3D Density Modeling of the Central American Isthmus

from Satellite Derived Gravity Data

Dissertation

zur Erlangung des Doktorgrades "Dr. rer. nat."

der Mathematisch-Naturwissenschaftlichen Fakultät

der Christian-Albrechts-Universität zu Kiel

vorgelegt von

Oscar H. Lücke

Institut für Geowissenschaften, Abteilung Geophysik

Kiel, 2012

Erstgutachter: Prof. Dr. Hans-Jürgen Götze

Zweitgutachter: Prof. Dr. Wolfgang Rabbel

Tag der mündlichen Prüfung: 21. August, 2012.

gez. Prof. Dr. Lutz Kipp, Dekan

Abstract

The combined geopotential models based on satellite and surface gravity data provide a homogenous gravity database with near global coverage. In this work, the data from the EGM2008 Combined Geopotential Model has been interpreted to prepare a comprehensive three dimensional model of the lithospheric density structure along the Central American Isthmus. The main focus of the model is the interpretation of the subduction process along the Middle American Trench and the segmentation of the oceanic Cocos and Nazca plates and the overriding Caribbean Plate. The viability of the EGM2008 data as input for the forward modeling has been assessed in terms of resolution and consistency with surface gravity data. For this purpose, a detailed surface gravity database was compiled and homogenized for Costa Rica and then compared with a subset of different data products from EGM2008. The Bouguer anomaly calculated from the gravity disturbance (geophysical anomaly) was determined to be the most consistent with the anomalies obtained from the surface stations, particularly in areas of high topography. The analysis also determined the areas in which the lower wavelengths from EGM2008 were dependent on the existence of surface gravity stations and the areas in which fill-in data may have been used to achieve its maximum spatial resolution.

From the processed data, a regional 3D density model of the lithosphere was constructed. The density model is constrained by available seismic velocity models, magnetotelluric cross-sections and receiver function data as well as the integration of seismic hypocenter data from local seismological networks. This regional model also integrates the available geological information and considers the tectonic segmentation of the crustal basement of the Caribbean Plate with separate units for the Chortis Block (2.77 Mg/m^3), Mesquito Composite Oceanic Terrane / Siuna Terrane (3 Mg/m^3) and the Caribbean Large Igneous Province (2.90 Mg/m^3). The upper crust of the Caribbean Plate also features several density bodies of lesser extent to account for local structures such as fore and back-arc sedimentary basins (2.45 - 2.65 Mg/m^3), granitoid and dioritoid intrusions (2.70 – 2.80 Mg/m^3) ophiolitic complexes (2.70 – 2.82 Mg/m^3) and magmatic bodies (2.35 – 2.40 Mg/m^3) among others. The crust for oceanic Cocos and Nazca plates was assigned an initial density of 2.80 Mg/m^3 and the changes in density caused by increase in pressure and temperature due to subduction at the Middle American Trench were modeled based on available petrological calculations constrained by thermal and lithostatic pressure conditions and metamorphic reactions.

Furthermore, first order boundary layers such as the Moho and the Cocos-Caribbean Plate interface were modeled and extracted for correlation with tectonic features and dynamic processes. The greater moho depths in the Caribbean Plate correlate with the presence of the Quaternary volcanic front and reaches a maximum of 44 km in western Guatemala. The Caribbean plate shows Moho depths between 20 and 12 km to the southeast of the continental shelf whereas to the north, values as shallow as 8 km are observed at the Cayman trough. For the Cocos Plate, Moho depths between 16 and 21 km were modeled along the Cocos Ridge contrasting with values between 15 and 12 km for the seamount segment and 8 and 11 km for the segments of the crust that are not volumetrically affected in a significant way by the Galapagos hot-spot.

For the Middle American Subduction Zone, an integrated interpretation of the slab geometry was carried out based on the three-dimensional density model constrained by seismological information from local networks. Results show the continuation of steep subduction from the Nicaraguan margin into northwestern Costa Rica transitioning to a shallower slab under central Costa Rica and the end of the Central American Volcanic Arc. To the southeast of the volcanic arc, the slab steepens and continues as a coherent structure until reaching the landward projection of the Panamá Fracture Zone. By integrating the seismological information into the 3D visualization of the density model, a correlation of the seismicity with the density units in the subducted slab was carried out. A gradual change in the depth of intra-plate seismicity is observed reaching 220 km for the northwestern part and becoming shallower toward the southeast where it reaches a maximum depth of 75 km. The changes in the depth of the observed seismicity correlate with changes in the density structure of the crust in the subducted slab. The initial 2.80 Mg/m^3 density for the crust of the Cocos Plate increases, according to petrological models and the calculated gravity, to 3.15 Mg/m^3 which correlates with the downdip extent of the Wadati-Benioff seismicity and then to 3.30 Mg/m^3 for the deepest sections of the slab where the seismicity is less frequent and the subducted crust is assumed to have become anhydrous. The increase in density occurs at variable depths along the subduction zone and may indicate that differences in the state of initial hydration of the oceanic lithosphere affect the depth reached by dehydration reactions.

Zusammenfassung

Die kombinierte Schweremodelle, die aus Satelliten- und an der Erdoberfläche gemessenen Schweredaten bestehen, bieten einen homogenen globalen Datensatz an. Für diese Dissertation wurden die Daten vom EGM2008 ausgewertet, um ein dreidimensionales Modell der lithospherischen Dichtenstruktur von Zentralamerika zu erstellen. Das Hauptthema ist die Modellierung der Subduktion am Mittelamerikanischen Graben und die Segmentierung der westlichen Karibischen Platte, sowie der ozeanischen Cocos und Nazca Platten. Die Viabilität der Schweredaten des EGM2008 als Eingabe für die Vorwärtsmodellierung wurde in Bezug auf die räumliche Auflösung und die Konsistenz mit bodengestützten Daten bewertet. Dafür wurde ein detaillierter Datensatz mit Schweredaten von Costa Rica kompiliert und homogenisiert. Dieser Datensatz wurde mit der EGM2008 Schweredaten von Costa Rica verglichen. Die Bouguer Anomalie, die aus der Störung des Schwerefeldes (geophysikalische Anomalie) berechnet wurde, stimmt mit dem bodengestützten Daten am besten überein, besonders in Gebiete mit hoher Topographie. Durch die Analyse und den Vergleich mit den EGM2008 Daten wurden Gebiete identifiziert, in denen EGM2008 von der Verfügbarkeit bodengestützter Stationen für die Berechnung der kürzeren Wellenlängen abhängig ist und in denen das EGM2008 „*fill-in*“ Daten enthält, damit die maximale räumliche Auflösung erreicht wird. Auf Basis der prozessierten Daten wurde durchs Vorwärtsmodellierung ein dreidimensionales Dichtemodell der Lithosphäre erstellt. Geophysikalische Daten, wie zum Beispiel: Geschwindigskeitmodelle aus der Seismik und seismischen Tomographie, magnetotellurische Profile und Daten aus *Receiver Functions* wurden als Randbedingungen im Modell integriert. Das Regionalmodell beinhaltet auch die Segmentation der unteren Kruste der Karibischen Platte die aus der Geologie und au tektonischen Modellen interpretiert wurde. Zu diesen Zweck wurden verschiedene Körper für die tektonischen Einheiten modelliert, zum Beispiel: der Chortis Block mit einer Dichte von 2,77 Mg/m^3, das Mesquito / Siuna Terrain (3 Mg/m^3) und die Größe Karibische Magmatische Region (2,90 Mg/m^3). Für kleinere Strukturen in der oberen Kruste, wurden mehrere Körper mit verschiedenen Dichten für die Sedimentbecken (2,45 - 2,65 Mg/m^3), granitischen/dioritischen Batholiten (2,70 - 2,80 Mg/m^3), ophiolitische Komplexe (2,70 - 2,82 Mg/m^3) und magmatische Körper (2,35 - 2,40 Mg/m^3) eingesetzt. Die Kruste der ozeanischen Platten (Cocos und Nazca) wurde mit einer Dichte von 2,80 Mg/m^3 modelliert. Die Änderungen in der Dichte der Kruste, die durch steigende Temperatur und Druck nach dem Eintritt der Platte in der Subduktionszone verursacht werden, wurden mit verschiedenen

Körpern steigender Dichte berücksichtigt. Diese Dichteverteilung in der Kruste der abtauchende Platte wurde mit petrologischen Randbedingungen gestützt. Die wichtigsten Grenzflächen wie die Moho und das interface zwischen Cocos- und Karibischer Platte wurden modelliert und für die spätere Korrelation mit anderen tektonischen Eigenschaften und dynamischen Verfahren extrahiert. Die größte Moho-Tiefe auf der modellierten Karibischen Platte hat einen Wert von 44 km und befindet sich im westlichen Guatemala. Für die Karibische Platte südwestlich vom Schelf wurden Tiefen zwischen 12 und 20 km modelliert. Im Bereich der Cayman Depression gibt es für die Moho Tiefen von 8 km. Für den Cocos Rücken auf der Cocos Platte wurden Moho Tiefen zwischen 16 un 21 km modelliert. Im Gegensatz dazu betragen sie Tiefen zwischen 12 und 15 km für das Seamount-Segment und 11 bis 8 km für die Segmente der Platte, die nicht vom Galapagos Hotspot beeinflusst sind. Die Geometrie der Mittelamerikanischen Subduktionszone wurde durch die dreidimensionale Vorwärtsmodellierung bestimmt. Dafür wurden die Hypozentren von lokalen Erdbebendatensätzen als Randbedingungen integriert. Das Modell zeigt eine fortlaufende steile Subduktion von Guatemala bis in nordwestliche Costa Rica. Im Zentralbereich von Costa Rica wird die Abtauchende Platte flacher bis zum Ende des Vulkansbogen wo es graduell wieder steiler wird. Im Südosten Costa Ricas wurde eine fortlaufende Struktur bis zur Bruchzone von Panama für die abtauchende Platte modelliert.

Seismologische Informationen wurden durch dreidimensionale Visualisierung im Dichtemodell integriert. Anhand Datenintegration wurde eine Korrelation zwischen Seismizität und Dichteverteilung interpretiert. Die Verteilung der Tiefen von Erdbeben Hypozentren zeigt, dass die Seismizität im Nordwesten Costa Ricas tiefer ist. Dort reichen die Erdbeben bis zu einer Tiefe von etwa 220 km, während die Hypozentren im Südosten eine maximale Tiefe von 75 km haben. Die Änderung in der maximalen Tiefe der Seismizität korreliert mit der Änderung in der Dichte der Kruste der abtauchende Platte korreliert. Die initiale Dichte der Kruste der Cocos Platte (2,80 Mg/m^3) nimmt nach petrologischen Modellen nach den Ergebnissen der Dichtemodellierung zu. Die Zone mit einer Dichte von 3,15 Mg/m^3 korreliert mit dem Bereich der Wadati-Benioff Zone. Ein dritter Körper mit einer Dichte von 3,30 Mg/m^3 wurde für die Kruste der abtauchende Platte modelliert; er entspricht der tiefsten Sektion der Subduktionszone im Modell, in der die Platte entwässert wird. Dieser Anstieg in der Dichte der abtauchende Kruste befindet sich im Modell in verschiedenen Tiefen und könnte den verschiedenen Zuständen der Hydration und späteren Entwässerung der abtauchenden Kruste entsprechen.

Resumen

Los modelos geopotenciales combinados, basados en datos gravimétricos satelitales y estaciones de superficie, proveen una base de datos consistente y con cobertura global. En este trabajo los datos derivados del modelo geopotencial combinado EGM2008 han sido interpretados con el fin de preparar un modelo tridimensional de la estructura litosférica del istmo Centroamericano. El enfoque principal del modelo es la interpretación del proceso de subducción a lo largo de la trinchera Centroamericana y la segmentación en la Placa Caribe así como en las placas oceánica del Coco y Nazca. La viabilidad del modelo EGM2008 como datos de entrada para el modelado de densidades, ha sido evaluada en términos de la resolución espacial y la consistencia con resultados obtenidos para estaciones superficiales. Con el fin de llevar a cabo esta evaluación, se compiló y homogeneizó una base de datos superficiales para Costa Rica que posteriormente fue comparada para un extracto de la base de datos regional del EGM2008. Se determinó que la anomalía de Bouguer calculada a partir de la perturbación gravimétrica (anomalía geofísica) es la más consistente con resultados obtenidos para los datos superficiales, particularmente en áreas de alta topografía. Este análisis determinó también las áreas en que las longitudes de onda más cortas del EGM2008 dependen de la cobertura de estaciones superficiales, así como las áreas en que datos "de relleno" habrían sido incluidos en la computación del modelo para alcanzar la máxima resolución espacial.

A partir de los datos procesados del EGM2008, se preparó un modelo tridimensional de las densidades litosféricas en la región. El modelo de densidades fue controlado por datos geofísicos disponibles, provenientes de modelos de velocidades sísmicas, perfiles magneto-telúricos y datos de funciones de receptor así como la integración de datos sismológicos de hipocentros a partir de redes locales. El modelo regional de densidades integra también la información geológica disponible y considera la segmentación tectónica del basamento cortical de la Placa Caribe. Para esto, distintas unidades fueron modeladas para el Bloque Chortis (2,77 Mg/m^3), el Terreno Oceánico Compuesto de Mesquito / Terreno de Siuna (3 Mg/m^3) y la Gran Provincia Ígnea del Caribe (2,90 Mg/m^3). La corteza superior de la Placa Caribe presenta también unidades de menor extensión con el fin de modelar estructuras locales como las cuencas sedimentarias del ante- y tras-arco (2,45 - 2,65 Mg/m^3), intrusiones granitoides y dioritoides (2,70 - 2,80 Mg/m^3), complejos ofiolíticos (2,70 - 2,82 Mg/m^3) y cuerpos magmáticos (2,35 - 2,40 Mg/m^3), entre otros. Para la corteza oceánica de las Placas del Coco y Nazca, se asignó una densidad inicial de 2,80 Mg/m^3 y posteriormente se

consideró el cambio en densidad de los materiales tomando en cuenta los cambios en las condiciones de presión y temperatura debido a la subducción en el margen convergente Centroamericano. Estos cambios fueron modelados considerando cálculos petrológicos controlados por condiciones de presión litostática, reacciones metamórficas y modelos térmicos.

Las discontinuidades litosféricas de primer orden como el Moho y la interfase entre la Placa Caribe y la Placa del Coco fueron modeladas y posteriormente extraídas para ser correlacionadas con estructuras tectónicas y procesos dinámicos. Las mayores profundidades del Moho fueron identificadas a lo largo del arco volcánico Cuaternario, con un máximo de 44 km para el occidente de Guatemala. La Placa Caribe presenta profundidades del Moho entre 12 y 20 km al sureste de la plataforma continental mientras que hacia el norte, valores tan someros como los 8 km fueron observados para la depresión de Caimán. Para la Placa del Coco, profundidades del Moho entre los 16 y 21 km fueron modeladas a lo largo de la dorsal asísmica del Coco. Esto contrasta con los valores entre 12 y 15 km obtenidos para el segmento de montes submarinos y 8 a 11 km para los segmentos corticales provenientes de los centros de dispersión y que no han sido afectados significativamente en términos volumétricos por el punto caliente de Galápagos.

Para la zona de subducción Centroamericana, se llevó a cabo una interpretación conjunta de su geometría basada en el modelado tridimensional de densidades, controlado por información sismológica proveniente de redes locales. Los resultados muestran la continuación de la subducción empinada a lo largo del margen Centroamericano hasta el noroeste de Costa Rica con una posterior transición a una subducción relativamente somera en la parte central de Costa Rica al término del arco volcánico Cuaternario. Al suroeste del arco volcánico, el ángulo de subducción incrementa y la placa subducida se presenta como una estructura coherente hasta alcanzar la proyección hacia el continente de la Zona de Fractura de Panamá.

Mediante la integración de la información simológica a la representación tridimensional del modelo de densidades, se estableció una correlación entre la ocurrencia de sismicidad y la distribución de las densidades en profundidad. A partir de esto se identifica un cambio gradual en la profundidad del la sismicidad intra-placa. Esta alcanza una profundidad máxima de 220 km para el segmento noroeste y se encuentra progresivamente más somera hacia el sureste del margen en donde alcanza una profundidad de 75 km. Los cambios en la profundidad de la sismicidad observada presentan una correlación con la estructura de

densidades en la corteza subducida. La densidad inicial de 2.80 Mg/m^3 para la Placa del Coco incrementa, según los modelos petrológicos y la gravedad calculada, a 3.15 Mg/m^3 lo cual se correlaciona con la extesnión en profundidad de la sismicidad de Wadati-Benioff. Posteriormente, la densidad incrementa a 3.30 Mg/m^3 en las secciones más profundas de la placa subducida para las que la sismicidad es menos frecuente y en donde se asume que la corteza oceánica subducida ha alcanzado un estado anhidro. El incremento en densidad ocurre a distintas profundidades a lo largo de la zona de subducción y podría indicar que las diferencias en el estado inicial de hidratación de la litósfera oceánica afecta la profundidad alcanzada por las reacciones de deshidratación.

Table of Contents

1 Introduction

The following dissertation focuses on results obtained from the forward modeling of satellite-derived and surface gravity data and is comprised of four scientific articles in various stages of publication. Chapter 2 of this dissertation is comprised of work originally published in the International Journal of Geophysics[1]. This publication is part of my collaboration with Hans-Jürgen Götze who provided input on the application of analytical methods for the interpretation of the gravity field and Guillermo Alvarado who contributed with insights into the composition and structure of the volcanoes of Central Costa Rica. For this work, the first, three-dimensional density model for Costa Rica was completed through cooperation with the Collaborative Research Center 574 (Sonderforschungsbereich 574): Volatiles and Fluids in Subduction Zones, the University of Kiel and the University of Costa Rica. This model was prepared by use of the inhouse the modeling software of the research group in Kiel and was interpreted from surface gravity data provided by GETECH Leeds. This local scale model is included in this dissertation in order to show the effect of local structures on the gravity field and to exemplify the limitations of the previously existing surface database. Furthermore, the insights gained by the local scale modeling of the magmatic processes in Central Costa Rica were applied for the Quaternary Central American Volcanic Arc and integrated in the regional scale model for Central America.

Though the available surface station database was successfully used as input for the modeling of small scale structures, specifically for Central Costa Rica, the quality and coverage of the surface data for the Central American region as a whole was considered insufficient for the modeling of structures on larger scales which is the main objective of this

[1] Lücke O.H., Götze, H-J. and Alvarado, G.E. (2010): A constrained 3D density model of the upper crust from gravity data interpretation for Central Costa Rica. *Int. J. Geophys.*, 2010, doi:10.1155/2010/860902.

work. The results obtained from the local model allowed to gain insights into the geometry of volcanic magma chambers. On the other side the 3D modeling helped to identify the deficiencies in terms of coverage, quality and consistency of the surface gravity databases for the region. It also provided motivation to inquire into the use of novel sources of data such as satellite derived gravity and combined gravity models. The application of these gravity models was sought with the objective of providing an adequate input in terms of resolution, consistency, and coverage, for the modeling of large scale structures such as the subducting slab and the Moho depths. The effect of these structures are expressed in the long wavelengths of the gravity field which were found to be adequately resolved in the satellite derived gravity models.

The third chapter on this dissertation is comprised of a joint scientific article which was accepted for publication in 2011 in the Journal of Geodynamics[2]. This chapter describes the results of cooperation with colleagues from the University of Kiel and the University of Jena and was carried out within the framework of the Special Priority Project SPP 1257 entitled "Mass Transport and Mass Distribution in the System Earth". My contribution for this work focuses on the assessment of the application of different satellite derived datasets to the research on mass distribution in the solid Earth, specifically in the area of Central America.

In order to determine which dataset was better suited for the geophysical interpretation of the lithospheric structure in Central America, a comparison of the satellite derived data with the existing surface gravity database was carried out for Costa Rica. Since the coverage and availability of ground gravity data in the rest of Central America is limited, the area of Costa Rica was considered as the best case scenario in which the surface data could be

[2] Köther, N., Götze, H.-J., Gutknecht, B.D., Jahr, T., Jentzsch, G., Lücke, O.H., Mahatsente R., Sharma, R. and Zeumann, S. (2011): The seismically active Andean and Central American margins: Can satellite gravity map lithospheric structures?, *J. Geodyn.*, (in press), doi:10.1016/j.jog.2011.11.004.

compared to the combined gravity models. For the purpose of this comparison, the surface database provided by GETECH and described for Chapter 2, was improved by compiling and processing additional surface station data and including it in a homogenous database. The additional data was obtained through a request to the Costa Rican Ministry of the Environment which provided the data for use in academic research. Furthermore, marine station data from SFB574 for the Pacific Ocean and open source data for the Caribbean Sea from the National Oceanographic and Atmospheric Administration of the United States were included.

The newly compiled dataset was then homogenized and constituted a state of the art surface gravity database for Costa Rica which was used as a reference to compare several data products, mainly from the GRACE satellite mission. This analysis, carried out for the region of Costa Rica, yielded new information on the reach and limitations of the combined geopotential models in terms of spatial resolution and consistency. The results also establish a comparison between the application of geodetic gravity anomaly (classical anomaly) and geophysical anomaly (gravity disturbance) to the modeling of the solid Earth.

For this assessment, results from a preliminary three dimensional model prepared solely from EGM2008 data for Central America were published. The characteristics of the different datasets were analyzed in the context of the modeled lithospheric structure and contributed to the comparison between the geodetic anomaly, the geophysical anomaly, and the surface station data for areas of varying topography and geological setting. The geophysical anomaly (gravity disturbance) from the EGM2008 Combined Geopotential Model (Pavlis *et al.*, 2008) was considered to have the best correlation with the surface gravity data particularly in areas of high topography. These results were consistent with the comparisons of data sources carried out simultaneously by colleagues working on the Chilean convergent margin.

The characteristics of the final version of the regional density model for Central America are described in chapter 4, which is comprised of a scientific article focusing on the Moho structure of Central America. This work was accepted for publication in 2012 in the International Journal of Earth Sciences[3] in a special issue along with other contributions from the SFB574. For this regional model, the gravity disturbance was chosen to be used as input for the regional three-dimensional forward modeling, based on the data analysis carried out in chapter 3. The constrained regional model of Central America takes into consideration the segmentation of the crustal basement of the Caribbean Plate with separate units for the Chortis Block (2.77 Mg/m^3), Mesquito Composite Oceanic Terrane / Siuna Terrane (3 Mg/m^3) and the Caribbean Large Igneous Province (2.90 Mg/m^3). The crust for oceanic Cocos and Nazca plates was assigned a density of 2.80 Mg/m^3. From the regional scale model, the Moho boundary surface was modeled and constrained by available geophysical data. This surface was then extracted from the model and the results were correlated with structures such as the volcanic arc, the Galapagos hotspot trace and the Nicaragua depression.

The subduction of the Cocos Plate along the Middle American Trench is the focus of chapter 5. This chapter is comprised of a manuscript which has been submitted for publication to the Geophysical Journal International and is currently under review[4]. This manuscript was prepared in collaboration with Ivonne Arroyo who provided the seismological data that was used to constrain the geometry of the density model. The regional geometry of the subduction zone and the density structure of the subducting slab were constrained by earthquake hypocenters as well as other geophysical and petrological constraints. The regional model shows a continuous steep subduction of the Cocos plate for

[3] Lücke, O.H. (2012): Moho structure of Central America based on three-dimensional lithospheric density modelling of satellite derived gravity data. *Int. J. Earth Sci.*, (in press), doi: 10.1007/s00531-012-0787-y.

[4] Lücke, O.H. and Arroyo, I., (in review): Density structure and geometry of the Costa Rican subduction zone from 3D gravity modeling and local earthquake data. *Geophys. J. Int.*, (submitted manuscript).

the crustal segments generated at the East Pacific Rise with major changes in geometry occurring in Central Costa Rica. A local, more detailed model of the Costa Rican subduction zone was prepared using the regional model as reference. For the local model, earthquake hypocenters from four distinct local seismological networks in Costa Rica were integrated as constraints, jointly interpreted and correlated with conceptual models (Ranero *et al.*, 2005) and petrological models (Bousquet *et al.*, 2005; Husen *et al.*, 2003a; Rüpke *et al.*, 2002). The presence of a continuous slab structure beneath southeastern Costa Rica was the preferred geometry considering the fit of the modeled gravity data and the available constraints. However, alternate models requiring a discontinuous slab and a shallow Moho structure were also considered and discussed in order to account for the lack of deep, slab-related seismicity in the region.

The final version of the density model is the result of the combined interpretation of gravity data from various sources as well as the integration of geophysical and geological constraints. The integration of the results from the forward modeling with the available constraining data provides a comprehensive, three-dimensional interpretation of the lithospheric structure of the region. The results presented in this dissertation provide the basis for further interpretations of the state of stress on the modeled boundary surfaces and the correlation with local seismicity.

The modeled structure for the Caribbean Plate provides an in-depth, three dimensional interpretation of the tectonic models that had previously been inferred mostly from surface geology or the qualitative interpretation of potential fields. The regional density model accounts for the lithospheric sources of the long wavelengths of the measured gravity field resolved by the satellite derived gravity models. The resulting density model will serve as a starting point for further, more detailed studies of the density distribution in the region,

providing that the resolution and quality of the databases improves and thus enabling the interpretation of local structures throughout the region.

1.1 Tectonic Setting of Central America

The present Central American land bridge links the South and North American land masses and is located on the western edge of the Caribbean Plate. The current lithospheric structure of the Caribbean Plate is the result of the tectonic processes that have followed the break-up of Pangaea and the dispersion of the resulting continental blocks since the Early Jurassic causing the migration of tectonic Terranes and the creation of early seaways (Pindell and Keenan, 2009). The crustal basement of the Caribbean Plate is thus highly heterogeneous and features large-scale differences in composition and physical properties.

The northern margin of the Caribbean Plate is a left-lateral strike-slip boundary formed by the Motagua-Polochic fault system in northern Guatemala, followed eastward by the Swan Islands Fault and along the Cayman Trough. The crustal basement in northern Central America is comprised of the Chortis Block first defined by Dengo (1969) as a Paleozoic continental block extending to northern Costa Rica. Further studies by Venable (1994) suggested the presence of an oceanic component (Siuna Terrane) on the southern part of the Chortis Block in the form of serpentinites which crop out in northern Nicaragua. The segmentation of the Chortis Block was described in further detail by Rogers *et al*. (2007) who, based on the correlation of surface geology and aeromagnetic data, defined 3 distinct magnetic provinces for the Chortis Block (Central, Southern and Eastern Chortis Terranes) and outlined a new limit for the mafic Siuna Terrane (Fig. 1.1).

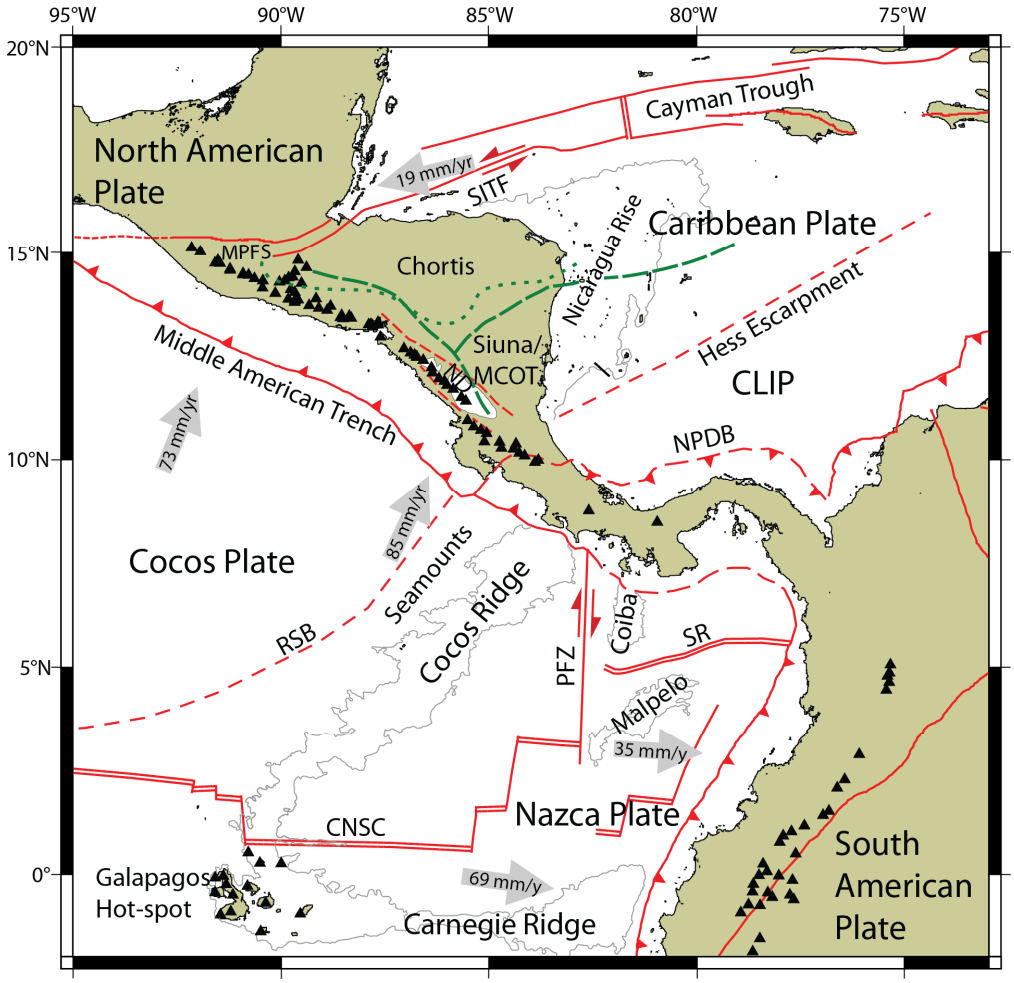

Figure 1.1. Tectonic setting of Central American. Red lines show plate boundaries (modified from Coffin *et al.*, 1998) and major tectonic structures. Triangles show Quaternary volcanoes (Siebert and Simkin, 2002). Gray arrows show plate motions relative to the Caribbean Plate after: Freymueller *et al.* (1993), Kellogg and Vega (1995) and DeMets (2001). CNSC: Cocos-Nazca Spreading Center. MPFS: Motagua-Polochic Fault System; ND: Nicaragua Depression; NPDB: North Panama Deformed Belt; PFZ: Panama Fracture Zone; RSB: Rough-Smooth Boundary modified from Hey (1977); SITF: Swan Islands Fault; SR: Sandra Rift (DeBoer *et al.*, 1988). Gray contours show the -2000 m bathymetric level outlining the Cocos Ridge and -500 m for the Nicaragua Rise. Green lines show the borders between the Chortis and the Siuna/Mesquito terranes according to Rogers *et al.* (2007) (stippled line) and Baumgartner *et al.* (2008) (dotted line).

Furthermore, based on surface geology and DSDP borehole data, Baumgartner *et al.* (2008) propose that the presence of the continental component of the Chortis Block is limited to eastern Guatemala and Honduras and that the mafic component in the form of the Mesquito Composite Oceanic Terrane (MCOT), extends to the northwest along the Central American fore-arc and southward to northern Costa Rica. The crustal basement on the southeastern part of the isthmus (Costa Rica and Panama) is composed of a Cretaceous oceanic plateau in the form of the Caribbean Large Igneous Province (Hoernle *et al.*, 2008).

This tectonic heterogeneity results in crustal basement units with contrasting physical properties i.e. crystalline Paleozoic rocks for the Chortis Block, ultramafic material (serpentinized peridotite) for the MCOT and oceanic basalts for the CLIP.

Along with this segmentation, the convergence of the oceanic Farallon Plate along the western margin of the ancient continental blocks resulted in different episodes of subduction. The current convergent margin on the western edge of the Caribbean Plate hosts the principal tectonic feature in the region with the subduction of the oceanic Cocos Plate along the Middle American Trench. According to Buchs *et al*. (2010), subduction-related volcanism may have affected the crustal basement of the current isthmus as early as the Coniacian (~89 Ma) for the Southern Central American Arc. The fission of the Farallon Plate at the beginning of the Miocene (Lonsdale, 2005), segmented the oceanic plate along the Panama Fracture Zone between the Cocos and Nazca Plate.

This, along with the interaction of the Oceanic Plate with the Galápagos Hotspot and the arrival of the Cocos Ridge to the Middle American Trench, has further influenced the subduction system. According to Lonsdale and Klitgord (1978), subduction of the Nazca plate may have ceased in the Late Miocene after which the margin transitioned to a strike-slip boundary. However, DeBoer *et al*. (1988) propose a reactivation of the subduction 3.4 to 5.3 million years ago and consider the existence of recent subduction. Although Neogene arc volcanism is present throughout the isthmus (Alvarado *et al.*, 2007) the Quaternary volcanic arc ends in Central Costa Rica with the exception of the Barú volcano and minor, eroded vents in western Panama. The tectonic segmentation of the Caribbean Plate along with lithospheric-scale processes such as the subduction of the oceanic Cocos Plate and its interaction with the Galapagos hotspot are reflected in the gravity field obtained from surface gravity data, satellite gravity data and combined geopotential model such as EGM2008 (Pavlis *et al.*, 2008).

1.2 Methods

The main focus of this work was the interpretation of gravity data by means of forward modeling of the solid Earth to create a comprehensive, three-dimensional model of the density distribution of the lithosphere in Central America. The modeling process followed the development of the software IGMAS+ (Götze *et al.*, 2010) which is based on the algorithm by Götze (1976) and Götze and Lahmeyer (1988). A previous model, which is presented in chapter 2, was constructed using the earlier version of the software (Schmidt and Götze, 1999). Since early 2009, the new version IGMAS+ (Götze *et al.*, 2010) became available to the research group. This new version emphasizes the interactive manipulation of the geometry and parameters, the optimized calculation of the modeled gravity, the integration of constraints and the three dimensional visualization. This software served not only as the primary method for the density modeling but also as an integration tool for geophysical constraints and results obtained by means of other analytical methods. The methods and their application to the analysis of the gravity field, will be explained further in each corresponding chapter of this dissertation.

2 A constrained 3D density model of the upper crust from gravity data interpretation for central Costa Rica

The map of complete Bouguer anomaly of Costa Rica shows an elongated NW-SE trending gravity low in the central region. This gravity low coincides with the geographical region known as the Cordillera Volcánica Central. It is built by geologic and morpho-tectonic units which consist of Quaternary volcanic edifices. For quantitative interpretation of the sources of the anomaly and the characterization of fluid pathways and reservoirs of arc magmatism, a constrained 3D density model of the upper crust was designed by means of forward modeling. The density model is constrained by simplified surface geology, previously published seismic tomography and P-wave velocity models, which stem from wide-angle refraction seismic, as well as results from methods of direct interpretation of the gravity field obtained for this work. The model takes into account the effects and influence of subduction related Neogene through Quaternary arc magmatism on the upper crust.

2.1 Introduction and tectonic setting

A constrained 3D density model of the upper crust along the Quaternary Central American Volcanic Arc (CAVA) was carried out based on complete Bouguer anomaly data. The main focus of the study was the modeling of the fluid pathways and reservoirs in the upper crust resulting from the magmatic processes associated with the subduction of the Cocos plate beneath the Caribbean plate.

The area of interest was the portion of the CAVA known as the Cordillera Volcánica Central in Costa Rica. Throughout Central America, the volcanic arc shows a segmented disposition along the isthmus marked by gaps in Quaternary volcanism as well as sudden changes in the distance from the Middle American Trench. The geographical and morphological region known as the Cordillera Volcánica Central of Costa Rica is comprised

by the Platanar, Barva, Poás, Irazú and Turrialba volcanic edifices. It is delimited to the NW by the absence of Quaternary stratovolcanoes up to the occurrence of the Arenal-Chato volcanic complex. To the SE the arc is interrupted by a major gap in Quaternary volcanism in the Talamanca region marking the southeastern end of the portion of the CAVA related to the subduction of the Cocos plate (Fig. 2.1).

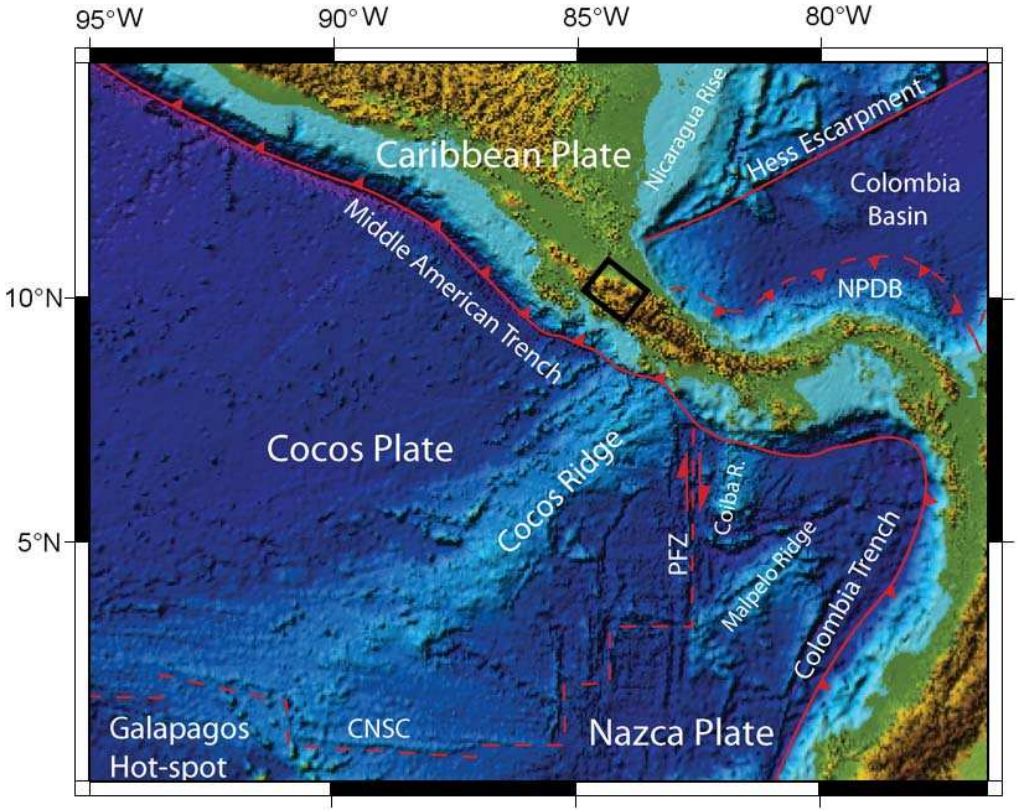

Figure 2.1. Tectonic setting of the Costa Rican subduction zone. Major plate boundaries and tectonic features are marked by red lines. Location of the 3D density model is indicated by a black polygon. NPDB: North Panamá Deformed Belt, PFZ: Panamá Fracture Zone, CNSC: Cocos-Nazca Spreading Center.

This portion of the Costa Rican arc is characterized also by unique morphological features such as the high volume of the volcanic edifices relative to the rest of the arc (i.e. Carr *et al*. (2007). Special interest was put on this portion of the arc because of the presence of an elongated gravity low in the complete Bouguer anomaly map. Until now, density modeling in the region was restricted mainly to regional 2D interpretations based on inhomogeneous gravity databases (Ponce and Case, 1987), also 2D sections along seismic refraction profiles on the northwestern part of the Costa Rican arc (Gödde, 1999; Sallarèz *et*

al., 2001) and across the volcanic gap in the Talamanca region (Stavenhagen *et al.*, 1997). Density models in the Cordillera Volcánica Central were restricted to the structure of the volcanic edifices (Thorpe *et al.*, 1981) thus accounting only for the effects of masses above the geoid . For this work, the homogenized complete Bouguer anomaly database compiled for the SFB574 was used to model in 3D, the crustal structure and the effects of Neogene to Quaternary volcanism on the densities along the arc.

2.2 Database and gravity field features

On-shore complete Bouguer anomaly maps were generated from the homogenized gravity database of the SFB574. The database includes approximately 20 000 stations and was compiled from previously existent on-shore gravity data from several government, industry and academic institutions such as: GETECH Leeds, BGI (Bureau Gravimétrique International), ICE (Instituto Costarricense de Electricidad). The complete Bouguer anomaly map shows an arc-parallel gravity low with a minimum of -57×10^{-5} m/s^2 along the Cordillera Volcánica Central (Fig. 2.2).

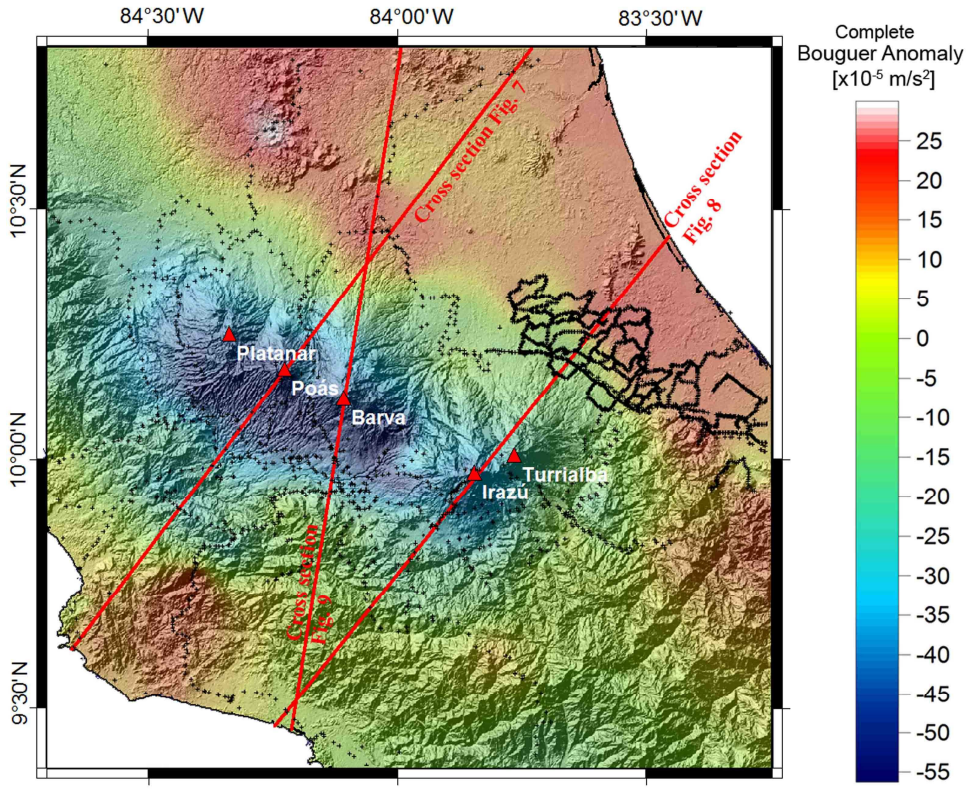

Figure 2.2. Modified from Lücke (2008).Complete Bouguer anomaly map of central Costa Rica draped over the shaded SRTM relief map. Red triangles show location of the main Quaternary volcanic vents. Black plus signs indicate the location of gravity stations. Red lines show locations of vertical cross sections presented on this work.

Previous works (Montero *et al.*, 1992; Ponce and Case, 1987), show a minimum of approximately -80x10^{-5} m/s^2 for this region. However, upon further review of the gravity database, the height above sea level reported for the single station with a complete Bouguer anomaly value of -75.9x10^{-5} m/s^2 differed in nearly 1000 m with the correspondent value of topographic height above sea level obtained from SRTM topography data. This, along with other aberrant values were corrected or taken out because of lack of metadata. The corrected database was then used for the forward modeling of the density structure and mass distribution of the upper crust.

Although the main gravity low coincides in extension and trend with the main volcanic edifices of the Quaternary arc, its axis is shifted approximately 8 km towards the Middle American Trench relative to the main volcanic axis comprised by the Platanar, Poás, Barva and Irazú volcanoes. The fore-arc region shows a relative Bouguer gravity low along

the Aguacate Mountains and on-shore data along the Pacific coast show a peak of approximately $20x10^{-5}$ m/s^2 on the Herradura promontory. Towards the back-arc region, the Bouguer anomaly values increase to a relative high of $15x10^{-5}$ m/s^2 in the northeastern Tortuguero plains. The northwestern end of the study area shows a gradual increase in the Bouguer anomaly values along the arc with an inflection at a value of $-35x10^{-5}$ m/s^2 at 20 km NW of the Platanar volcano from which the values plateau until they decrease again towards the Pacific coast in SW Nicaragua. To the SE, the main gravity low shows a strong positive gradient culminating at an alignment between the port towns of Quepos and Limón.

2.3 Constraints of the 3D density model

The data analysis methodological approach emphasized the integration of geological and geophysical constraints into the forward modeling. For geological constraints, a simplified map (Fig. 2.3) outlining the main superficial lithostratigraphic units was summarized from previously existing geological information (Denyer and Alvarado, 2007; Tournon and Alvarado, 1997) together with the integration of the inferred location of main volcanic vents related to the Neogene Aguacate arc (Alvarado, 2000). The geological information was complemented by borehole stratigraphy data from Pizarro (1993).

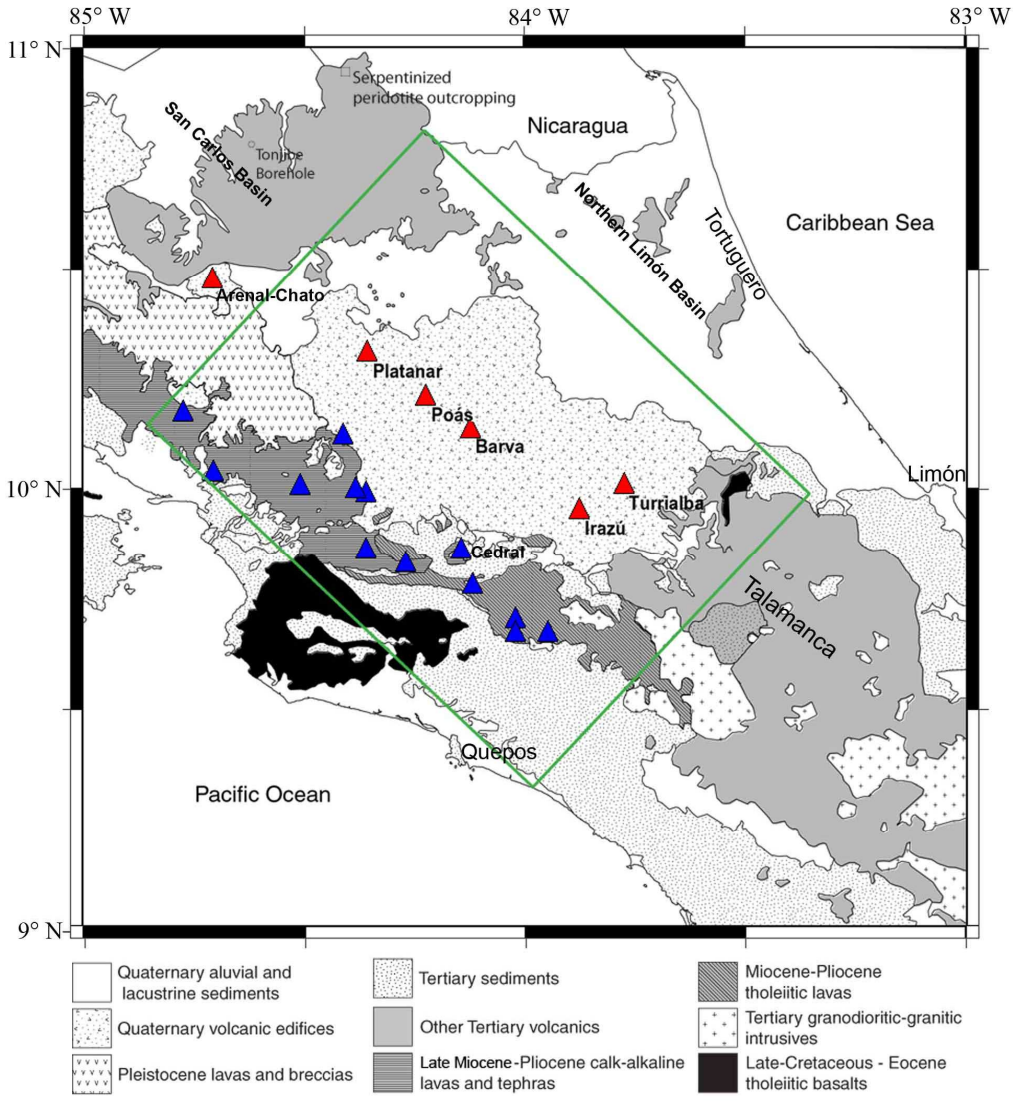

Figure 2.3.. Simplified surface geology of the study area based on cartography by Tournon and Alvarado (1997) and Denyer and Alvarado (2007). The green box shows the extent of the modeled area. Red triangles show the locations of main Quaternary volcanic vents. Blue triangles show the locations of paleo-volcanic vents for the Neogene "Aguacate" volcanic paleo-arc, inferred from surface geology and morphology.

Geophysical constraining focused on direct interpretation of the gravity field (i.e. Euler deconvolution source points and power spectrum analysis) and the inclusion of local earthquake seismic tomography data generated by SFB574 collaborators (Arroyo, 2008) and previously published works as well as 2D velocity models based on wide angle seismic refraction surveys (Lizarralde *et al.*, 2007).

2.3.1 Euler deconvolution

For the Euler deconvolution solutions, the software REDGER (Pašteka, 2006) was used which advantages the calculus by means of regularized derivatives (Pašteka and Richter, 2005). The calculation of the Euler source points is based on Euler's homogeneity equation and results in clusters used to constrain the overall geometry of the model. In this case, a structural index of 0.01 was used to for the approximation of planar structures thereby outlining the main boundaries between bodies of contrasting density (Fig. 2.4).

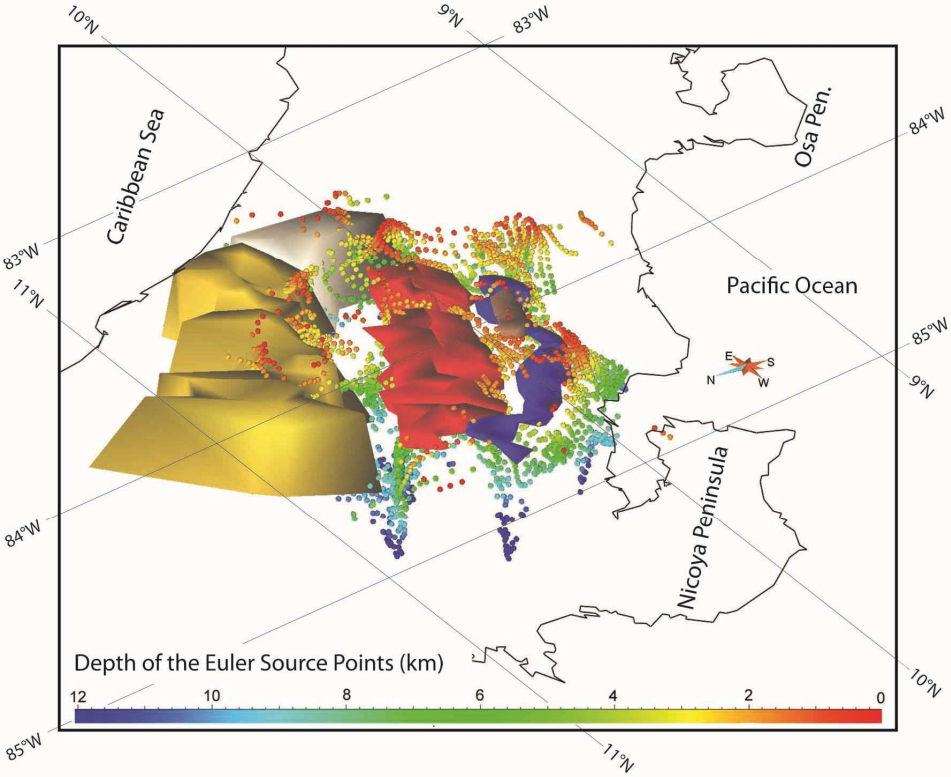

Figure 2.4. Modified from Lücke (2008). Semi-perspective view of the modeled area. Colored dots show locations of Euler deconvolution source points relative to the modeled bodies. Main modeled bodies are shown as colored polyhedra. The yellow polyhedron represents the back arc structural high with a density of 2.82 Mg/m^3. The red polyhedra represent the low density zones beneath the arc with densities between 2.35 and 2.38 Mg/m^3. The blue polyhedra represents the paleo-arc bodies with densities between 2.40 and 2.45 Mg/m^3. Coastline is shown in black.

The Euler source points showed clustering between geological units mainly on the southwestern and northeastern boundaries of the Quaternary volcanic arc. The clustering of the source points outlines in depth, the heterogeneities in the upper crust caused by the Quaternary volcanism. The location of the source point clusters also correlates well with

surface geology in the sense that they coincide with the contacts between the lithostratigraphic units that represent major events in Cenozoic volcanism as well as basement structure towards the back-arc. The distribution of the shallower Euler source points may also outline the upper boundary of heterogeneous bodies in the upper crust.

2.3.2 Power spectrum analysis

Power spectrum analysis was carried out through 2D Fast Fourier Transformation to estimate depths for the structures which cause the measured anomaly. According to this method (Döring, 1995), the depth of a corresponding "monopole source point" is obtained from the negative slope of the linear relationship between the logarithmic power spectrum and the wavenumber of the gravity field. Results show two tendencies for the correlation between energy and wavenumber (Fig. 2.5).

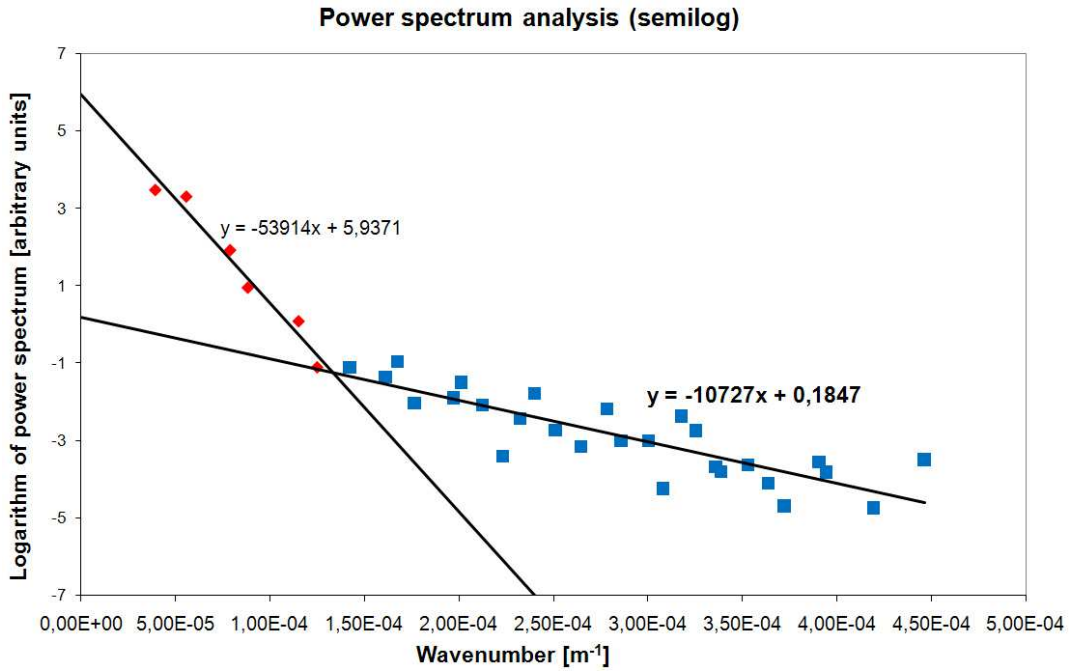

Figure 2.5. Modified from Lücke (2008). Results of the power spectrum analysis of the Bouguer gravity field using 2D Fast Fourier Transform. Black lines represent the trends of the linear regression separating the spectrum in a local trend (blue squares) and a regional trend (red diamonds).

The local part of the spectrum results in depths of some 11 km. The regional part of the spectrum appoints to greater depths of about 54 km. The source of this/these causing mass/masses is not yet clear. We put the main focus of the modeling on the shallower

structures because they are better constrained by other geophysical data such as the seismic tomography. 3D modeling together with the results of Euler deconvolution, constrained the local modeling in the upper 15 km of the crust. Until now the effect of deeper located structures are not investigated and may account for wider wavelengths of the regional field outside of the area of study and outside the area of interest.

2.3.3 Correlation with local earthquake seismic tomography

Further constraints included previously published local earthquake seismic tomography cross sections (Colombo *et al.*, 1997; Husen *et al.*, 2003a; Protti *et al.*, 1996), as well as data from SFB574 collaborators (Arroyo, 2008). Based on the slab location relative to the volcanic arc as observed on the seismic tomography cross sections and the shallow results for the source of the local gravity anomaly obtained from power spectrum analysis, it is interpreted that the effects of the distribution of mass directly related to the slab, does not have an effect on the gravity field at a local scale. However, low velocity zones shown by Husen *et al*. (2003a) in the upper mantle at a depth of approximately 60 km may have a regional effect on the gravity field. Local low velocity heterogeneities in the upper crust are present beneath the Quaternary volcanic arc in the Cordillera Volcánica Central as observed in the values of perturbation in V_p from Arroyo (2008). As for the geometry of such heterogeneities, the integration of the data as constraints in the density model shows trenchward-dipping, low velocity structures, originating from the slab and ascending to the upper crust beneath the Quaternary arc. Remarkable is also the presence of similar structures beneath the Neogene Aguacate arc which hints of remnant effect of paleo-volcanism on the upper crust. With regards to the issue of resolution of the seismic tomography data directly integrated as constraints (Arroyo, 2008), the better resolved portions of the Quaternary arc in the upper crust domain are those beneath the Irazú-Turrialba volcanic complex as well as the Poás volcano. This is mainly due to the location of seismologic stations.

2.4 Results and Discussion

The constrained 3D density model was carried out by the interactive modeling with the software IGMAS (Interactive Gravity and Magnetics Application System, Schmidt and Götze (1998). This modeling is based on the initial algorithm by Götze (1976) and further enhanced by Götze (1984), Götze and Lahmeyer (1988), Schmidt and Götze (1998). Modeling is carried out interactively by creating cross sections from which constant density bodies are triangulated based on the location of the input vertices. Densities are directly assigned to each body or may be calculated via inversion based on the given geometry.

For this model, 22 modeling cross sections were created trending perpendicular to the volcanic arc with a NE-SW trend. Geometry is based on available constraints as well as fit between the measured and the modeled gravity field. Overall fit between measured and calculated complete Bouguer anomaly is shown on figure 2.6.

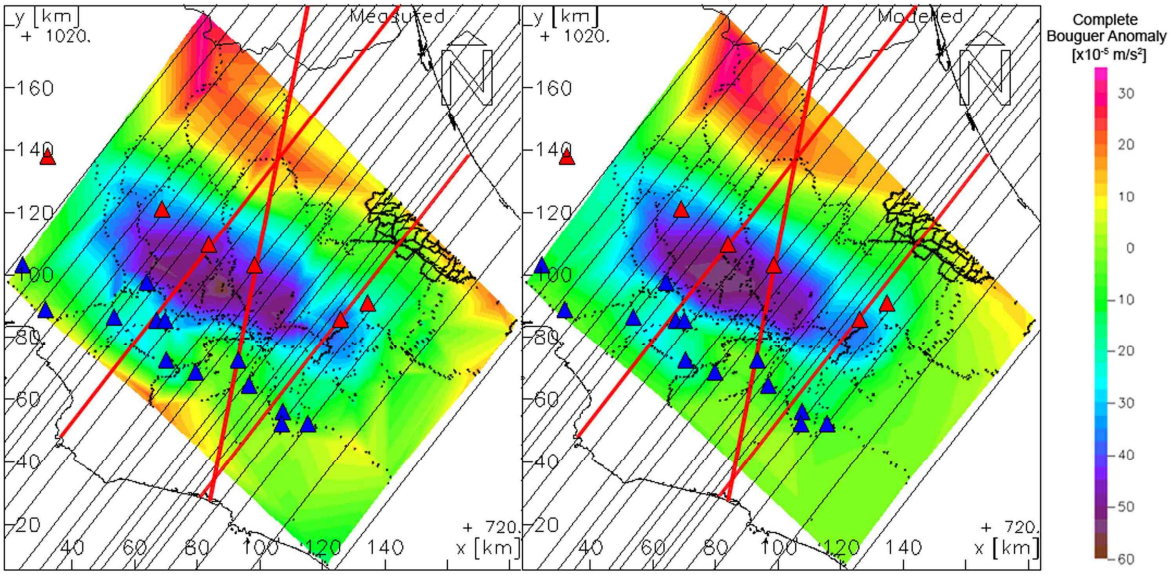

Figure 2.6. Modified from Lücke (2008). Comparison of measured (left) and calculated (right) complete Bouguer anomalies. Location and trend of model cross sections are shown as NE-SW trending black straight lines. The cross sections presented on this work are highlighted in red. Location of the main Quaternary volcanic vents are shown as red triangles. The Neogene "Aguacate" paleo-volcanic vents inferred from surface geology are shown as blue triangles. Black dots represent the location of gravity stations. Coastline and political borders are shown in bold black lines.

2.4.1 Overall context and horizontal discontinuities

In order to model the effects of volcanism in the upper crust, an overall background structure was modeled in accordance with available constraints. An important discontinuity in the upper crust is shown in a one-dimensional velocity model by Matumoto et al. (1977) with a change on P wave velocities from 5.05 km/s to 6.2 km/s at a depth of between 8 and 10 km for northwestern Costa Rica. A discontinuity at an approximate depth of 10 km is also shown by a P wave velocity model from Gödde (1999) based on wide angle refraction survey. Due to lack of constraining data for the Central region, this discontinuity was extrapolated to the area of interest and modeled as a change in density to 2.80 Mg/m^3 below the 10 km depth. This density represents a mafic igneous basement assumed for the southwestern part of the Caribbean plate. A middle layer with densities between 2.70 Mg/m^3 and 2.74 Mg/m^3 was modeled to account for an andesitic composition of the next to uppermost crustal domain. Lateral variations were modeled to account for broad changes in the gravity field. An uppermost layer with a density of 2.60 Mg/m^3 was modeled representing a 1-2 km thick layer comprised mainly of volcanoclastic Tertiary marine sediments, tephra deposits and Quaternary alluvial sediments.

2.4.2 Effects of magmatic processes on the upper crust

The main features modeled beneath the Quaternary arc are elongated lower density bodies with densities ranging from 2.35 Mg/m^3 to 2.38 Mg/m^3. Such bodies represent low density heterogeneities in the upper crust brought on by the effects of Quaternary volcanism. These effects may be comprised of a complex interaction between magma derived components such as fluids and volatiles, and the surrounding crust. Also, higher temperatures from higher heat flow along the active arc may play a role in lowering the overall density. In addition, the presence of melts may also be taken into account, although the relatively high volumes and broad lateral extension of the modeled bodies make it unlikely for these to be

occupied entirely by melts. Thus, these are not interpreted to be magma chambers in their full extent but low density zones in the upper crust directly related to processes such as hydrothermal alteration, higher heat flow and the presence of melts.

As for the geometry and lateral variations of such bodies, the qualitative interpretation of the complete Bouguer anomaly map yields an indirect hint as for the disposition of these low density zones. The main gravity low corresponds in extent and trend to the main volcanic edifices in the Cordillera Volcánica Central and appears as an elongated body constricted only in the region between the Barva volcano and the Irazú-Turrialba volcanic complex. This constriction coincides with a relatively larger gap between the main vents of the Barva and Irazú volcanoes (32 km) as compared with smaller more regular gap of about 15 km between the main vents of the Barva-Poas-Platanar volcanic edifices. This may indicate that the overlap of the effects of magmatism in the upper crust for each volcanic vent is attenuated by the greater distance represented by such gap. However, a non-constricted gravity low may also be a product of the current sparse gravity station coverage which may merge the low wavelengths into a continuous signal. A low density body (2.35 Mg/m^3) was modeled separately for the Irazú-Turrialba volcanic complex; this separation concerns the basic geometry but maintains a constant density (Figs 2.7 and 2.8).

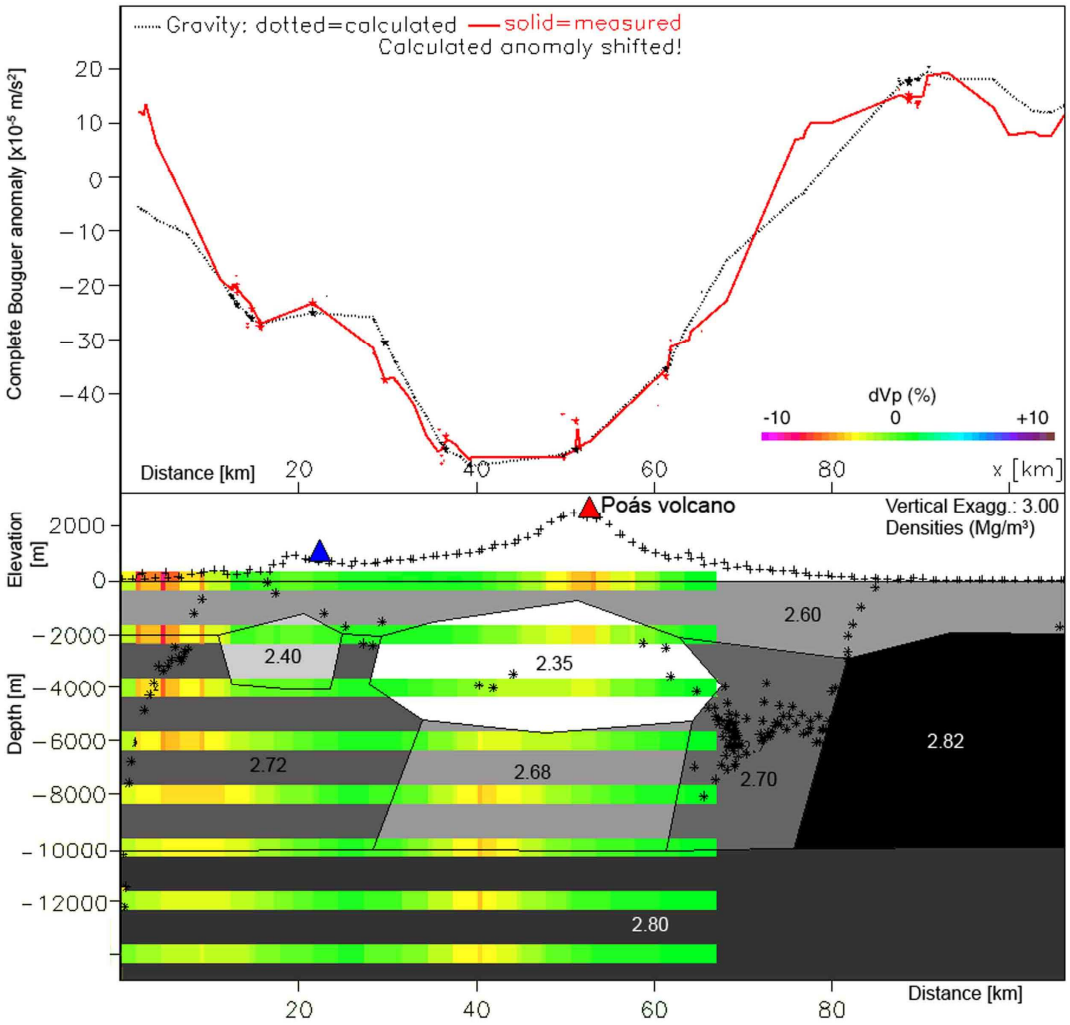

Figure 2.7. 3D density model cross section across the Poás volcano and surrounding regions. Red and black curves in the upper box show the measured and calculated gravity anomalies respectively. Black plus-signs indicate topography derived from SRTM 3 arc sec grid which is projected on the cross section, black stars in the lower box show Euler source points. Grayscale polygons represent modeled crustal bodies with corresponding densities. Colored pixels and bars show percentage of change in V_p velocities which were calculated by Arroyo (2008). Red triangle indicates the location of the main Quaternary volcanic vent, blue triangle indicates the locations of inferred paleo-volcanic vent.

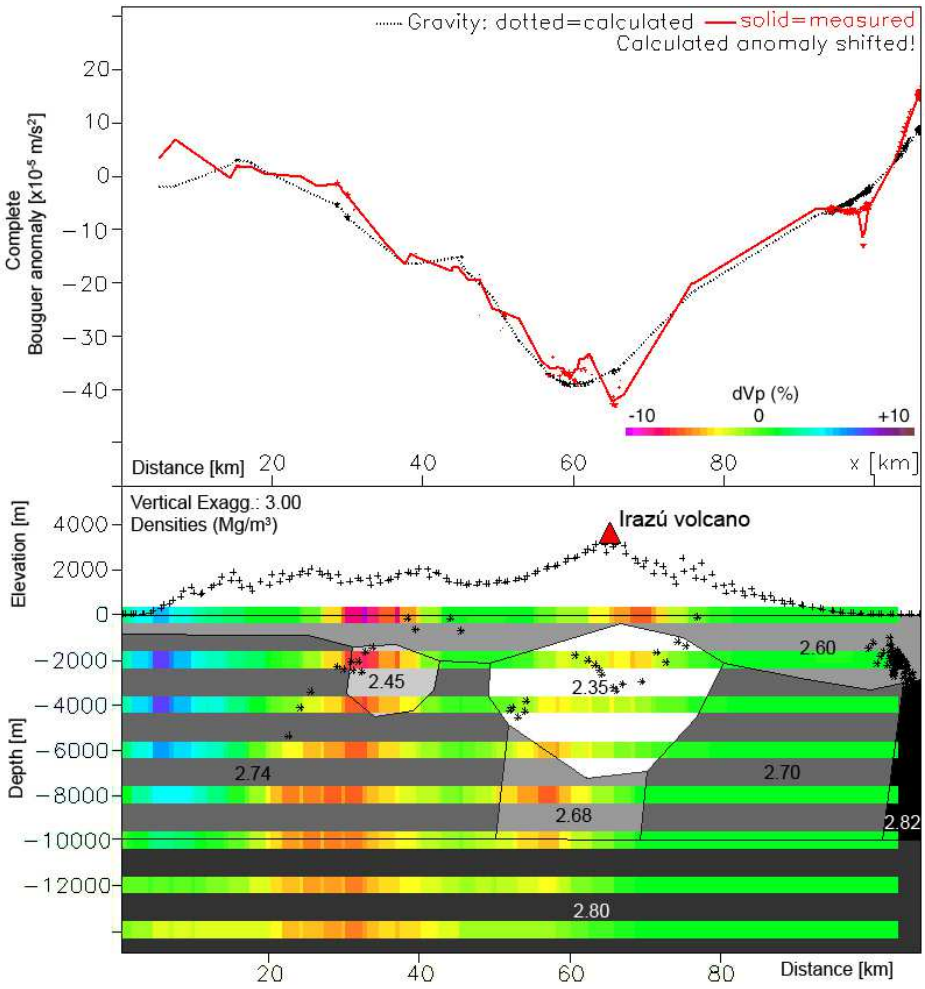

Figure 2.8. 3D density model cross section across the Irazú volcano and surrounding regions. Red and black curves in the upper box show the measured and calculated gravity anomalies respectively. Black plus-signs indicate topography derived from SRTM 3 arc sec grid which is projected on the cross section, black stars in the lower box show Euler source points. Grayscale polygons represent modeled crustal bodies with corresponding densities. Colored pixels and bars show percentage of change in V_p velocities which were calculated by Arroyo (2008). Red triangle indicates the location of the main Quaternary volcanic vent.

A joint low density body (2.35 Mg/m^3) was modeled for the upper crust beneath the Barva and Poás volcanoes (Fig. 2.8 and 2.9). As for the underground structures of the Platanar-Porvenir volcanic complex, a slightly higher density of 2.38 Mg/m^3 was calculated through inversion for the given geometry and assigned to the heterogeneous body resulting on a better fit between measured and calculated gravity. This is in accordance with the lower volume and lack of historical activity of the volcanic complex relative to the others, which may indicate a lower flux of magma and volatiles to the vent. Beneath the main heterogeneous low density bodies (2.35 Mg/m^3), a trenchward dipping low density (2.68 Mg/m^3) zone was modeled based on the orientation of low velocity zones observed on the

seismic tomography results. This zone is interpreted as a zone of passage of fluids and melts from the lower to the uppermost crustal domains.

As for the near fore-arc, local earthquake seismic tomography data (Arroyo, 2008) show low velocity zones beneath the paleo-arc. The location of these zones also shows a relative gravity low trending NW-SE which itself coincides with the surface geology units corresponding to the Neogene Aguacate volcanic arc. Constrained also by Euler deconvolution source points obtained for this work as well as the inferred location of paleo-volcanic vents (Alvarado, 2000), low density bodies (2.40 - 2.45 Mg/m^3) were modeled for the Neogene volcanic arc to account for the effects of paleo-magmatic processes on the upper crust. The lower densities may be the result of pervasive hydrothermal alteration which can be recognized from surface geology. Also, the presence of granitic intrusions (Denyer and Alvarado, 2007) which crop out in limited extent along the paleo-arc may contribute to this signal. A limited extent crustal body with a density of 2.80 Mg/m^3 was modeled at the location of the Cedral mountains to account for the presence of an outcropping dioritic stock.

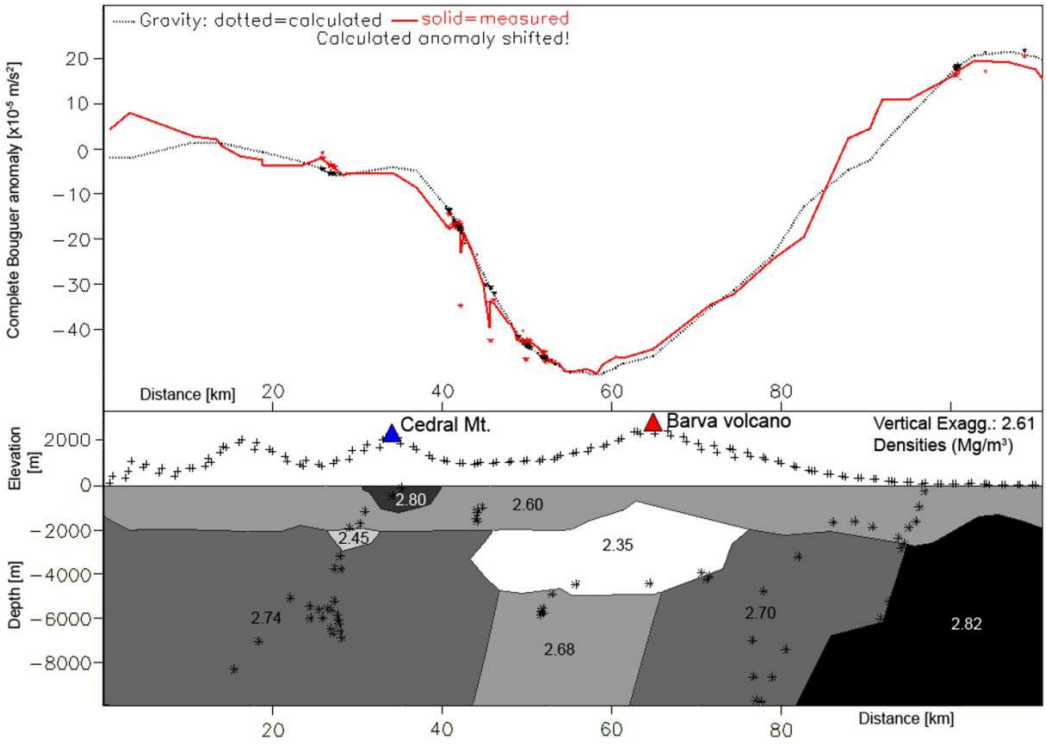

Figure 2.9. 3D density model cross section across the Barva volcano and surrounding regions. Red and black curves in the upper box show the measured and calculated gravity anomalies respectively. Black plus-signs indicate topography derived from SRTM 3 arc sec grid which is projected on the cross section, black stars in the lower box show Euler source points. Grayscale polygons represent modeled crustal bodies with corresponding densities. Red triangle indicates the location of the main Quaternary volcanic vent, blue triangle indicates the location of the Cedral inferred paleo-volcanic vent.

2.4.3 Back-arc structure

Towards the back-arc, a less constrained body with a density of 2.82 Mg/m^3 (Figs 2.7, 2.8 and 2.9) was modeled as a basement high located beneath the Caribbean plains. It's structure follows the trend of a Bouguer gravity high in the back-arc and represents a shallow mafic basement in accordance with outcroppings of serpentinized peridotite near the Costa Rica-Nicaragua border (Tournon *et al.*, 1995). The presence of such material in the back-arc at depths of less than 2 km corresponds with borehole stratigraphy logs (Pizarro, 1993). The basement high marks the boundary between the San Carlos sedimentary basin related to the Nicaragua graben, and the Northern Limón sedimentary basin towards the Caribbean passive margin. The sedimentary fill of the San Carlos basin was modeled as thickening of the uppermost layer (2.6 Mg/m^3).

2.5 Conclusions

A total of 22 cross sections were designed to construct a constrained 3D density model for the upper crust in the central region of Costa Rica. Power spectrum analysis of the gravity field results in a maximum depth of approximately 11 km for sources of the local along-arc gravity anomaly modeled thus suggesting a shallow depth for the main heterogeneities beneath the Quaternary volcanic arc. Such heterogeneities were modeled by low density (2.35 - 2.38 Mg/m^3) zones which are interpreted as the effects of arc magmatism derived from the subduction of the Cocos plate beneath the Caribbean plate. The geometry of these bodies was constrained by seismic tomography data and Euler deconvolution source points. Along the Cordillera Volcánica Central, the low of the Bouguer anomaly is segmented towards the SE where shorter wavelengths are observed suggesting a change in the geometry of the low density bodies. To account for this feature, separate low density bodies were modeled for the Irazú-Turrilaba volcanic complex and the Barva and Poás volcanoes. However, these features consist of a unique 2.35 Mg/m^3 density. Towards the NW a slightly higher (2.38 Mg/m^3) density was modeled beneath the Platanar-Porvenir volcanic complex.

Low velocity zones from local earthquake seismic tomography results from the work of Arroyo (2008), and quantitative interpretation of the gravity field with Euler deconvolution source points suggest the presence of shallow heterogeneous low density bodies beneath the Neogene “Aguacate” volcanic arc. These bodies were modeled with densities of 2.45 Mg/m^3 for segments of the paleo-arc which have a predominantly tholeiitic composition. A density of 2.40 Mg/m^3 was modeled for the segments of mainly calk-alkaline composition and with greater presence of pyroclastic rocks.

Along the back-arc, a 2.82 Mg/m^3 body was modeled and interpreted as a basement high. This density accounts for the presence of a shallow mafic basement which consists of

serpentinized peridotite which crops out in northeastern Costa Rica and is present in borehole logs at a shallow depth of approximately 2 km towards the back-arc.

3 The seismically active Andean and Central American margins: Can satellite gravity map lithospheric structures?

The spatial resolution and quality of geopotential models (EGM2008, EIGEN-5C, ITG-GRACE03s, and GOCO-01s) have been assessed as applied to lithospheric structure of the Andean and Central American subduction zones. For the validation, we compared the geopotential models with existing terrestrial gravity data and density models as constrained by seismic and geological data. The quality and resolution of the downward continued geopotential models in the Andes and Central America decrease with increasing topography and depend on the availability of terrestrial gravity data. High resolution of downward continued gravity data has been obtained over the Southern Andes where elevations are lower than 3000 m and sufficient terrestrial gravity data are available. The resolution decreases with an increase in elevation over the north Chilean Andes and Central America. The low resolution in Central America is mainly attributed to limited surface gravity data coverage of the region. To determine the minimum spatial dimension of a causative body that could be resolved using gravity gradient data, a synthetic gravity gradient response of a spherical anomalous mass has been computed at GOCE orbit height (254.9 km). It is shown that the minimum diameter of such a structure with density contrast of 240 kg m^{-3} should be at least ~ 45 km to generate signal detectable at orbit height. The batholithic structure in Northern Chile, which is assumed to be associated with plate coupling and asperity generation, is about 60-120 km wide and could be traceable in GOCE data. Short wavelength anomalous structures are more pronounced in the components of the gravity gradient tensor and invariants than in the gravity field. As the ultimate objective of this study is to understand the state of stress along plate interface, the geometry of the density model, as constrained by combined gravity models and seismic data, has been used to develop dynamic model of the

Andean margin. The results show that the stress regime in the fore-arc (high and low) tends to follow the trend of the earthquake distributions.

3.1 Introduction

Novel satellite gravity missions aim at a breakthrough in recovering signals associated with mass transport, mass distribution and the underlying dynamic processes on the Earth's surface, the lithosphere and upper mantle. The missions significantly improved the coverage and availability of gravity data. In the year 2000, CHAMP started to measure the global gravity field with a spatial resolution of about 550 km for Eigen-2, (Reigber *et al.*, 2005). The following GRACE mission measured gravity with an increased spatial resolution of approximately 140 km of ITG-GRACE03s (Mayer-Guerr, 2007). In 2009, the GOCE mission has begun measuring the gradients of the gravity field. Compared to scalar measurements, gradiometry offers better signal to noise ratio, de-emphasizes regional trends (Holstein *et al.*, 2007) and provides enhanced sensitivity of geological structures (Fedi *et al.*, 2005; Pedersen and Rasmussen, 1990). Thus, the direct use of gradients is a new scope for geophysical modeling. However, it has to be determined whether the resolution of downward continued GOCE gradient data is sufficient for direct application to lithospheric studies. One recent high-resolution gravity model of GOCE is GOCO-01s which is a combined model of GRACE solutions for lower degrees and GOCE data for higher degrees (Pail *et al.*, 2010). Higher resolution is provided by combined models of terrestrial and satellite data. The EIGEN-5C (Förste *et al.*, 2008) and the EGM2008 (Pavlis *et al.*, 2008) provide gravity data with spatial resolution of 56 km and 10 km, respectively.

In this paper, we investigate the resolution and quality of various geopotential models as applied to lithospheric structures and mapping of regions of high seismic moment release (asperities) using the active plate boundaries of Central America and Southern Central Chile as case studies. The origin and role of asperities in earthquake recurrence in these regions are

much debated (Wells *et al.*, 2003). Many source time functions of large earthquakes show distinct onsets of sub-events and episodes of moment release, which signify co-seismic failure of asperities. As causes for these sub-events, varying physical properties such as geometrical and/or material heterogeneities and dynamically generated complexities are suggested (Aochi *et al.*, 2003; Madariaga and Cochard, 1996; Marsan, 2006). Inhomogeneities on the subducting plate (e.g. seamounts, ridges, transform faults) could lead to stronger coupling (Barckhausen *et al.*, 1998; Cloos, 1992; DeShon *et al.*, 2003; Kirby *et al.*, 1996). Deep-sea terraces and sedimentary basins along convergent margins are other proposed indicators of asperities (Fuller *et al.*, 2006; Song and Simons, 2003; Wells *et al.*, 2003).

In regions of high seismic moment release, trench-parallel gravity anomalies positively correlate with topography. Thus, the spatial gravity variations over the fore-arc could serve as proxy for the long-term state of stress on the plate interface (Song and Simons, 2003). Furthermore, Wells *et al*. (2003) showed that epicenters of major earthquakes often tend to concentrate on the pronounced gravity gradients from the fore-arc basins towards gravity highs. Recent studies in the South-Central Chile suggest that pressure exerted by batholitic structure and buoyancy force acting on the Nazca plate could be one of the possible mechanisms of asperity generation (Sobiesiak *et al.*, 2007). An analysis of the 1995 Antofagasta earthquake showed that high b-values correlate with isostatic residual gravity anomalies of the region (Sobiesiak *et al.*, 2007). The isostatic residual anomalies are caused by batholitic bodies of the Jurassic to early Cretaceous magmatic arc system and help to lock the interface of the seismogenic zone. This is also indicated in the local tomography as high P-wave velocity (Husen, 1999). Tassara (2010) expanded this hypothesis for the entire Chilean-Pacific margin and suggested that hazardous earthquakes predominantly occur in

regions of positive vertical stress anomalies associated with positive density anomalies of the crust in the fore-arc region.

The scope of this work is to test the resolution of satellite-only and combined models as applied to lithospheric structure, tectonic processes and dynamic evolution of convergent plate boundaries. In order to test the resolution and unravel the 3D structure as well as the dynamic evolution of the two convergent plate margins, three steps have been followed: (1) all terrestrial gravity data from the region of interest have been combined into a single database; (2) satellite-derived gravity data have been used to fill in regions lacking terrestrial gravity coverage; and (3) the combined gravity database has been used to develop 3D lithospheric structures of the two convergent plate margins. Then, the geometry and physical parameters obtained from the well-constrained 3D density models have been used to refine the dynamic models of the Andean margin. The satellite gravity data have been obtained from the ICGEM portal of the GFZ Potsdam (http://icgem.gfz-potsdam.de/ICGEM/).

3.2 Tectonic setting

The Andes mountain belt is the result of subduction of the Nazca beneath South America plate. The dynamics of subduction are mainly controlled by the convergence rate and age of the subducting plate. Several studies indicate the differences in tectonic style between the Central and Southern Andes (Allmendinger *et al.*, 1997; Ramos and Aleman, 2000). The Central Andes can be divided from west to east into the fore-arc, magmatic arc and backarc (Reutter and Götze, 1994). The fore-arc comprises the Coastal Cordillera, the Longitudinal Valley, the Precordillera and the Preandean depression (Fig. 3.1). Since the Jurassic, the magmatic arc front has migrated more than 200 km to the east (Scheuber *et al.*, 1994), with the Jurassic arc now present along the Coastal Cordillera and on the slope of the fore-arc (about 50 to 150 km east of the trench). Repeated micro-gravity and GPS measurements reveal the on-going deformation and relaxation processes after the 1960

Valdivia earthquake (Klotz *et al.*, 2001). The main causes for these tectonic differences are changes in slab dip, age and convergence obliquity (Gutscher *et al.*, 2000). Young and buoyant slabs produce shallow dips and strong seismic coupling. Convergence was always oblique, with obliquity changing with time and latitude. Convergence velocity also fluctuated considerably and has been decreasing throughout the Neogene (Norabuena *et al.*, 1999). However, it was always amongst the faster convergence rates observed on Earth.

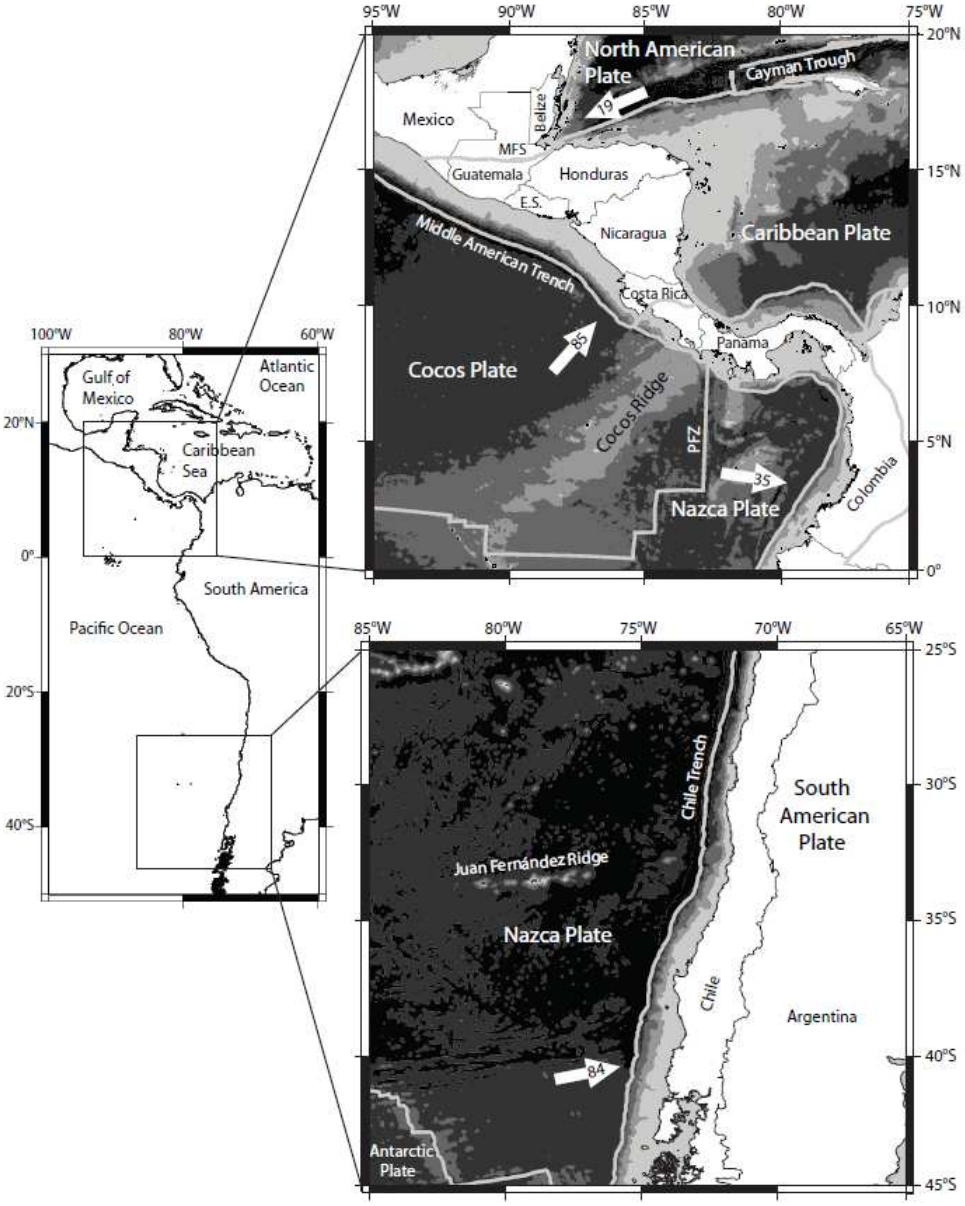

Figure 3.1. Geologic setting of Central (top) and South (bottom) America. The white arrows show the plate movement per year in mm. Grey lines offshore indicate plate boundaries. Dark colors indicate deep, light colors shallow seafloor.

In this paper, we will focus on the structures and processes affecting the fore-arc region. For comparison, we will use the gravity field and results of the density modeling from Central America. Therefore, we provide a brief introduction to the geology of the region. For more detail, refer to Lücke *et al.* (2010). The outstanding tectonic feature is the subduction of the oceanic Cocos plate beneath the Caribbean plate along the Middle American Trench. Throughout Central America, the volcanic front is segmented along the isthmus presenting gaps in Quaternary volcanism as well as changes in distance from the Middle American Trench. Such changes have been attributed to both the state of stress in the overriding plate and the disposition of the subduction zone leading to changes in depth to the slab (Bolge *et al.*, 2009). The heterogeneity of the structure of the oceanic Cocos plate due to the influence of the Galapagos hot-spot (Sallarès *et al.*, 2003) leads to inconsistencies upon the arrival of bathymetric features to the subduction zone and may cause seismogenic asperities and uplift (Barckhausen *et al.*, 1998; Meschede *et al.*, 1998). Furthermore, the subduction of seamounts on the oceanic Cocos plate acts as an agent of upper plate erosion (Ranero and von Huene, 2000). At the western end of the Middle American Trench, the plate boundary between the Cocos and Nazca plates is marked by the seismically active Panama Fracture Zone. Subduction of the Nazca plate along the southern Panama segment is now considered to be inactive showing instead evidence of left lateral shearing between the Nazca and Caribbean plates (Lonsdale, 2005).

3.3 Gravity database and geophysical constraints

Onshore gravity data collected under the framework of the Collaborative Research Centre 267 (Oncken *et al.*, 2006) have been homogenized to compile Bouguer anomaly map of the Central Andes. The database comprises data acquired over the past 30 years in Argentina, Chile and Bolivia (20° S to 29° S and 74° W to 64° W). Approximately 2000 gravity stations covering the region in Argentina between the Andes and the Atlantic coast

were measured along the southern traverse in 2000 (36° S and 42° S and 71° W and 62° W) and along the northern traverse between 1982 and 1990 (Alasonati-Tašárová, 2007; Götze *et al.*, 1994; Hackney *et al.*, 2006; Schmidt and Götze, 2006). Additional data have been obtained from industry (ENAP; Chile and Repsol-YPF; Argentina), the Universidad de Chile and the United States National Imagery and Mapping Agency. All measurements are tied to the IGSN71 gravity datum. Bouguer anomalies were computed using the normal gravity formula of 1967 and a spherical Bouguer cap correction (cap radius 167 km, density 2670 kg m^{-3}). Terrain corrections on land were computed using triangular facets to approximate topography up to a distance of 167 km from stations. The corrections were applied using the 1×1 km GLOBE (onshore) and ETOPO5 (offshore) digital elevation models. Offshore gravity and seismic data are obtained from shipborne measurements of the SPOC (Subduction Processes Off Chile) project (Reichert and Schreckenberger, 2002). The former are merged with the KMS-2001 global free-air gravity anomaly database (Andersen and Knudsen, 1998).

A series of 3-dimensional density models showing mass distribution at different scales in the western continental margin of South America have previously been developed (Alasonati-Tašárová, 2007; Kirchner *et al.*, 1996; Prezzi *et al.*, 2009; Tassara *et al.*, 2006). Tassara *et al*. (2006) presented a sub-global density model (410 km depth) encompassing the Pacific Ocean (85° W) and the Andean margin between the northern Peru (5° S) and Patagonia (45° S). At a regional scale, 3D density models of the Central (between 36°S – 43°S) and South Central Andes have been developed by Kirchner *et al*. (1996), Alasonati-Tašárová (2007) and Prezzi *et al*. (2009). All models traverse the Andes and provide complete picture of lithospheric density distributions. Modeling was done using the 3D gravity modeling package IGMAS (Götze and Lahmeyer, 1988; Schmidt *et al.*, 2010). Model constraints were taken from active and passive seismic campaigns conducted under the

framework of the Collaborative Research Centers 267 (Giese *et al.*, 1999; Oncken *et al.*, 2006; Sick, 2006) and 574 (Brasse *et al.*, 2009; Ranero *et al.*, 2003). Moreover, results of the previous seismic experiments from: PISCO Proyecto de Investigación Sismológica de la Cordillera Occidental (Lessel, 1997; Schmitz *et al.*, 1999), ANCORP Andean Continental Research Program (ANCORPWorkingGroup, 2003; Buske *et al.*, 2002) and ISSA Integrated Seismological experiment in the Southern Andes (Bohm *et al.*, 2002; Lüth *et al.*, 2003) have been used to constrain major structures such as Moho, upper slab surface, lithosphere-asthenosphere boundary and intra-crustal inhomogeneities.

For Central America, a similar database was compiled and homogenized. Offshore databases consisting of ship borne gravity and seismic data acquired within the activities of the Collaborative Research Centre 574 have been used to cover mainly the area along the Middle American trench and the Pacific continental shelf. Seismic reflection, refraction and tomography data sets provided constraints for the modeling (Arroyo *et al.*, 2009; Husen *et al.*, 2003a; Sallarès *et al.*, 2001; Sallarès *et al.*, 2003). The onshore gravity database was also compiled by SFB574 members and consists of data from various government and academic institutions. Bouguer and terrain corrections were carried out following similar processing procedures as for the Andean gravity dataset.

3.4 Results and discussion

3.4.1 Geophysical and Geodetic Bouguer anomaly

The definition of Bouguer anomalies is different in Geophysics and Geodesy. In order to avoid confusion, the differences between “gravity anomalies” and “gravity disturbances” will be explained. Detailed discussions about this issue can be found in the work of Li and Götze (2001) and Hackney and Featherstone (2003). In general, for geophysical interpretation and modeling, “geophysical Bouguer anomalies” will be used. Here, the measured gravity is corrected for the normal gravity formula at station elevation as well as for the Bouguer slab and the topographic variations. The measured gravity value is still interpreted at its original height (Fig. 3.2). In terms of geodesy, gravity values that are corrected for the normal gravity but still defined at station elevation are called disturbances. The Bouguer anomaly provided by the ICGEM is defined as the gravity calculated at the geoid and corrected for both the normal gravity at the ellipsoid and a plain Bouguer slab (called “classic anomaly” according to ICGEM terms; Fig. 3.2; Barthelmes, (2009). In the discussions to follow, we will continue to call this the "geodetic Bouguer anomaly". Downward continuation of the geodetic Bouguer anomaly to the geoid is only valid when it is assumed that all singularities of the gravity field lie below the geoid. This is not the case in regions of high topography. Furthermore, density anomalies located between the geoid and the top of the topography are of interest for geophysical interpretation. Hence, differences between geophysical and geodetic Bouguer anomalies can be high. Moreover, the use of disturbances (geophysical anomalies) is consistent with reduction techniques of existing geophysical terrestrial datasets. Thus, the geophysical Bouguer anomaly should be used in regions of high topography.

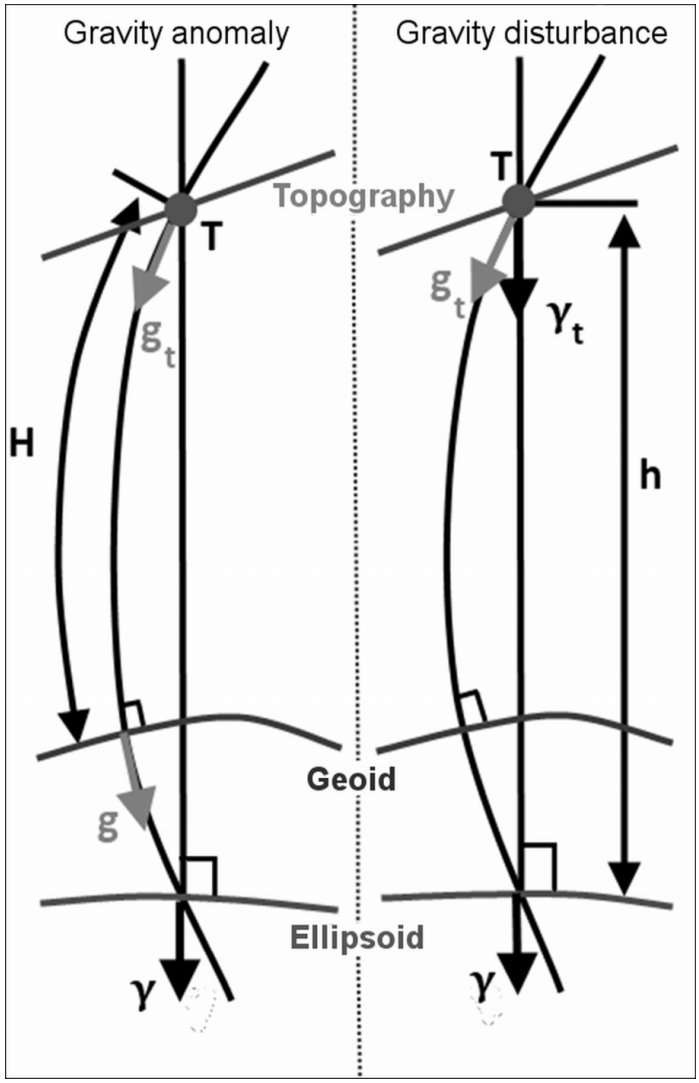

Figure 3.2. After Köther *et al.*(2011). Gravity anomaly and gravity disturbance. The gravity anomaly (left) is downward continued from the observation point T to the geoid (g_t to g) and then reduced by the normal gravity from the ellipsoid (γ). Downward continuation is an unstable procedure over mountainous regions. Gravity disturbance (right) can be determined at any level (g_t) and is reduced by the upward continued normal gravity value (γ_t). This procedure is stable.

3.4.2 Data quality of the EGM2008

The EGM2008 consists of GRACE satellite data up to a spatial resolution of approximately 140 km. Data from 140 km spatial resolution up to 10 km are derived from other sources such as terrestrial, satellite altimetry and "fill-in" data (Pavlis *et al.*, 2008). Regarding the additional onshore data, several inconsistencies appear because its availability and distribution is not homogeneous. Moreover, in areas void of any terrestrial gravity data, ''fill-in'' data were used. These datasets were synthesized from GRACE data and augmented

with data from the EGM96 and gravity derived from topography by means of residual terrain model (RTM) (Pavlis *et al.*, 2007). At locations, where confidential terrestrial gravity datasets are available, the data were used up to the maximum resolution permitted by the restrictions and then augmented with RTM anomalies. This approximated gravity solution lacks high frequency anomalies (> degree 1650) (Pavlis *et al.*, 2007). For the present study, we used terrestrial datasets collected by Schmidt and Götze (2006). It is expected that these data are included in the EGM2008. Thus, the EGM2008 should correlate well with the surface data at its maximum spatial resolution. If the data do not coincide, errors or inconsistencies in the EGM2008 may be assumed.

In the Andes, two onshore areas with different topography were investigated: The North Chilean part is located between 74° W – 67° W/19° S – 30° S. Elevation in this region reaches up to 5800 m above sea level. The southern part (between 73° W – 60° W and 36° S-43° S) has elevations up to 3000 m. In Central America, the study area is located between 86.5° W – 82° W/8° N – 11.5° N with elevations up to 3800 m. The number of onshore gravity stations used for the Northern Chile, Southern Chile and Central America are 8373, 14210 and 13387, respectively.

Table 1 shows the correlation between the EGM2008 anomalies (geodetic and geophysical) and terrestrial gravity data for the Andes and Central America. In general, the EGM2008 shows high correlation (> 95%) in the Andes. However, low correlation has been obtained over the regions with rough topography, where deviations of about 40 % are observed (e.g. 128 x 10^{-5} m s^{-2}). The data correlation in Central America is even lower (about 68 % deviations for the geodetic anomaly and ~ 86 % for the geophysical anomaly). This is mainly attributed to sparse terrestrial gravity data coverage.

Table 3.1. Correlation of the EGM2008 with terrestrial data. The maximum deviations of each model are shown. The correlation values in brackets are for the Andes west of 69°W. Thus, only stations located around

mountainous areas and the coastal line are considered. In Costa Rica, the brackets show the correlation of stations located above 1000 m of altitude.

	North Andes (19° S-30° S) onshore		South Andes (36° S-43° S) onshore		Central America onshore	
	Geophysical BA	Geodetic BA	Geophysical BA	Geodetic BA	Geophysical BA	Geodetic BA
Correlation between EGM2008 and terrestrial data (%)	99.48 (98.29)	98.91 (95.63)	96.51 (93.26)	97.48 (94.32)	85.8 (49.37)	68.2 (40.66)

Figure 3.3 shows the gravity maps of Central America and the Southern Andes in which the geodetic and geophysical Bouguer anomalies are compared with terrestrial data. The histograms in Fig. 3.4 show the deviation of the geodetic (checked) and geophysical (hatched) anomaly compared to the terrestrial data in the Andes. The deviation of the geodetic anomaly compared to the geophysical anomaly is larger (~0.6%) in the northern part where topography is higher. In the southern part, the geodetic anomaly is slightly better (~1%) than the geophysical anomaly. However, both datasets show significant deviations from the terrestrial data with values higher than 20 x 10^{-5} m s^{-2}.

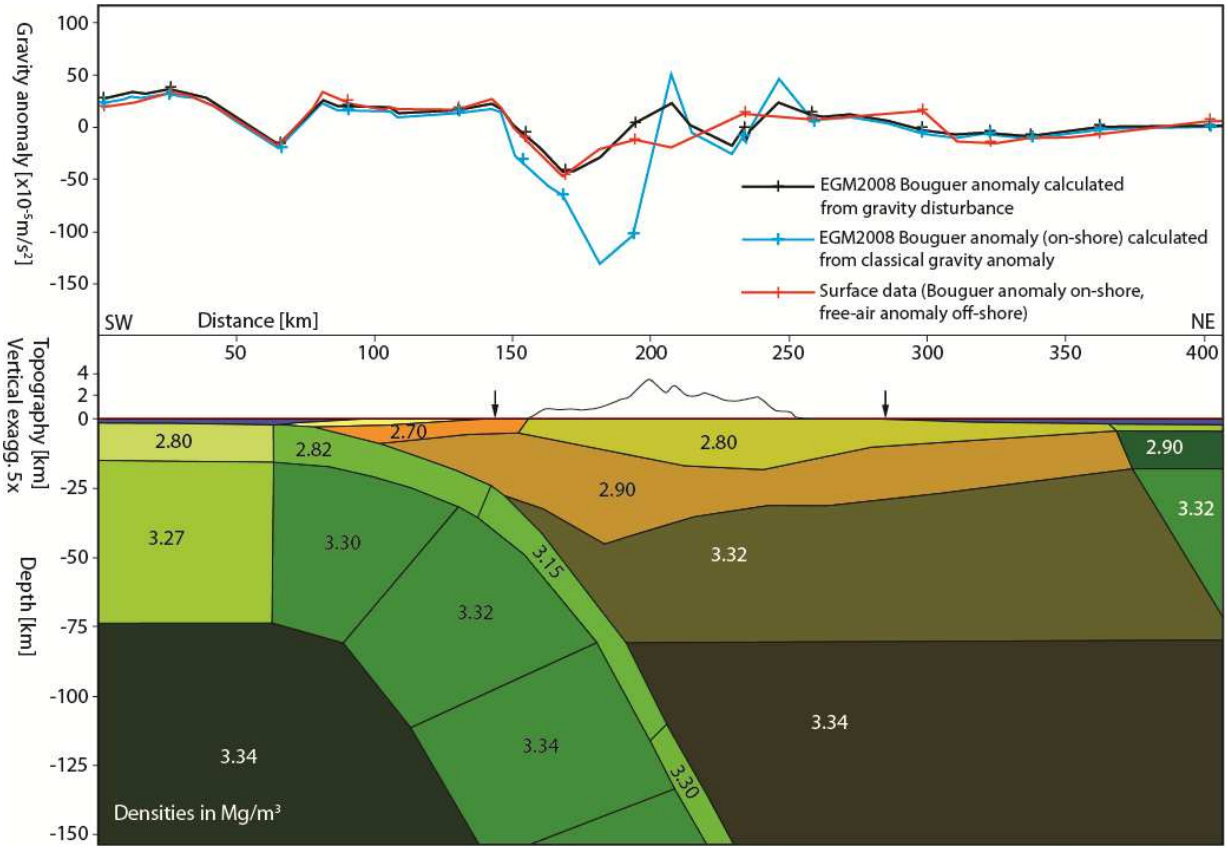

Figure 3.3. Vertical cross-section of a 3D density model from Central America. Different gravity anomalies are shown in the upper panel. The dotted line (with boxes) is derived from surface gravity data and shows the geophysical Bouguer anomaly on-shore and free-air anomaly off-shore (shoreline indicated by arrows). The dashed line (with triangles) shows the geodetic Bouguer anomaly on- and off-shore calculated from the classical gravity anomaly using EGM2008 model (off-shore without Bouguer reduction). The black line (with crosses) shows the geophysical Bouguer anomaly. Offshore, all datasets correlate. Onshore, however, there is still correlation with surface data, but the geodetic Bouguer anomaly shows errors of about 80 x 10^5 m s^{-2} for this cross section. In this region, elevation reaches up to 3700 m. The errors emphasize the uncertainty of the combined gravity models and instability of the downward continuation method.

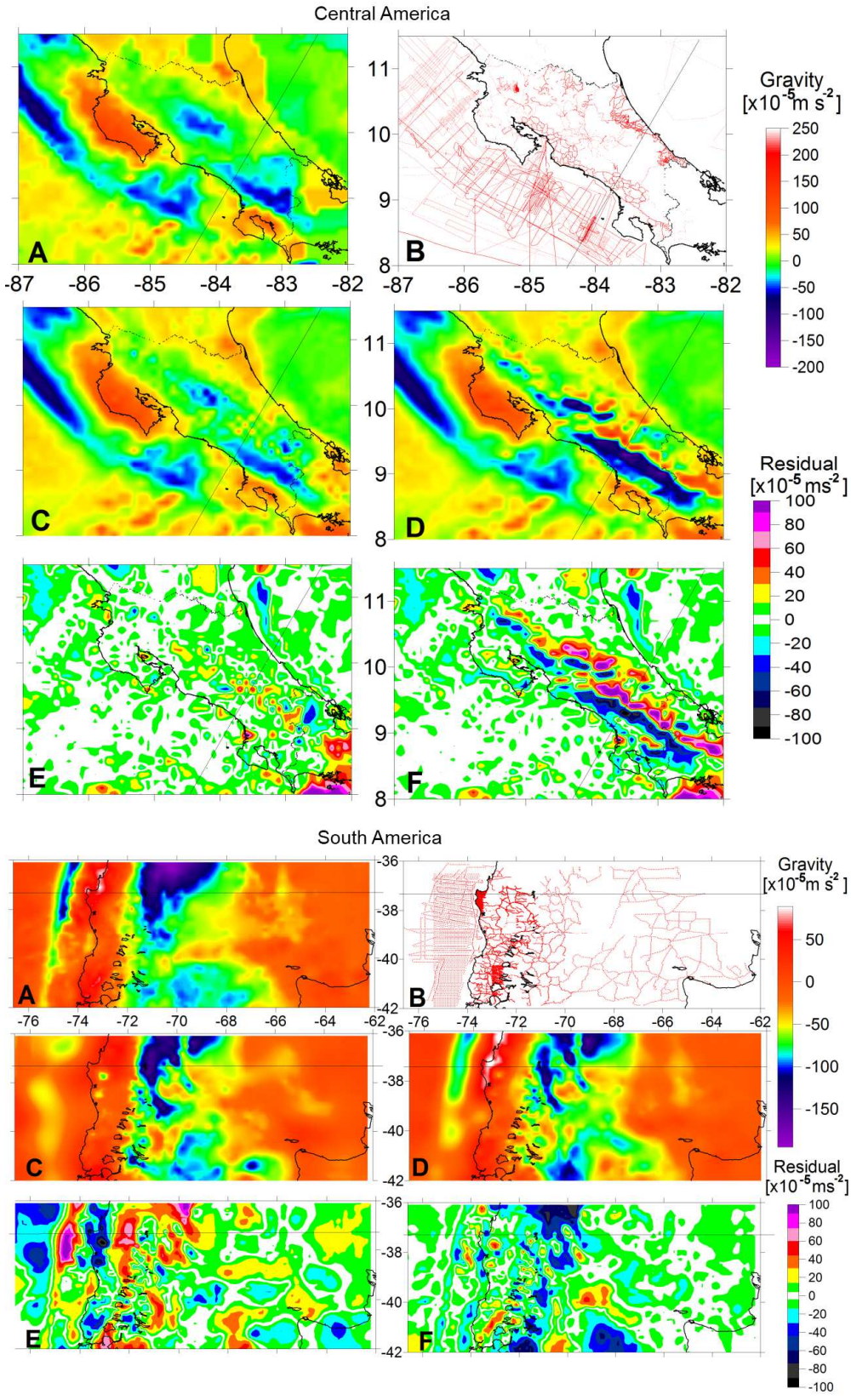

Figure 3.4. Comparison of the EGM2008 with surface gravity data from Costa Rica (top) and Chile (bottom, after Köther *et al.* (2011)). (a) Data from surface stations with Bouguer gravity anomaly on-shore and free-air gravity anomaly off-shore; (b) Location of surface stations; (c) Geophysical Bouguer anomaly (from EGM 2008); (d) Geodetic Bouguer anomaly (from EGM2008); (e) Residual map obtained by subtracting (a) from (c); (f) Residual map obtained by subtracting (a) from (d). Bold black lines show the coastline and borders. Straight line shows location of cross- section of the 3D density model shown in Figures 3.3 and 3.6.

For Central America, a three dimensional density model is being developed within the framework of the SPP1257. The density model is based on gravity data from the EGM2008 geopotential model. So far, results on well constrained areas such as Costa Rica have shown that the resolution of the gravity model (EGM2008) is appropriate for the modelling of regional lithospheric mass distribution and major tectonic structures such as the Middle American subduction zone, the continental and oceanic Moho as well as first order crustal discontinuities represented by the heterogeneities in the crustal basement and the upper crust.

Figure 3.5 shows a cross-section of the 3D density model through central Costa Rica in which different datasets are compared and put into the context of the modelled structures. In the offshore areas, a good correlation has been obtained between the EGM2008 satellite gravity model and surface data. The geophysical Bouguer anomaly (offshore) is located on the geoid (on the ocean surface). Thus, it coincides with the geodetic Bouguer anomaly. Onshore, the geophysical Bouguer anomaly shows better correlation to the surface data than the geodetic Bouguer anomaly. In the mountainous areas of Costa Rica, the geodetic Bouguer anomaly (dashed line) differs significantly from the surface data (dotted line) as well as from the geophysical Bouguer anomaly (black).

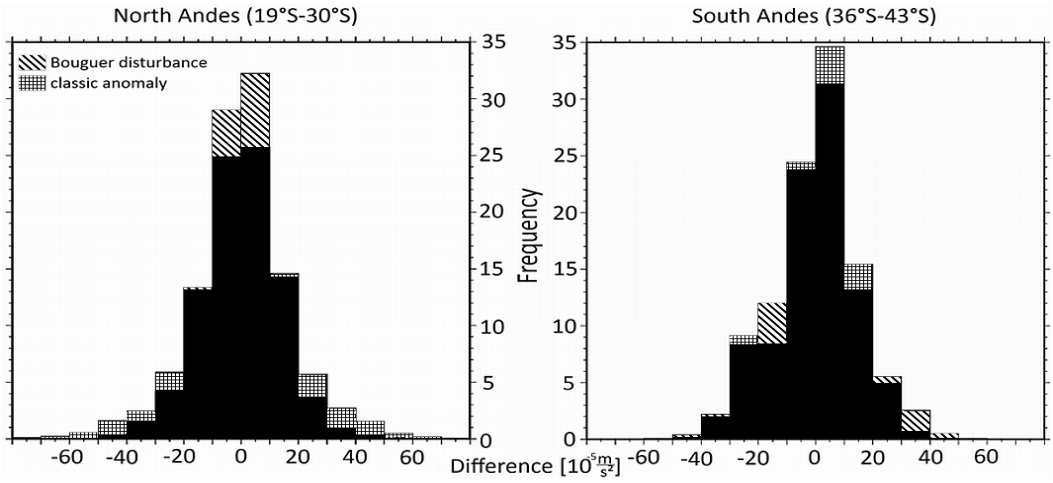

Figure 3.5. After Köther *et al.* (2011). The deviation of the geodetic Bouguer anomaly (checked) and geophysical Bouguer anomaly (hatched) from terrestrial data. The area, marked in black, indicate the overlapping of both datasets. In the northern Andes, the fit of the geophysical Bouguer anomaly is better. Most values are in the range of ±10 x10^{-5} m/s^2. In the southern part, the geodetic Bouguer anomaly fits much better to the terrestrial data. Thus, the resolution of the geophysical anomaly is better in areas of large topography. However, large deviations from original datasets make the EGM2008 less reliable in these regions.

The analysis of the present study shows that rugged topography downgrades the spatial resolution of the EGM2008 featuring large outliers in the Andes and Central America. Results in Central America show that high and unexpected deviations can be present in areas void of any terrestrial gravity data. Thus, the quoted spatial resolution of 10 km is not valid for all regions. Our case studies in these regions show that in areas of rugged topography, the geophysical anomaly often provides better results (up to 9% in mountainous regions; Table 3.1). Moreover, the use of geophysical anomalies in the calculation is consistent with the existing reduction techniques of terrestrial geophysical datasets.

3.4.3 Spatial resolution of different satellite gravity models

The main geophysical objective of using satellite-derived gravity data is the interpretation of lithospheric structures. We have used a well-constrained 3D density model of the South-Central Chile (Alasonati-Tašárová, 2007) to assess the spatial resolution of different satellite gravity models. The comparison emphasizes the areas of the models in which problems may occur when using different satellite gravity models (EGM2008, EIGEN-5C, ITG-GRACE03s, and GOCO-01s).

Figure 3.6 shows a section of the 3D density model from the Central Chile at 37.4° S. Also shown on the top panel are gravity fields derived from different satellite models, measured surface gravity data, and the calculated gravity field from the density model. The dashed black line illustrates the calculated gravity from the density model and the red line shows the measured surface data. The EGM2008 (black) and the EIGEN-5C (yellow) show overall good correlation with the calculated gravity field. In the area of high topography (e.g. at 100 km of the x-axis), the EGM2008 exhibits significant deviations. The EIGEN-5C is smoother and correlates better with the predicted field. However, a deviation of about 15 x 10^{-5} m s^{-2} is observed between 350 and 400 km. The same misfit is visible in the GRACE solution (dark blue). The GRACE-GOCE satellite model (light blue) provides a better fit to

the calculated gravity. Here again, deviations at 200 and 420 km are observed. However, the gravity low below the Andes at 300 km is better resolved by the GRACE-GOCE model. The gravity low of the deep-sea trench is well fitted by the combined models but the GRACE model does not comprise a distinct gravity low. Compared to other models, the deep-sea trench and the root of the Andes are more visible in the GRACE-GOCE model. The Coastal Cordillera is also shown as gravity high, but not well fitted in amplitude. The new GRACE-GOCE satellite model shows the best fit. The EIGEN-5C provides a good fit over the entire section. The deviation of the EGM2008 in regions of high topography is clearly visible in areas where no surface data is available. The higher degree models such as the EGM2008 and EIGEN-5C cannot provide a high spatial resolution.

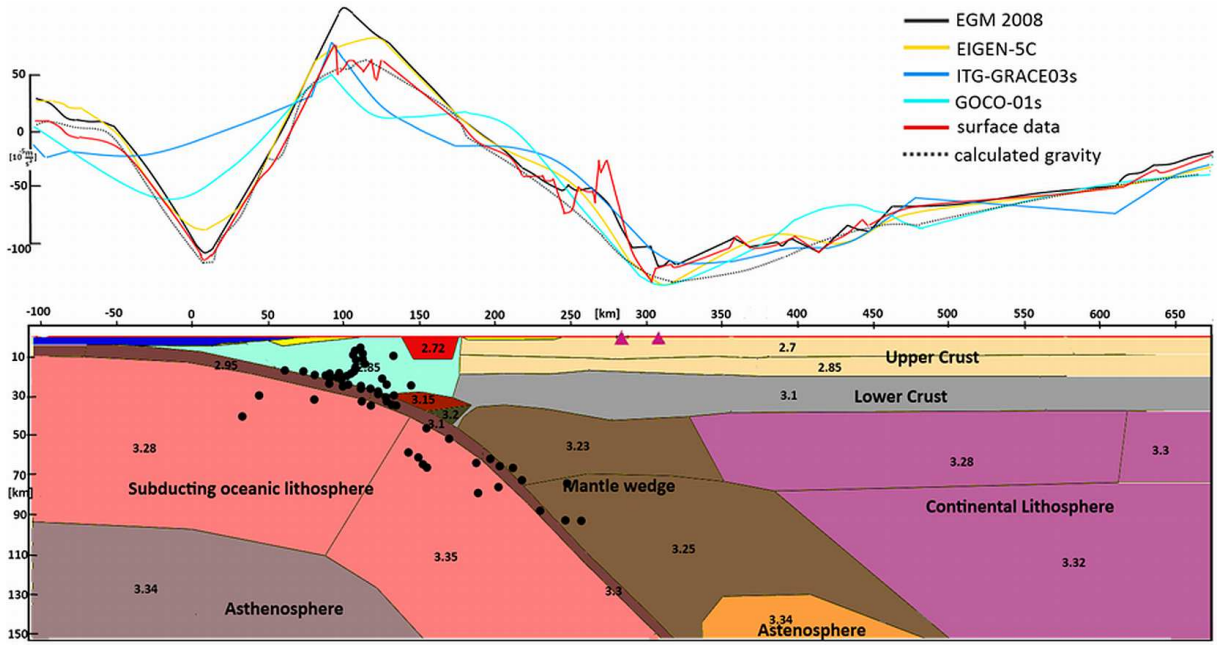

Figure 3.6. After Köther *et al.* (2011). Vertical cross-section of a 3D density model from Central Chile at 37.4°S (Alasonati-Tašárová, 2007). The model is constrained in part by geological and seismological information (e.g. seismicities are shown in black circles). The dashed line shows the calculated gravity from the model matched to the surface gravity data (red curve). The combined EIGEN and EGM2008 models fit well to the data. The EIGEN-5C (yellow) correlates well with the predicted gravity values, but it also shows some deviations. The ITG-GRACE03s model does not show sufficiently the gravity lows of the deep sea trench (at 10 km) and crustal root (at 300 km). The GOCO-01s (light blue) model shows the best correlation of all satellite only models.

Overall, the GRACE-GOCE model shows an increased spatial resolution relative to the GRACE derived field. Since large-scale density models do not resolve local features, the calculated gravity field is smooth and comparable with wavelengths obtained from satellite-only gravity models. Combined models with new GOCE data could be sufficient for compiling density models of regional scale in frontier regions. Although combined gravity models can be used for density modeling of relatively smaller features such as shallower crustal structures, satellite-only models are not appropriate for this purpose due to the low spatial resolution.

3.4.4 Asperity mapping and resolution of gravity gradient data

Delineation of potentially hazardous provinces using gradiometry is one of our objectives. In order to examine the applicability of GOCE gradients for asperity detection in a simple way, the minimum dimension of a spherical anomalous mass below the geoid producing gravity and gravity gradient amplitudes of the order of GOCE's accuracy at orbit height (254.9 km) has been calculated. The curves in Fig. 3.7 show the minimum diameter of such a mass of given density contrast required to produce signal differences of 1×10^{-5} m s^{-2} and 12×10^{-12} s^{-2} at orbit height. These values are close to the expected accuracies of the gravity and vertical gravity gradient of GOCE global data, respectively (Pail 2011, pers. comm.). As shown in Fig. 3.7, an anomalous structure with density contrast of 240 kg m^{-3} could be detected in a gravity data at orbit height, if its diameter is at least ~ 45 km. However, if the diameter of an anomalous structure increases by up to 100 %, its density contrast should not be less than 33 kg m^{-3} to be detected. If gradients are considered, even bodies of about half of that size could produce signal in the range of GOCE's gradient data sensitivity. The dimension of Jurassic arc batholiths in Northern Chile is about 60-120 km (Götze *et al.*, 1994; Götze and Krause, 2002; Husen, 1999; Sobiesiak *et al.*, 2007). This supports the idea

that batholithic structures, which are assumed to be related to asperity generation, can be detected using GOCE data.

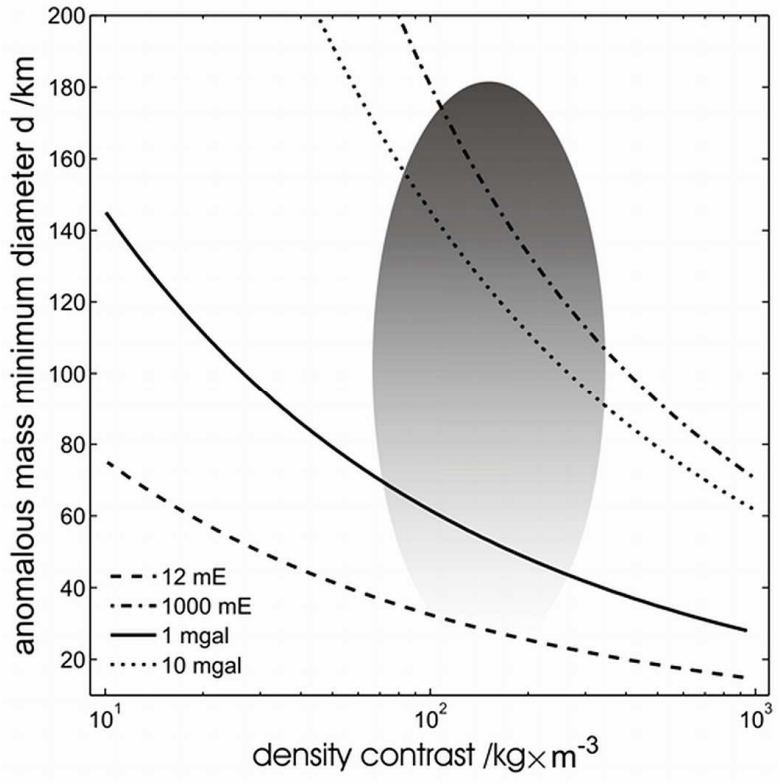

Figure 3.7. After Köther *et al*. (2011). Differential gravity and gradient signal caused by a minimum diameter of an anomalous spherical mass of given density contrast below geoid at an orbit height of 254.9 km. The signal is in the range of GOCE's resolution. The thick solid and dotted lines represent differential gravity signals of 1 x10^{-5} and 10 x10^{-5} m/s^2 at an altitude of 254.9 km, respectively. The thin dashed and dash-dotted lines represent gradients of 12 and 1000 mE, respectively. The grey shaded area shows the possible combination of parameters of a potentially asperity generating batholithic structure near subduction zones.

Furthermore, we set up a synthetic model of an arbitrary subduction zone for 3D-density forward modeling. The geometry and density parameters have been adapted from the models developed by Sobiesiak *et al*. (2007) and Alasonati-Tašárová (2007). In order to test the signal response of asperity generating structure at different station heights using forward modelling, a three dimensional anomalous structure (115 x 200 x 45 km) with physical properties resembling the Chilean batholiths has been included in the modelling. A density of 3 x 10^3 kg m^{-3} (density contrast of 0 to 300 kg m^{-3}) has been chosen for the batholith body in the model. At the height of 254.9 km, the magnitude of the gravity gradient anomaly ranges from few to some hundred mE (1 mE= 1 × 10^{-12} s^{-2}). Being the second spatial derivatives of

the gravity potential, gradients provide sharper images of anomalies and can be combined into coordinate independent invariants (Pedersen and Rasmussen, 1990). Invariants sharpen density contrasts and help to emphasize structural boundaries. Fig. 3.8 shows how well anomalous underground structures of interest can be detected using gravity gradients at orbit height. Different tensor components give valuable information for geo-scientific interpretation. The above analysis shows that gradient maps from GOCE data may help to delineate major geological structures like fault zones, rims of sedimentary basins and intrusions.

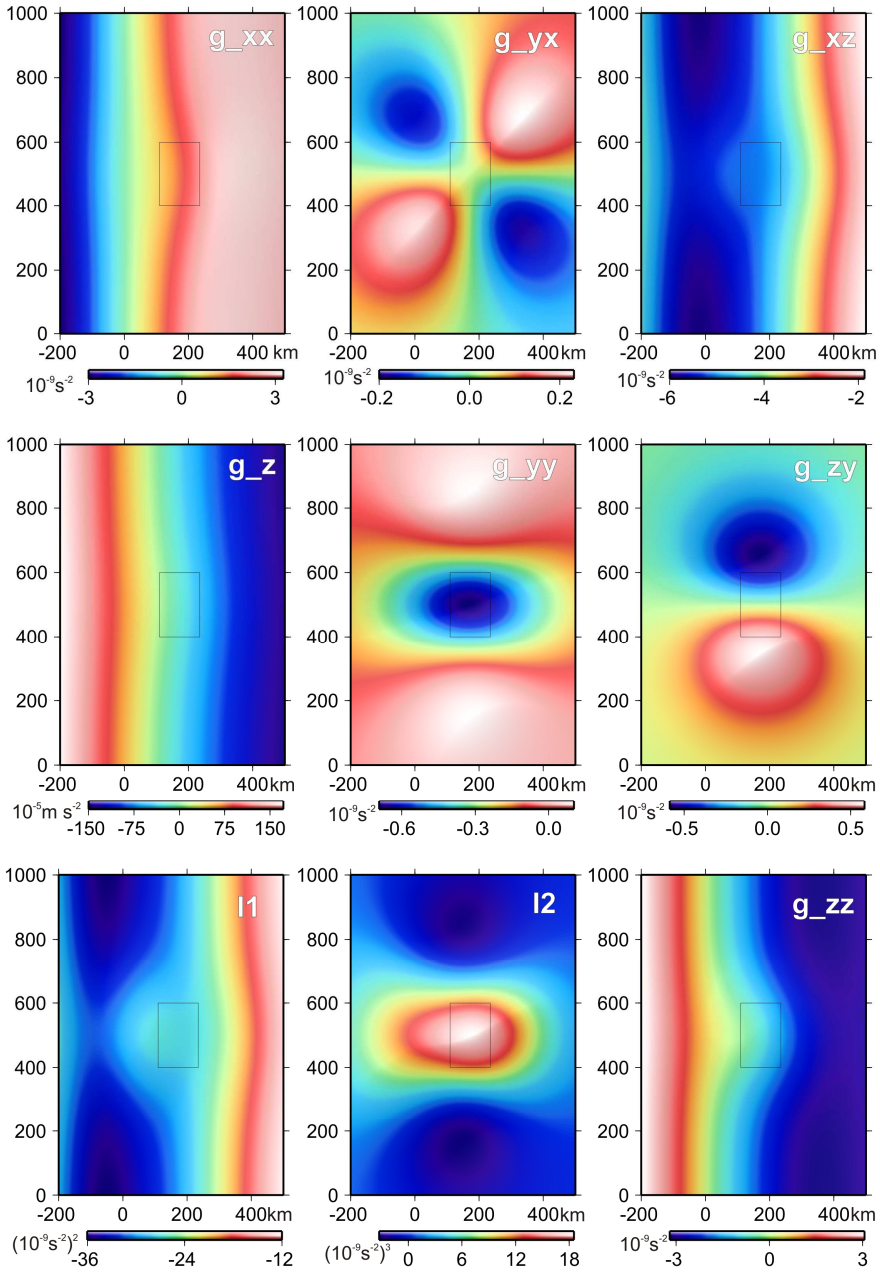

Figure 3.8. After Köther *et al.*(2011). Modeling of synthetic gravity gradient tensor and invariants (I1 and I2) of subduction zone using vertical gravity field as measured at 250 km height. A batholitic structure has been included on top of the down-going slab to test the resolution of gravity gradient signal. The gradient maps emphasize the location of the batholitic structure and the general geological strikes of the subduction zone.

3.4.5 Geodynamic model of the Andean margin as constrained by satellite gravity data

The present mass distribution is the result of long and complex geodynamic processes. Therefore, dynamic modeling is necessary to include the effects of time factor to the static density models. The dynamic evolution of the Andean margin has been extensively studied using numerical modeling. This includes studies of the dynamics of the plateau foreland (Babeyko *et al.*, 2006), the factors controlling the intensity of tectonic shortening (Sobolev *et al.*, 2006) and the influence of curvature of the convergent plate margin on the stress distributions (Boutelier and Oncken, 2010). These existing models are constrained by geophysical and geological data, but are based on generalized geometries. One of the objectives of this study is to develop a dynamic model of the Andean margin using realistic geometries from a well-constrained density model. In the present study, the geometries of the 3D dynamic model have been imported from the regional 3D density model of the Andean margin (Tassara *et al.*, 2006). The model has 16 tectonic units including the lithosphere and the upper mantle down to a depth of 410 km.

Figure 3.9 shows the visco-elastic 3D dynamic model of the Andean margin. The size of the model is 1730 km x 725 km (area between 16-22°S and 78-63°W). The densities of the units have been adopted from the density model of Tassara *et al*. (2006). Young's moduli have been calculated using the V_p velocities from the ANCORP profile (ANCORPWorkingGroup, 2003) and the P-S wave velocity relation $V_p=3^{1/2}V_s$. The corresponding Poisson ratio for all units is 0.25. The parameters of the geological units are shown in Fig. 3.9. The asthenosphere has been modeled as a viscous-elastic medium. The lithosphere is pure elastic. In the modeling, it is assumed that the South American plate is fixed and the Nazca plate moves by 7.8 cm/year for 200,000 years (Somoza, 1998). It is

assumed that friction occurs only in the uppermost part of the contact up to approximately 40 km depth with a frictional coefficient of 0.1.

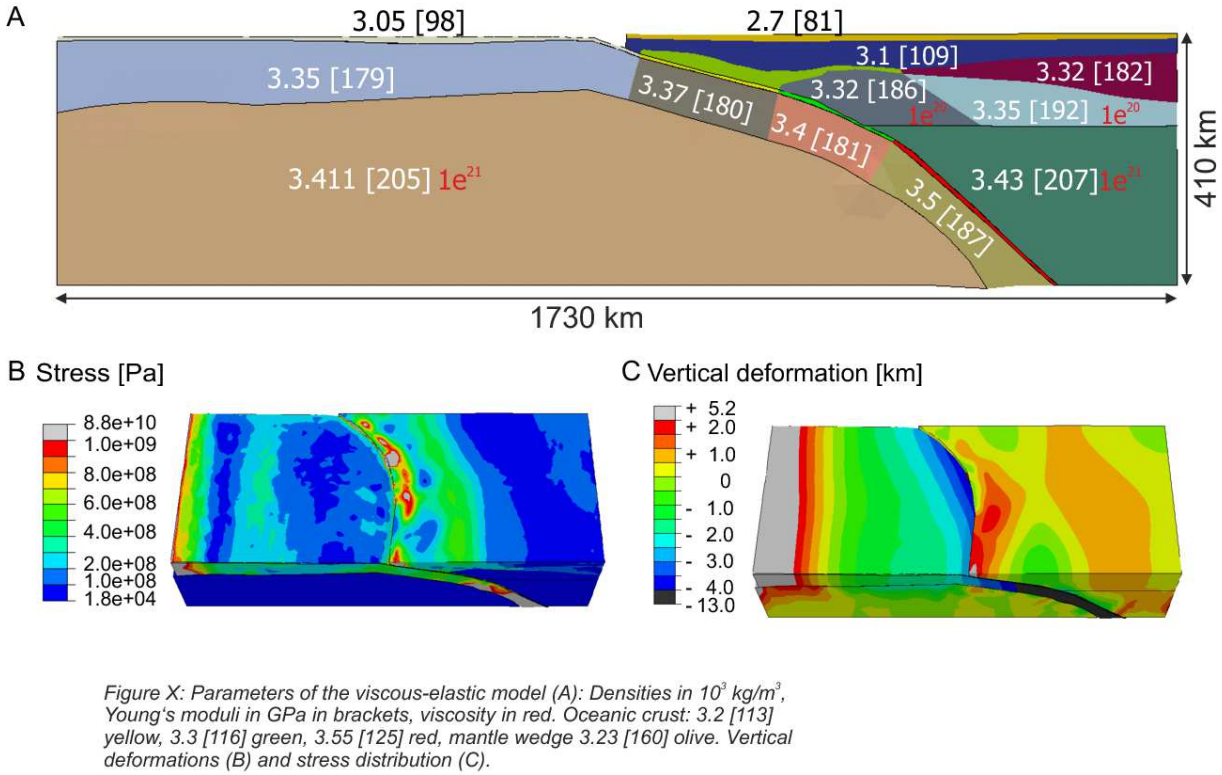

Figure X: Parameters of the viscous-elastic model (A): Densities in 10^3 kg/m^3, Young's moduli in GPa in brackets, viscosity in red. Oceanic crust: 3.2 [113] yellow, 3.3 [116] green, 3.55 [125] red, mantle wedge 3.23 [160] olive. Vertical deformations (B) and stress distribution (C).

Figure 3.9. After Köther *et al.* (2011). Used parameters for the viscous-elastic model (A). Densities [*10³ kg/m³], Young's moduli [GPa] in brackets, viscosity in red. Oceanic crust: 3.2 [113] yellow, 3.3 [116] green, 3.55 [125] red, mantle wedge 3.23 [160] olive. Vertical deformations (B) and stress distribution (C).

Beside density, however, Young's modulus, width of coupling zone, frictional coefficient and obliquity of the subducting Nazca plate could influence the dynamics of plate interfaces (Heuret and Lallemand, 2005). In order to study the effects of these controlling parameters, rheologies (e.g. plasticity, viscoelasticity and visco-elasto-plasticity) and temperature on the dynamics of the thrust zone area, more generalized and realistic 3D models have been developed.

Figure 3.9b shows the resulting vertical deformations. The calculated uplift is ~ 1.5 km and this corresponds to 7.5 mm/year. The expected surface uplift is smaller than 2 mm/year (Jordan *et al.*, 1997; Klotz *et al.*, 2006). Though our model neglects erosion, the estimated uplift from the numerical modeling is in the right order of magnitude. Figure 3.9c

shows the stress distributions. The stress (high and low) tends to follow the trend of the earthquake distributions in the region. The green belt indicates where the slab is at depth of 100 km.

The present study shows that well constrained geometries are crucial for dynamic modeling. The availability of satellite-derived gravity data has significantly improved the density models of the Andean region lacking terrestrial data. This in turn refined the geometries and densities of the geodynamic models. In particular, the long wavelength satellite-derived gravity anomaly is suitable to constrain the deep structures of the models. The resulting stress fields and new petrologic models can help to improve the density structure of the static models. Thus, a direct link between the static and dynamic models could be established.

3.5 Conclusions

Thorough understanding and interpretation of dynamic processes associated with hazardous regions is one of the major research interests in geosciences. Combined gravity models can provide valuable information for density modeling and geological interpretation where terrestrial gravity data of high resolution are available. In this study, it is shown that gravity prediction and downward continuation in some areas, e.g. the mountain ranges over Costa Rica and Central Andes, could lead to large errors and reduce the reliability of gravity data. Gravity prediction based on topography may not be appropriate for those regions. This calls the need to improve reduction techniques such as Bouguer calculation, topographic correction as well as downward continuation. The satellite only models have low spatial resolution compared to terrestrial data. However, the resolution is sufficient for interpretation of large-scale structures. Especially, in frontier regions such as parts of the Andes or Central America, where terrestrial gravity data coverage is limited, these models are valuable. 3D modeling of synthetic gradients and invariants of subduction zones, using the Andean as case study, proved the applicability of gradient measurements for detection of the edge of geological structures. Therefore, gradients from GOCE mission can resolve structural information and improve interpretation of asperities. The long term and complex geodynamic processes of subduction could only be fully understood if model predictions are constrained with surface observables such as satellite gravity data. In the present study, a geodynamic model of the Andean margin has been developed with a realistic geometry based on density model constrained by gravity data and other relevant prior information. The stress distributions in the fore-arc, as determined from the dynamic modeling, mostly coincide with the locations of the earthquake of the region. Finally, mapping and interpretation of hazardous regions require good gravity database (among others) to constrain lithospheric and dynamic processes. Satellite gravity data provide globally best information about frontier

regions. Therefore, it is possible to interpret structures globally without limitations and combine regional interpretation of different regions into a one big picture.

4 Moho structure of Central America based on three-dimensional lithospheric density modeling of satellite derived gravity data

The Central American isthmus hosts a highly variable Moho structure due to the diverse origin and composition of the crustal basement and the influence of large scale neotectonic processes. Gravity data from the combined geopotential model EGM2008 was interpreted via forward modeling to outline the three dimensional lithospheric density structure along the Middle American Trench, as well as the segmentation of the oceanic Cocos and Nazca plates and the overriding Caribbean plate. In this work, results for the depth of the Moho obtained from the density model are presented. The Quaternary volcanic arc correlates with a maximum Moho depth of 44 km in western Guatemala. To the southeast of the continental shelf, the Caribbean plate shows Moho depths between 20 and 12 km whereas to the north, values as shallow as 8 km are observed at the Cayman trough. For the oceanic Cocos Plate, depths between 16 and 21 km are obtained for the Moho along the Cocos ridge contrasting with values between 15 and 12 km for the seamount segment and 8 and 11 km for the segments of the crust that are not affected by the Galapagos hot-spot track.

4.1 Introduction

The origin and tectonic history of the Central American isthmus has resulted in a heterogeneous density distribution of the crustal basement which, in combination with neotectonic processes and magmatism produce a highly variable crustal thickness. This paper describes a density model of the Central American lithosphere that is derived from constrained forward modeling of gravity data.

The aim of the density model is to provide a large scale picture of the density distribution of the lithosphere in the region in order to further comprehend the segmentation of the Caribbean Plate. The model takes into consideration the influence that dynamic

processes such as subduction and volcanism have had on the overall composition and structure of the crust. In this work, the modeled Moho depth results from three dimensional density modeling are presented for the study area. Moreover, the implementation of satellite derived gravity data and combined geopotential models as input for the forward modelling of the solid Earth will contribute to the understanding of global Earth models as a tool for geophysical interpretation.

4.2 Tectonic setting

The characteristics of the Central American land bridge are closely linked to the tectonic segmentation and the interaction of five major tectonic plates. The northern limit of the isthmus is marked by the Motagua-Polochic fault system (Fig. 4.1), a left-lateral shear zone that continues off-shore along the Swan Islands transform fault. This transform plate boundary between the Caribbean and North-American plates averages 18-20±3 mm/y of along-boundary motion (DeMets, 2001).

The Caribbean coast of the isthmus shows characteristics of a passive margin extending southeast from the Swan Islands Fault to the central Caribbean coast of Costa Rica. The passive margin is interrupted by the North Panama Deformed Belt, a fold-and-thrust belt which, according to Marshall *et al*. (2000) is linked to the Middle American Trench through the Central Costa Rica Deformed Belt, a diffuse fault zone outlining the western boundary of the Panama micro-plate. The crustal basement of the Caribbean plate is highly heterogeneous in composition and origin presenting blocks with contrasting densities. The northernmost segment is predominantly composed of crystalline rocks of the Paleozoic continental Chortis block. This block of crystalline basement was believed to extend southward to the Nicaragua-Costa Rica border region (Dengo, 1985). However, the presence of ultramafic rocks in northern Nicaragua has led to the suggestion of an ultramafic basement unit in the form of the Siuna Terrane (Rogers *et al.*, 2007; Venable, 1994) and has placed the southernmost limit of

the Chortis continental basement at the area of the Honduras-Nicaragua border (Fig. 4.2). Baumgartner *et al*. (2008) include the Siuna Terrane as part of the Mesquito Composite Oceanic Terrane, a block of Mesozoic igneous rocks of oceanic origin and deep ocean sediments which extends along the Central American Volcanic Arc and fore-arc, the Nicaraguan mainland and part of the Nicaragua Rise. For the area of Costa Rica, western Panamá and the Colombia basin, the crustal basement is predominantly composed of basalts which have been linked with a Large Igneous Province event (Baumgartner *et al.*, 2008; Hoernle *et al.*, 2004).

The Central American Volcanic Arc begins at an approximate latitude of 15°N at the Tacaná volcano and extends 1100 km parallel to the Middle American Trench ending at the Irazú-Turrialba volcanic complex at a latitude of 10°N. To the east of this complex, the only major Quaternary volcano is the Barú volcano which stands at a distance of 190 km from the rest of the Central American Volcanic Arc. The Nicaraguan and southeastern Salvadorian section of the volcanic front is located inside the Nicaragua depression interpreted by Marshall (2007) as a half-graben bounded by transtensional faults.

Bounding the Pacific edge of the Caribbean plate is the Middle American Trench along which the Cocos plate subducts at a rate of 73 mm/y for the northwestern part off-shore Guatemala and 85 mm/y to the southeast off-shore Costa Rica (DeMets, 2001). Subduction along the Middle American Trench is interrupted by the Panama Fracture Zone, a right-lateral shear zone forming a transform boundary between the Cocos and Nazca plates. Eastward from the Panama Fracture Zone, the boundary between the Caribbean plate and the Nazca plate in southern Panamá is marked by a portion of the trench characterized by Lonsdale (2005) as a fossil structure. According to Lonsdale and Klitgord (1978), subduction of the Nazca plate beneath the Caribbean plate ended in the Late Miocene after a period of 18 to 20 m.y. of subduction and transitioned to a strike-slip boundary. However, DeBoer *et al*. (1988)

propose a reactivation of the subduction 3.4 to 5.3 million years ago and consider the existence of recent low-angle subduction. In this region, both the Cocos and Nazca plates feature a complex crustal structure due to the presence of oceanic ridges.

Offshore Costa Rica, von Huene *et al*. (2000) describe the segmentation of the Cocos plate and define 3 different segments according to morphology. The smooth segment, generated at the East Pacific Rise and the Cocos-Nazca Spreading Center, is bordered to the southeast by a rough-smooth boundary (Hey, 1977) beyond which the oceanic crust has been affected by the Galápagos hot spot track. The hot spot trace is divided into a seamount segment and the Cocos ridge. Seismic cross-sections presented by von Huene *et al*. (2000), Walther (2003) and Sallarès *et al*. (2003) show that the Cocos and Malpelo ridges feature a maximum crustal thickness of 19-21 km contrasting with the surrounding oceanic basins in which the crust features thicknesses between 7 and 11 km. On the Nazca plate, the Coiba and Malpelo ridges are separated by the defunct Sandra rift (DeBoer *et al.*, 1988; Lonsdale, 2005).

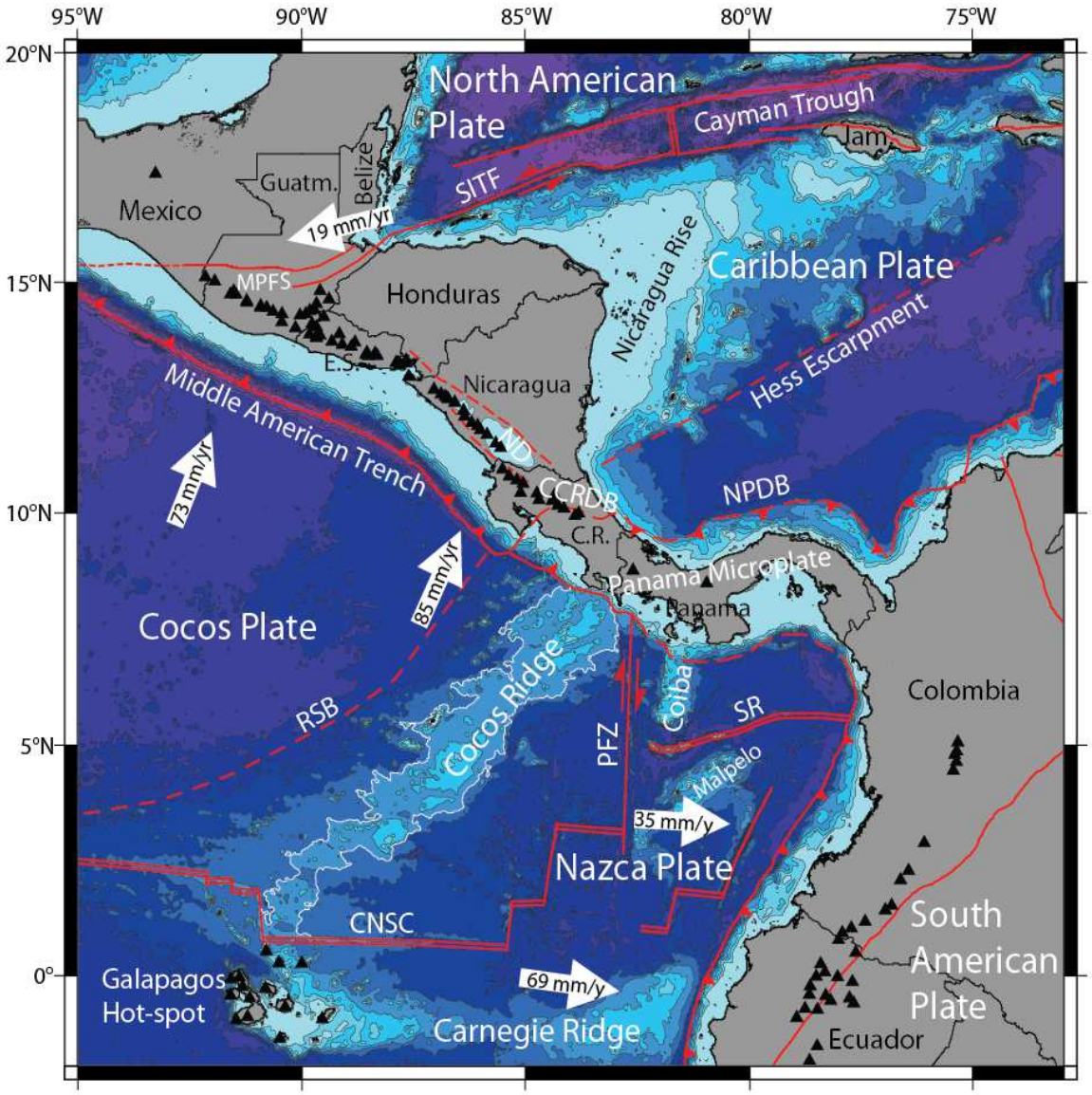

Figure 4.1. Tectonic setting of the Central American Isthmus. Red lines show plate boundaries and major tectonic structures. Black triangles show main Quaternary volcanoes modified from Siebert and Simkin (2002). White arrows show direction and rate of plate motions relative to the Caribbean plate according to Freymueller *et al*. (1993), Kellogg and Vega (1995) and DeMets (2001). Plate Boundaries modified from Coffin *et al*. (1998) and Lonsdale (2005) . Black lines depict the coastline and international borders. C.R.: Costa Rica; E.S.: El Salvador; Guatm.: Guatemala; Jam.: Jamaica; CCRDB: Central Costa Rica Deformed Belt; CNSC: Cocos-Nazca Spreading Center. MPFS: Motagua-Polochic Fault System; ND: Nicaragua Depression; NPDB: North Panamá Deformed Belt; PFZ: Panamá Fracture Zone; RSB: Rough-Smooth Boundary modified from Hey (1977); SITF: Swan Islands Fault; SR: Sandra Rift (DeBoer *et al.*, 1988). White contour represents the -2000 m bathymetric level outlining the Cocos Ridge, bathymetric data from Global Multi-Resolution Topography by Ryan *et al*. (2009).

4.3 Data

This work focused on the use of gravity data from a global geopotential model as input for the forward modeling. The data was chosen in order to overcome the difficulties posed by the vast extent of the study area and the problems in terms of data quality, station coverage and the availability of meta-data that describe the surface gravity databases. The

EGM2008 combined geopotential model (Pavlis *et al.*, 2008) was used as the main source of gravity data for the study. With a maximum spatial resolution of approximately 10 km, this geopotential model combines data from the GRACE satellite mission as well as satellite altimetry data off-shore and surface stations data on-shore (where available) which are reduced to a 5'x5' grid.

The gravity data for this work was obtained through the International Centre for Global Earth Models (ICGEM, under: http://icgem.gfz-potsdam.de/ICGEM/ICGEM.html). From this portal, several products may be obtained for different global geopotential models. The Bouguer anomaly provided directly by the ICGEM calculation service consists of the classical gravity anomaly minus the effect of the Bouguer plate with a density of 2.67 Mg/m^3. The classical anomaly considered for the calculation is obtained by subtracting the normal potential on the ellipsoid from the magnitude of the gradient of the potential which is continued downward to the geoid. The gravity disturbance as defined in the ICGEM calculation service (Barthelmes, 2009) is obtained by subtracting the magnitude of the gradient of the normal potential from the magnitude of the gradient of the potential at a given point.

In order to assess which individual dataset was adequate for the density modeling, different anomalies for Central America were calculated and compared with surface station data compiled from datasets provided by GETECH Leeds and the General Bureau for Hydrocarbons of the Costa Rican Ministry of the Environment. A detailed comparison of the surface station data with different values obtained from the EGM2008 geopotential model was carried out for a data subset for Costa Rica and has been published by Köther *et al.* (2011). From the comparison with surface station data, it was concluded that due to its consistency with anomalies calculated from surface stations, the use of the Bouguer anomaly calculated from the gravity disturbance is preferable for this work. Further discussions on

gravity anomalies and disturbances have been published by Li and Götze (2001) and by Hackney and Featherstone (2003). Figure 4.2 shows a compilation of Bouguer anomaly onshore and free-air anomaly offshore for the study area.

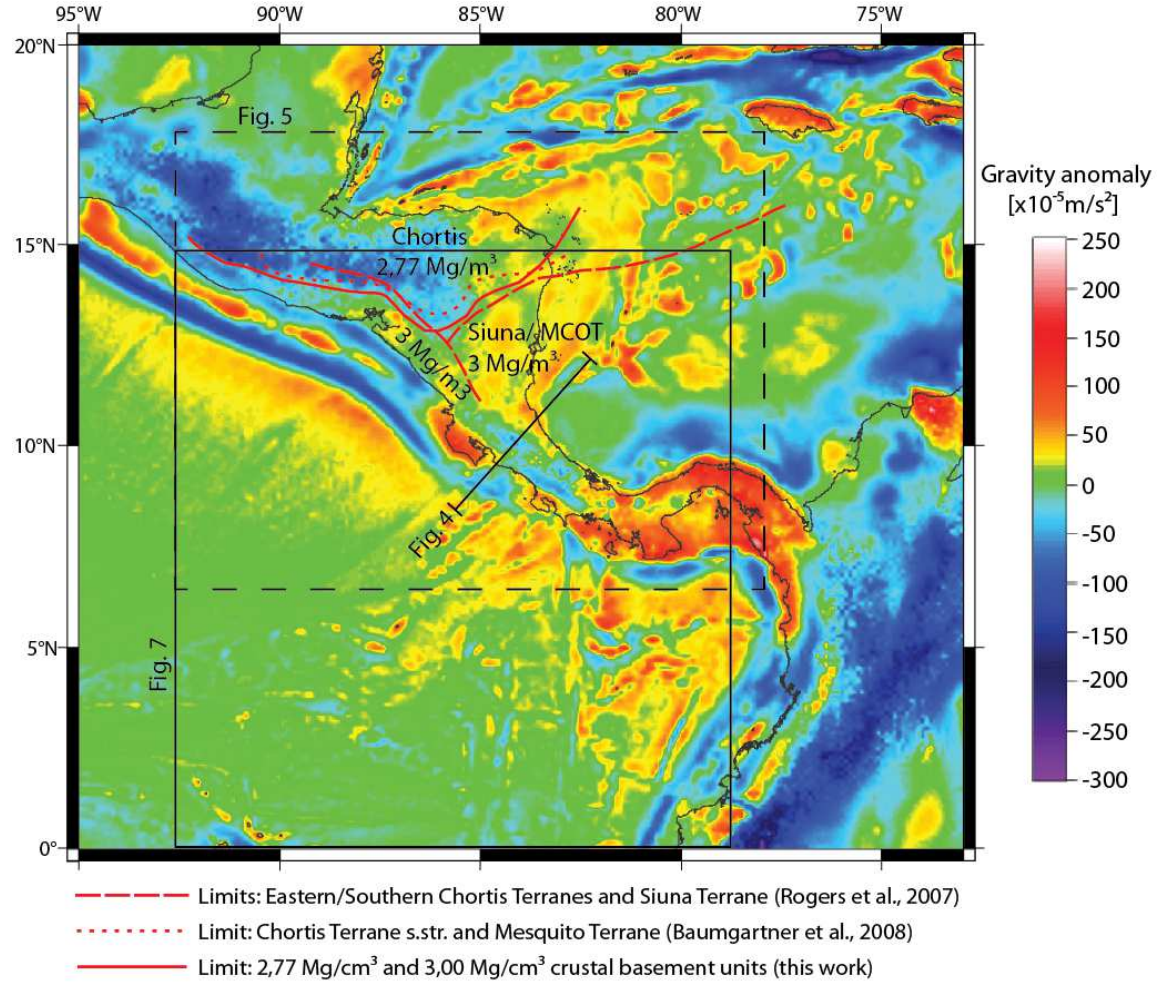

Figure 4.2. Gravity field data for the Central American isthmus and surrounding areas. Bouguer anomaly onshore and free-air anomaly offshore calculated from the gravity disturbance data from EGM2008 (Pavlis *et al.*, 2008). Black lines indicate the coastline. Red lines outline the proposed boundaries for tectonic terranes in northern Central America: Siuna Terrane (Rogers *et al.*, 2007; Venable, 1994), MCOT: Mesquito composite Oceanic Terrane and Chortis Terrane *s.str.* (Baumgartner *et al.*, 2008).

4.4 Methods

The 3D density model was constructed via interactive forward modeling using the software IGMAS+ (Götze *et al.*, 2010). A total of 45 cross-sections were constructed from which the three-dimensional structure is triangulated to form polyhedra of constant density. The resulting geometry represents the structure of the subsurface. The calculation of the effect on the gravity field from each polyhedron is carried out by the algorithm of Götze (1976) and Götze and Lahmeyer (1988). The calculated gravity field is then compared with

the measured gravity data and the model geometry and body densities are adjusted, within the limits of constraining information, to achieve the best fit. Figure 4.3 shows the orientation of the modeling cross-sections and the residual from the comparison of the modelled gravity field and the gravity data from EGM2008.

In order to constrain the model, additional geophysical and geological data were incorporated to provide information on the structure and the density distribution of the lithosphere. Geophysical constraints include: wide-angle seismic refraction (Sallarès *et al.*, 2003), local earthquake seismic tomography (Arroyo *et al.*, 2009; Husen *et al.*, 2003a; Syracuse *et al.*, 2008) and receiver functions results (Dzierma *et al.*, 2010; Linkimer *et al.*, 2010; Syracuse *et al.*, 2008). The surfaces representing the continental and the oceanic Moho were extracted from the 3D density model to provide a comprehensive representation of the Moho depth.

4.5 Results

4.5.1 Overview of the 3D Density Model

Since the gravitational effect at the given point (station) is a sum of the effects of the subsurface masses, in order to adequately model the Moho structure, the overall density distribution of the lithosphere must be considered. The general density distribution provides a framework of the density contrasts from which the Moho was modeled. Several local features have been included to account for anomalies of lower wavelengths in the gravity dataset. However, these local structures will not be discussed in detail in this work since it is the regional density distribution that significantly influences the modeling of the Moho structure. The structure of the lithosphere and the values of the densities were modeled interactively along the cross-sections to achieve the best fit between the calculated and the measured gravity while integrating the available constraining information. Figure 4.3 shows the

differences between the measured gravity anomaly from EGM2008 and the calculated anomaly from the three dimensional model as well as the location of the available geophysical constraints on the Moho depth.

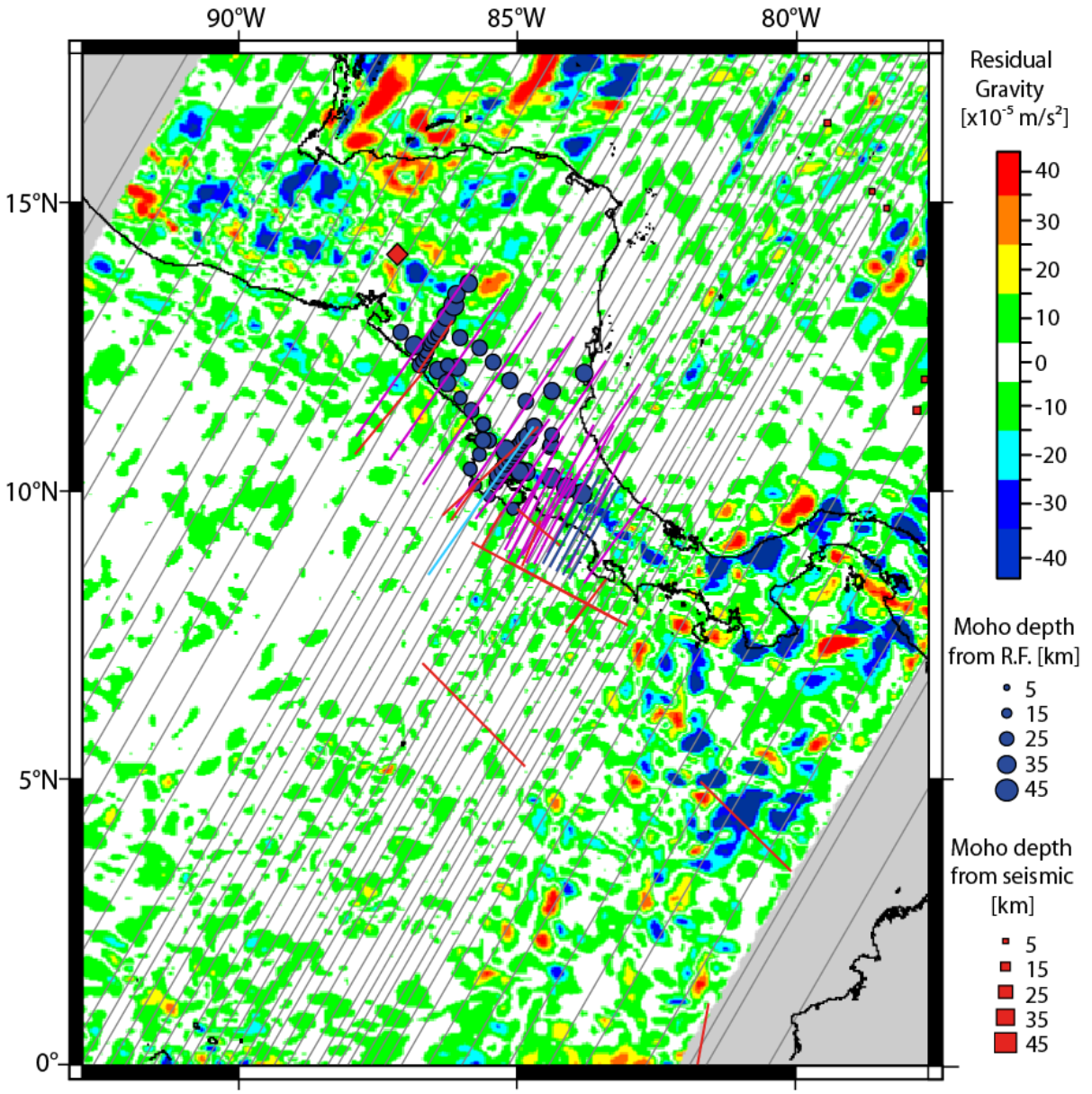

Figure 4.3. Fit between the calculated and the measured gravity anomaly and location of constraining geophysical data. Grey lines show the location of modeling cross-sections for the triangulation of the 3D density model. Blue circles show the location of 1D depth to the Moho solutions from receiver functions (R.F.) by MacKenzie *et al.*(2008) and Linkimer *et al.* (2010). Red lines show the location of refraction/reflection profiles from Ye *et al.* (1996), Walther *et al.* (2003), von Huene *et al.* (2000), Sallarès et al.(2001), Sallarès *et al.* (2003). Magenta lines show the location of seismic tomography cross-sections by Husen *et al.* (2003a), Syracuse *et al.* (2008) and Arroyo *et al.* (Arroyo *et al.*, 2009). Dark blue lines show the location of receiver function cross sections by Dzierma *et al.* (2010). Cyan line shows the location of magnetotelluric survey by Worzewski *et al.* (2011). Red squares and diamond show the location of 1D depth to the Moho solutions from seismic studies by Ewing *et al.* (1960) and Kim *et al.* (1982) respectively. Black lines depict the Central American coastline.

The 3D density model extends 200 km in depth and includes structures such as the asthenospheric mantle with a density of 3.34 Mg/m^3, and the lithospheric mantle with a density of 3.30 Mg/m^3 for the Cocos and Nazca plates and 3.32 Mg/m^3 for the Caribbean plate. For these two layers, the density is constant with the exception of the changes in density of the subducting lithosphere. Regarding the crust, a heterogeneous density distribution was modelled considering the available geological and geophysical data. The oceanic crust of the Cocos and Nazca plates was modelled with a density of 2.8 Mg/m^3. The oceanic basins of the Caribbean plate were modelled with a separate layer of 2.55 Mg/m^3 for the sediment cover and 2.8 Mg/m^3 for the oceanic crustal basement.

In the continental domain of the isthmus, different densities were considered for the diverse crustal basement blocks. The density and extent of each crustal basement unit was determined by correlation of local geology, available tectonic models and the characteristics of the gravity field. On-shore, a Bouguer anomaly low ranging from $-135x10^{-5}$ to $-35x10^{-5}$ m/s^2 is in strong contrast with a Bouguer anomaly high ranging between $10x10^{-5}$ and $45x10^{-5}$ m/s^2. This gravity gradient correlates with the location of the limits between the Chortis Terranes or Chortis Block and the Siuna or Mesquito Terrane outlined by Rogers *et al*. (2007) and Baumgartner *et al*. (2008) respectively (Fig. 4.2) based on surface geology. For this work, to account for the measured Bouguer anomalies, the crystalline Chortis block was modelled with a density of 2.77 Mg/m^3 while predominantly ultramafic material of the Mesquito Terrane has a model density of 3.00 Mg/m^3. The basaltic crustal basement associated with the Caribbean Large Igneous Province and other units composed of crustal basalts were modeled together with a density of 2.90 Mg/m^3 (Fig 4.4).

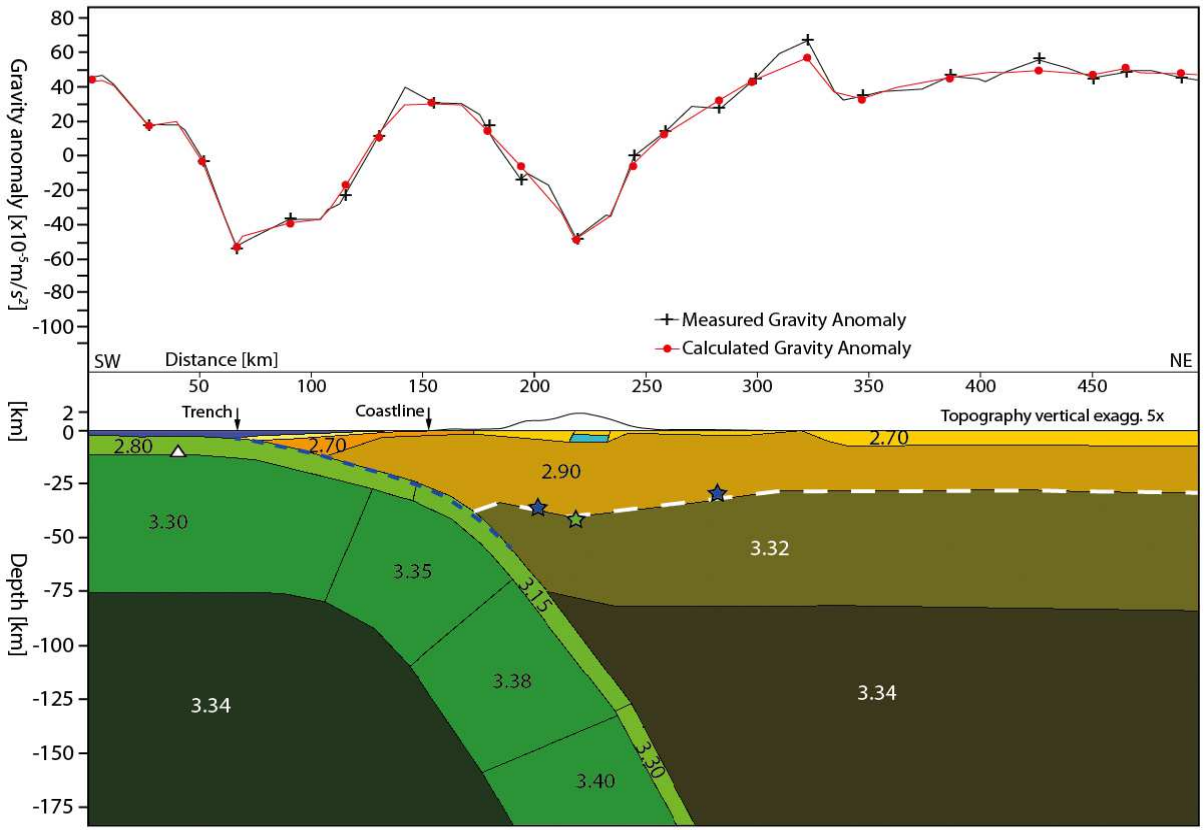

Figure 4.4. Cross-section from the 3D density model for Central Costa Rica (see location in figure 4.2). Densities given in Mg/m^3. The white stippled line shows the Moho on the overriding Caribbean Plate. Star symbols shows constraining data on the depth of the Moho by means of receiver functions from Linkimer et al. (2010) (green), MacKenzie *et al*. (2008) (blue). White triangle shows the Moho depth at the intersection with the seismic profile published by von Huene *et al*.(2000). The blue stippled line shows the top of the subducting slab interpreted from local earthquake seismic tomography by Arroyo *et al*. (2009).

4.5.2 Constraints on Lithospheric Densities

The final densities for the three-dimensional bodies in the density model have been determined through the interactive forward modeling process to achieve best fit between the modeled and measured gravity field. The initial conditions for the model were determined by a combination of integration of geophysical constraints, the correlation with surface geology and the regional tectonic interpretation.

In order to constrain the densities used in the three-dimensional model, the V_p structure from available velocity models from wide angle seismic refraction (Sallarès *et al.*, 2001; Sallarès *et al.*, 2003; Stavenhagen *et al.*, 1997; Walther *et al.*, 2000; Walther, 2003) and seismic tomography (Arroyo *et al.*, 2009; Husen *et al.*, 2003a; Syracuse *et al.*, 2008) were

taken into account. Though highly variable, the densities obtained from V_p through empirical formulas help to constrain the range in which the densities for the 3D model may vary. Table 4.1 shows a comparison of the densities calculated from V_p and the densities of some of the units of the final 3D model.

Table 4.1. Modeled densities and constraints from seismic velocities

Layer in Density Model	Density in Gravity Model (Mg/m^3)	Seismic Velocity Vp (km/s)	Reference for Velocity	Equivalent Density (Mg/m^3)	Reference Empirical Formula
Upper Crust Caribbean	2.70	5.1 - 5.9	(Sallarès *et al.*, 2001)	2.61 - 2.71	(Gardner *et al.*, 1974)
				2.55 - 2.70	(Brocher, 2005)
		4.0 - 6.0	(Stavenhagen *et al.*, 1997)	2.46 - 2.72	(Gardner *et al.*, 1974)
				2.39 - 2.72	(Brocher, 2005)
Lower Crust MCOT	3.0	6.8	(Sallarès *et al.*, 2001)	2.95	(Godfrey *et al.*, 1997)
				2.99	(Christensen and Mooney, 1995)
				2.85	(Birch, 1960)
Lower Crust CLIP	2.90	6.0 - 6.6	(Stavenhagen *et al.*, 1997)	2.89 - 2.94	(Godfrey *et al.*, 1997)
Lower Crust Chortis	2.77	6.14	(Kim *et al.*, 1982)	2.75	(Brocher, 2005; Christensen and Mooney, 1995)
				2.60	(Birch, 1960)
Crust Cocos	2.80	4.30 - 7.17	(Walther, 2003)	2.76 - 2.98	(Godfrey *et al.*, 1997)
Upper Mantle Caribbean	3.32	7.5	(Sallarès *et al.*, 2001)	3.12	(Birch, 1960)
				3.16	(Birch, 1960)
		7.5 - 8.5	(Syracuse *et al.*, 2008)	3.12 - 3.48	(Brocher, 2005)
				3.16 - 3.60	(Birch, 1960)
Upper Mantle Cocos	3.20	8.1	(Sallarès *et al.*, 2001)	3.3	(Brocher, 2005)
				3.42	(Birch, 1960)
		7.6 - 7.8	(Walther, 2003)	3.15 - 3.22	(Brocher, 2005)
				3.20 - 3.30	(Birch, 1960)

The densities for the oceanic crust of the subducting Cocos plate were constrained by petrological modelling carried out by Bousquet *et al*. (2005) assuming an initial Mid-Ocean Ridge Basalt composition. The petrological models show the changes in density considering

temperature, pressure, initial composition, and metamorphic reactions. The temperature was obtained from thermal models by Peacock *et al*. (2005) and the lithostatic pressure was calculated from the initial density model for the overriding plate.

4.5.3 Caribbean Plate Moho

Results obtained from the modeling of the Moho structure of the Caribbean plate (Fig. 4.5) show a sharp contrast in the crustal structure of the continental land bridge and the oceanic basins. Due to the diverse tectonic environments present in the region, results for the Caribbean plate Moho are presented separately for the continental domain (considered from a morpho-tectonic point of view including the continental shelf) and the oceanic domain.

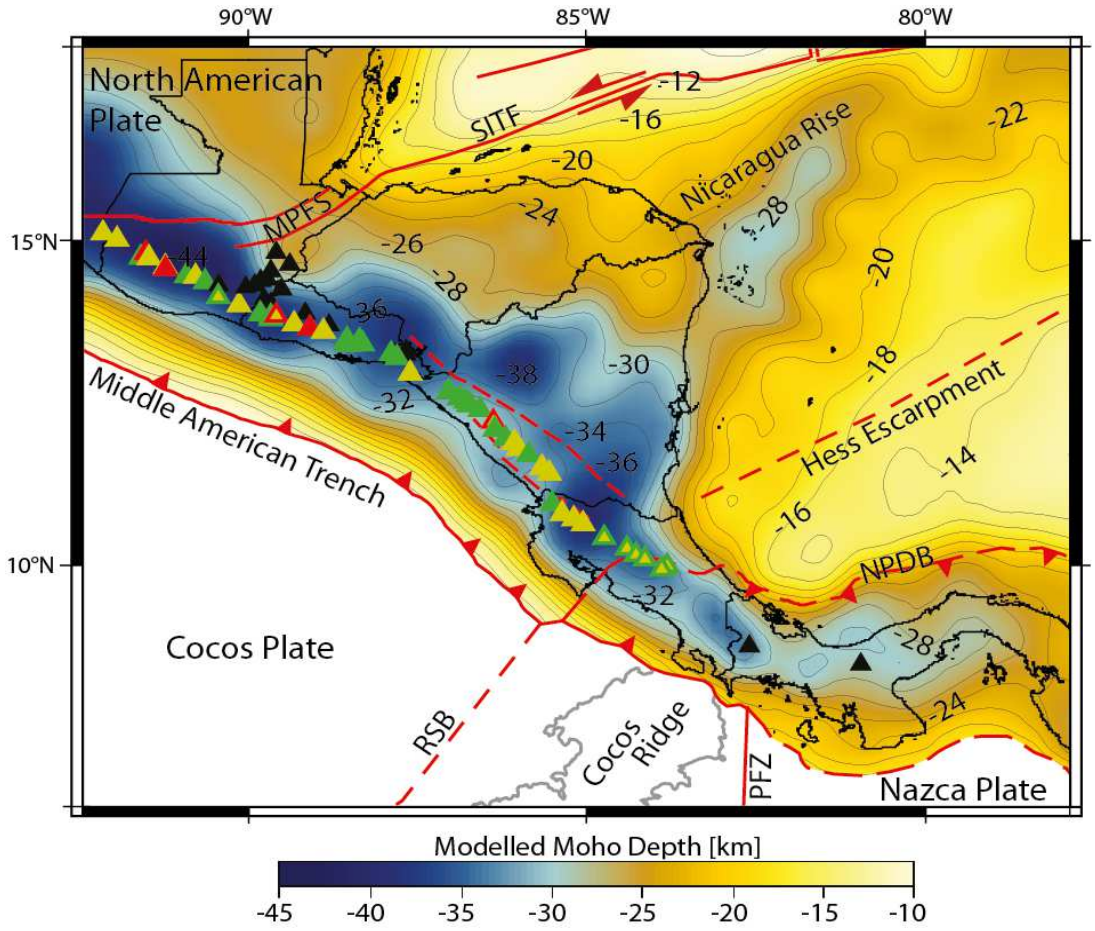

Figure 4.5. Moho depth results from the 3D density model for the Caribbean plate. Contours show the depth to the modeled Moho in 2 km intervals. Red lines show plate boundaries and major tectonic structures. Triangles show main Quaternary volcanoes modified from Siebert and Simkin (2002) and classified by general chemical composition (color legend in figure 4.6). Plate Boundaries modified from Coffin *et al*. (1998) and Lonsdale (2005). Bold black lines depict the coastline and international borders. MPFS: Motagua-Polochic Fault System; NPDB: North Panama Deformed Belt; PFZ: Panama Fracture Zone; RSB: Rough-Smooth Boundary modified from Hey (1977); SITF: Swan Islands Transform Fault.

4.5.3.1 Continental domain

The modelled continental Moho is deepest towards the eastern edge of the isthmus and shows a strong correlation with the presence of the Quaternary volcanism of the Central American Volcanic Arc. The deepest Moho follows the trend of the volcanic arc, with depths between 36 km and 44 km. An exception is noted for the Nicaraguan portion of the arc where the trend in the lower depth of the Moho is shifted some 50 km towards the back of the Quaternary arc. The correlation of the deeper Moho with the volcanic arc resumes in northern Costa Rica. For central Costa Rica, the Moho shows a relatively shallow section toward the end of the Quaternary arc but returns to values deeper than 32 km toward eastern Costa Rica and western Panama. The continental domain of the Moho is extended off-shore Honduras and Nicaragua as a northeast trending feature with Moho depths between 24 and 30 km for the Nicaragua Rise which joins with a similarly thickened crust for the island of Jamaica and the area adjacent to its southern coast. Towards the South American continent, in the eastern Panamanian section of the isthmus, the Moho is noticeably shallower and flat with depths between 22 and 28 kilometers and is bound to the north by a strong gradient towards the ocean basin.

Considering a two dimensional cross section of the Moho depth along the Central American Volcanic Front (Fig. 4.6), a pattern of four different domains with relatively flat sections is observed. Each section is separated by a steeply sloping Moho which forms a transition zone and correlates with areas where major volcanic edifices are less frequent. The northwestern section extends between the Tacaná and the Izalco volcanoes. This section is characterized by Moho depths between 40 and 44 km and ends in a transition zone between the Izalco and Ilopango volcanoes where the Moho climbs from 41 to 36 km in depth. A second “flat” section is observed between Ilopango and Conchagüita volcanoes with Moho depths between 36 and 38 km and ends in a 100 km long transition zone to the San Cristobal

volcano. This particular transition zone coincides with a 70 km gap in major Quaternary volcanoes along the axis between the Cosigüina and San Cristobal volcanoes. The shallowest section of the Moho along the arc is observed between the San Cristobal and Maderas volcanoes varying from 32 to 30 km in depth. A third transition zone is observed toward the southwest of the Maderas volcano and coincides with a trenchward shift in the axis of the volcanic front. A fourth section with the Moho depth between 37 and 39 km along the volcanic front can be defined between the Rincón de la Vieja and the Irazú volcanoes. This trend is interrupted by anomalous Moho depths for the Miravalles and Tenorio volcanoes reaching close to 42 km.

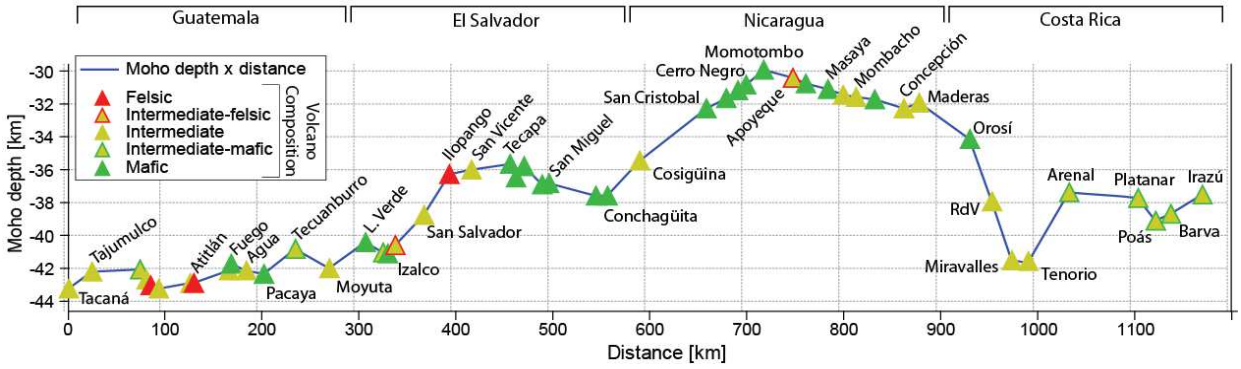

Figure 4.6. Depth to the Moho profile along the Central American Volcanic Front. Generalized chemical composition is based on Siebert and Simkin (2002). Location of the cross-section and volcanoes is shown in figure 4.7.

4.5.3.2 Caribbean Oceanic domain

The Swan Island Fault and the Cayman Trough act as a distinct segment boundary between the Caribbean and the North American plate and a clear distinction between the continental domain of the Caribbean plate and the oceanic segment of the North-American Plate is observed. Along this plate boundary, a shallow Moho is observed with depths of close to 8 km at the Cayman Trough. This structure bounds the thicker crust of the Nicaragua Rise and the oceanic basin of the Gulf of Mexico. To the south of the Nicaragua Rise, two different sections can be distinguished by following the characteristics of the modeled Moho. To the southeast of the edge of the continental shelf, results show a segmented area with

depths between 22 and 16 km. This heterogeneous segment with variable Moho depths is observed until reaching the Hess Escarpment. The escarpment outlines the boundary with the oceanic basin which features a smooth sloping Moho structure with depths between 12 and 16 km culminating at the North Panama Deformed Belt.

4.5.4 Cocos Plate Moho

The most important feature affecting the Moho structure on the Cocos plate is the Galapagos hotspot track which can be separated into the Cocos Ridge (depicted in figure 4.1 considering the -2000 m bathymetric contour) and the seamount segment which extends parallel to the ridge up to approximately 150 km to the northwest. The ridge extends from the Cocos-Nazca spreading center at an approximate latitude of 1° N with a northeasterly trend culminating at the Middle American Trench off the coast of Costa Rica. Results show the effects of the thickened crust on the Moho which presents depths between 15 and 21 kilometers below sea level along the area directly related to the ridge (Fig. 4.7). Accounting for bathymetry, this corresponds to a crustal thickness between 13 and 19 kilometers contrasting with the values between 5 and 8 kilometers obtained for the crust originated at the East Pacific Rise. Along the seamount segment of the Cocos Plate, a uniformly thickened crust north of the Rough-Smooth Boundary is observed. This area shows crustal thicknesses between 8 km at the edge of the Rough-Smooth Boundary and 12 km at the neighboring Cocos Ridge which is consistent with seismic results of 11 to 12 km depth obtained by von Huene *et al*. (2000) and Walther (2003) for the northwestern flank of the Cocos Ridge.

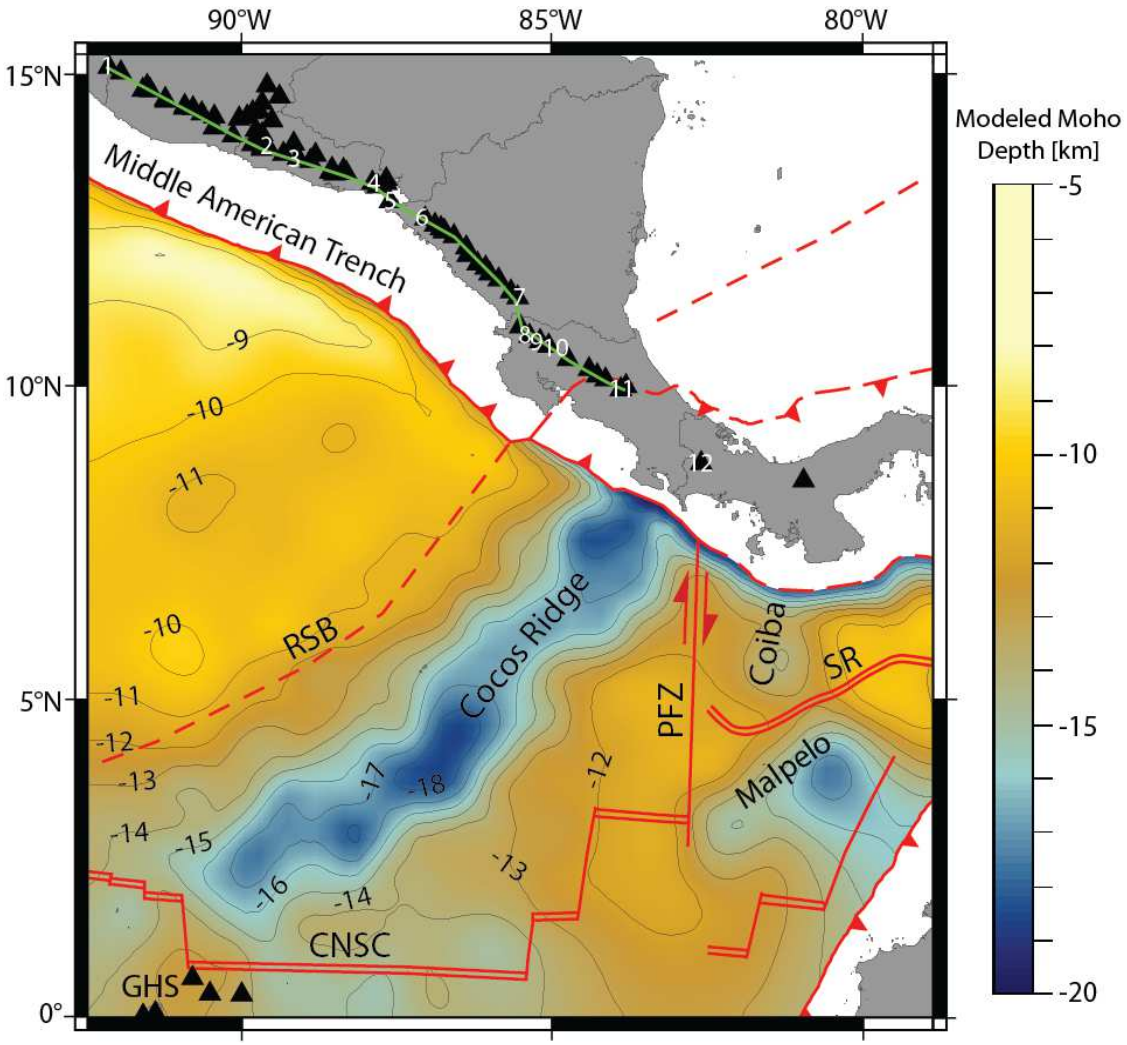

Figure 4.7. Moho depth results from the 3D density model for the Cocos and Nazca plates. Contours show the depth to the modeled Moho in 1 km intervals. Red lines show plate boundaries and major tectonic structures. Black triangles show main Quaternary volcanoes modified from Siebert and Simkin (2002), labeled volcanoes are: 1: Tacaná, 2: Izalco, 3: Ilopango, 4: Conchagüita, 5: Cosigüina, 6: San Cristobal, 7: Maderas, 8: Rincón de la Vieja (RdV), 9: Miravalles, 10: Tenorio, 11: Irazú, 12: Barú. Green line shows the location of the cross-section in figure 4.6. CNSC: Cocos-Nazca Spreading Center; GHS: Galápagos Hot Spot; PFZ: Panamá Fracture Zone; RSB: Rough-Smooth Boundary modified from Hey (1977); SR: Sandra Rift (DeBoer *et al.*, 1988).

Crustal thickness on the Cocos Plate decreases to the northwest of the Rough-Smooth Boundary outlining a segment with thicknesses between 6 and 8 km off the coast of Nicaragua and northwestern Costa Rica. The shallowest parts of the Cocos Plate Moho lie off-shore Guatemala with a depth of less than 8 km featuring a crustal thickness between 7 and 4 kilometers when the bathymetry is subtracted.

4.5.5 The Panama Fracture Zone and the Nazca Plate

A wide, north-south trending feature showing a relatively shallow Moho is consistent with the presence of the Panama Fracture Zone which marks the plate boundary between the Cocos plate and the eastern part of the Nazca plate. Along the fracture zone, Moho depths between 11 and 12 km have been modeled. The Nazca plate between the Panama Fracture Zone and the Colombia trench shows a highly heterogeneous Moho structure with depths up to 15 km for the Coiba ridge and a maximum of 19 km for the northeastern part of the Malpelo ridge. The Coiba and Malpelo ridges are separated by a SW-NE trending feature showing a shallower Moho along the Sandra rift.

4.6 Discussion

Considering the available constraints on the Moho structure for the Cocos Ridge, the crustal density along the ridge and the seamount segment does not differ from the density of the surrounding oceanic plate. A constant density of 2.8 Mg/m^3 was assumed for the Cocos Plate, including the seamount segment and the Cocos Ridge. This value was obtained after taking into account the constraining data on the depth of the Moho from von Huene *et al.* (2000), Walther (2003) and Sallarès *et al.* (2003), the range of density values for obtained from V_p and the analysis of the fit between the measured and the calculated gravity. Considering this results, the interaction of the Cocos Plate with the Galápagos hot spot does not seem to have long term effects on the density of the lithosphere beyond the thickening of the crust as observed on the results for the Moho depth. Locally, the crust-upper mantle system is altered by means of a thicker crust resulting in less dense material (2.80 Mg/m^3) replacing denser mantle material (3.30 Mg/m^3). Assuming a less dense oceanic crust (e.g. as an effect of the interaction with the Galapagos hot spot) would yield large misfits for the modeled gravity. For a given Moho depth of 18 km which is in agreement with the seismic constraints (Sallarès *et al.*, 2003; von Huene *et al.*, 2000; Walther, 2003), the calculated

gravity would create a misfit of up to $40x10^{-5}$ m/s^2 relative to the measured gravity if the existence of a less dense Cocos ridge crust with a density of 2.75 Mg/m^3 is assumed. A density of 2.775 Mg/m^3 would create a misfit between $10x10^{-5}$ and $20x10^{-5}$ m/s^2.

In spite of an apparent homogeneous density distribution for the oceanic crust, the influence of the origin of the oceanic crust on the Moho structure is observed for the Cocos plate. From the modeled Moho results, a distinction between 4 different segments can be drawn which correlates with morpho-tectonic domains defined by von Huene *et al*. (2000). First, the Cocos Ridge itself which shows the deepest areas of the Moho reaching a maximum of 21 km in depth. Northwest of the Cocos Ridge, the adjacent seamount segment features a smooth gradient in Moho depth between 16 and 12 km. Northwest of the Rough-Smooth-Boundary, an area with Moho depths between 11 and 9 km correlates with the oceanic crust originated at the East Pacific Rise ranging in ages between 19 and 24 m.y. according to Barckhausen *et al*. (2001). The shallowest Moho for the Cocos plate is observed offshore Guatemala and El Salvador. This area with depths shallower than 9 km corresponds to the oldest oceanic crust in the region with ages between 22 and 25 m.y. (Müller *et al.*, 2008). For the Panama Fracture Zone, a diffuse north-south trending alignment with Moho depths between 11 and 12 km is observed. On the Nazca plate, the Coiba and Malpelo ridges are separated by a NE-SW lineament of a shallower Moho which coincides with the Sandra rift.

On the Caribbean plate's continental domain, the segmentation of the crustal basement into tectonic blocks of contrasting densities and the influence of Neogene magmatism correlate with changes in the depth of the Moho. The deepest sections of the Moho are consistent with the location of the Southern Chortis Terrane and the Siuna Terrane defined by Rogers *et al*. (2007) and interpreted by Baumgartner *et al*. (2008) as the Mesquito Composite Oceanic Terrane. The presence of a thicker crust in an area where an oceanic component of the crustal basement is present instead of the crystalline Chortis Block seems contradictory.

However, it is consistent with interaction of this crustal segment with subduction related magmatism since the Miocene. Results from seismological analysis by Linkimer *et al*. (2010) show *Vp/Vs* values for the Mesquito Terrane which are related to continental crust and interpret these values as an indication of subduction related magmatism modifying the crust of the Caribbean Plate along the volcanic arc.

In Guatemala, El Salvador and northwestern Costa Rica, the crust appears to be thickened along the arc and fore-arc regions. In Nicaragua however, the axis along the Quaternary volcanic front shows a shallower Moho in comparison to the back-arc which corresponds to the Neogene arc. This section of the Moho along the Central American Volcanic Front may be explained by a shallower upper mantle as a result of extension in the overriding plate along the most pronounced sections of the Nicaragua depression. Additional evidence of the effects of magmatism on the overriding plate is observed for the back-arc of the Nicaraguan segment of the Central American Volcanic Arc. For this section, the trend in the Moho depth results and its correlation with the Quaternary arc is interrupted. Here, the axis of the deepest section of the modeled Moho shows an offset towards the Holocene back-arc which is consistent with receiver functions results from McKenzie *et al*. (2008). This trend correlates with the location of the Early Miocene volcanic arc for Nicaragua (Alvarado *et al.*, 2007) showing the influence of Neogene magmatism. The change in Moho depth between the Nicaraguan and the Costa Rican portions of the volcanic front is well constrained by published receiver function data from MacKenzie *et al*. (2008) and Linkimer *et al*. (2010) and may be related to extension along the Nicaragua depression.

The oceanic basin on the eastern part of the Caribbean Plate is outlined by the Hess escarpment and the North Panama Deformed Belt. For this region, crustal thicknesses between 12 and 17 km were obtained when accounting for bathymetry. Overall, the results from the modeled Moho show a much smoother trend in the crustal thickness for the oceanic

basin when compared with seismic results by Ewing *et al*. (1960) which show a much more heterogeneous distribution of depths between 8.5 and 17.9 km. However, the range of crustal thicknesses obtained from the density model for this area varies from 6 to 17 km which is consistent with the seismic data. For the North Panama Deformed Belt a strong gradient is observed where the Moho depth changes from 18 to 26 km consistent with crustal thickening occurring along this structure.

For the Quaternary volcanic arc, a generalized categorization for the composition of volcanic material based on Siebert and Simkin (2002) and its relation to the Moho depth is shown in figure 4.6. A general mafic trend is observed between the Tecapa and Concepción volcanoes, this correlates to the shallower Moho observed for the Nicaraguan section of the volcanic arc. This trend is in agreement with results by Carr (1984) in which a lower minimum silica content for Nicaragua relative to Guatemala and Costa Rica is observed. In addition to the regional variation in minimum silica contents, Carr (1984) shows a similar pattern for NaO_2 and correlated this segmentation in geochemistry to variations in the crustal thickness. In order to establish a correlation between geochemical variations and Moho depth, Carr (1984) presented an along-arc crustal thickness model interpreted from regional topography based on an empirical relation by Wollard (1969), as well as three schematic one-dimensional density models for the crust of the Caribbean plate. For these models, Carr (1984) assumed a constant three layer crustal model for Central America based on a one-dimensional model by Matumoto *et al*. (1977). Though it is difficult to compare a 3D model with a one dimensional model, the densities reported by Carr (1984) are generally lower than the densities obtained for this work. However, the trend in Moho depth observed along the volcanic arc is similar, with the shallowest Moho located at the Nicaraguan section of the volcanic arc and a thickened crust present toward the Guatemala and Costa Rica segments.

4.7 Conclusions

The deepest Moho for the Cocos Plate is observed along the axis of the Cocos ridge and reaches 21 km, similar values are observed for the Malpelo Ridge. On the Caribbean plate, the maximum Moho depth obtained from the density model is 44 km. The trend of the deepest sections of the continental Moho extends from southwestern Guatemala to central Costa Rica and correlates with the presence of the Central American Volcanic Arc. The influence of subduction related magmatism dating back to the Early Miocene can be observed on the recent Moho structure throughout Central America resulting on a thicker crust and more heterogeneous depth distribution relative to the back-arc. Trends in the Moho depth along the volcanic arc show the segmentation of the crustal basement with relatively flat blocks separated by transitional areas of steeply dipping Moho. The shallowest section of the Moho along the volcanic arc is observed for the Nicaraguan section where the Nicaragua depression is more pronounced. The area associated with the crystalline crustal basement of the Chortis Block features a flatter Moho relative to the surrounding crust with crustal thicknesses between 22 and 32 km. The Nicaragua Rise shows NE-SW segmentation on the Moho structure of the continental domain and a transition zone to the oceanic domain from the edge of the continental shelf to the Hess Escarpment. The oceanic basin is bound by strong gradients in the Moho depth along the North Panama Deformed Belt and to the northwest of the Hess escarpment and features crustal thicknesses between 14 and 18 km.The modeled Moho provides insights into the tectonic segmentation of the crustal basement of the Caribbean plate as well as the effects that dynamic processes such as volcanism and crustal extension may have on the present structure of the crust along the isthmus. Furthermore, the modeled boundary may be considered as a reference for local density modeling and the evaluation of the contribution of heterogeneities on the solid earth to the gravity field observed on satellite derived gravity data.

5 Density structure and geometry of the Costa Rican subduction zone from 3D gravity modeling and local earthquake data

The eastern part of the oceanic Cocos Plate presents a heterogeneous crustal structure due to diverse origins and ages as well as plate-hot spot interaction. The complex structure of the oceanic plate directly influences the dynamics and geometry of the subduction zone along the Middle American Trench. In this work, an integrated interpretation of the slab geometry is presented based on three-dimensional density modeling of satellite-derived gravity data constrained by seismological information obtained by local networks. Results show the continuation of steep subduction from the Nicaraguan margin into northwestern Costa Rica followed by a shallower slab under the Central Cordillera toward the end of the Central American Volcanic Arc. To the southeast of the termination of the volcanic arc, the slab appears to steepen and continue as a coherent structure until reaching the landward projection of the Panama Fracture Zone. Overall a gradual change in the depth of intra-plate seismicity is observed reaching 220 km for the northwestern part and becoming shallower toward the southeast where it reaches a maximum depth of 70-75 km. The changes in the depth of the observed seismicity correlate with changes in the density structure of the subducting slab and may indicate that differences in the state of initial hydration of the oceanic lithosphere affect the depth reached by dehydration reactions in the subduction zone.

5.1 Introduction

The southeastern end of the Middle American convergent margin is characterized by segmentation of the subducting oceanic lithosphere and a heterogeneous crustal basement on the overriding plate. The oceanic Cocos Plate is composed of crustal segments generated at two different spreading centers and affected by hot spot interaction (Barckhausen *et al.*, 2001). This diverse morpho-tectonic environment on the oceanic plate causes heterogeneities

that carry over to the subduction zone and affect the manner in which plate interaction occurs. Differences in the response of the lithosphere upon arrival to the trench are recognizable starting from the structure of the outer rise, the morphology of the margin and the characteristics of the subduction zone (von Huene *et al.*, 2000). This paper focuses on the geometry of the subduction zone and the density distribution of the subducting slab under Costa Rica as well as the relationship between the density structure and the distribution of seismicity. The three-dimensional density modeling based on interpretation of the satellite derived gravity data is constrained by seismological information from local networks. This joint interpretation of seismological and potential fields data allows for an integrated analysis of the geometry of the slab and its interaction with the overriding plate. The determination of the slab structure is a major task in the study of subduction zones, providing also a platform to gain a better understanding of subduction processes. Further geoscientifc studies, such as thermal and stress modeling, geochemical and petrological models, and seismic hazard assessments may benefit from detailed knowledge about the slab and overriding plate configuration

5.2 Tectonic Setting

The Central American isthmus is located in the western edge of the Caribbean Plate (Fig. 5.1), a predominantly convergent margin defined mainly by the subduction of the oceanic Cocos Plate along the Middle American Trench (MAT). Costa Rica is located in the eastern portion of the isthmus where subduction of the Cocos Plate along the MAT is bound by the Panama Fracture Zone (PFZ), a right-lateral shear zone acting as a transform boundary between the Cocos and Nazca plates. The overall structure of the southeastern part of the Cocos Plate is highly heterogeneous due to the multiple origins of the highly segmented crust (Fig. 5.1). Offshore Costa Rica, segments of oceanic lithosphere created at the East Pacific Rise (EPR) and the Cocos-Nazca Spreading Center (CNS) are present (Barckhausen *et al.*,

2001). The latter shows direct influence of the Galapagos Hot Spot adding to the heterogeneous nature of the plate and resulting in three different morphotectonic domains defined by (von Huene *et al.*, 2000): a northwestern section with smooth relief which contrasts with a central seamount province outlining a Rough-Smooth Boundary and an eastern domain characterized by the Cocos Ridge. These morphotectonic domains correlate with significant changes in Moho depth for the Cocos Plate from 8 to 10 km for the EPR section (Sallarès *et al.*, 2001), to 10 to 12 km for the seamount province (von Huene *et al.*, 2000; Walther, 2003) and a maximum of 21 km for the crust of the Cocos Ridge (Sallarès *et al.*, 2003).

Convergence rates are variable for different domains with 85 mm/y for the northwestern EPR section and 90 mm/y for the Cocos Ridge domain (DeMets *et al.*, 1994). Furthermore, oblique subduction along the MAT appears to take place in the region with a 10° counter clockwise difference in convergence direction relative to trench normal (DeMets, 2001).

Subduction related volcanism is present in the form of the Central American Volcanic Arc (CAVA) which begins at latitude 15°N and extends 1100 km parallel to the MAT ending at the Irazú-Turrialba volcanic complex in central Costa Rica (Fig. 5.1). At this point the CAVA is interrupted by a 190 km gap in the Quaternary volcanism in the Talamanca region. This gap ends at the Barú volcano, the only major Quaternary volcanic vent located in the eastern edge of the isthmus. This gap in Quaternary volcanism coincides with the convergence of the Cocos Ridge with the Middle American Trench.

Seismic tomography studies have been carried out for the area of Nicaragua and northwestern Costa Rica (DeShon *et al.*, 2006; Syracuse *et al.*, 2008), central Costa Rica (Arroyo *et al.*, 2009; Dinc *et al.*, 2010) as well as a comprehensive study of the Costa Rican subduction zone by Husen *et al*. (2003a). A previous work on the geometry of the subduction

zone based on earthquake hypocenters has been published by Protti *et al*. (1994) where segmentation of the subducting slab in northwestern Costa Rica is described and a change in the dipping angle is interpreted as a sharp contortion. Moreover, those authors propose a termination of deep intraslab seismicity in southeastern Costa Rica and interpret it as shallow underthrusting of the Cocos Ridge. Husen *et al*. (2003a) however, observe a gradual decrease in maximum depth from northern to southern Costa Rica. More recently, Dzierma *et al*. (2011) interpret a steeply dipping slab to a depth of approximately 70 to 100 km based on receiver function analysis for the northwestern part of the Talamanca region. Furthermore, local earthquake data from a temporal network present evidence of a steep slab down to ~70 km in southern Costa Rica (Arroyo *et al*., 2003; Arroyo, 2001).

Eastward from the PFZ, the boundary between the Caribbean and the Nazca plates in southern Panamá is marked by a segment of the trench which according to Lonsdale and Klitgord (1978) has transitioned since the Late Miocene to a strike-slip boundary after a period of 18 to 20 m.y. of subduction. However, deBoer *et al*. (1988) propose a reactivation of the subduction 3.4 to 5.3 million years ago and consider the existence of recent low angle subduction.

The Caribbean coast of Costa Rica appears segmented into a northwestern section extending to the Hess Escarpment and the slope of the Nicaragua Rise and a southeastern section defined by the North Panama Deformed Belt. According to Marshall *et al*. (2000), this fold-and-thrust belt is linked with the MAT through the Central Costa Rica Deformed Belt, a diffuse fault zone outlining the western boundary of the Panama Micro-plate.

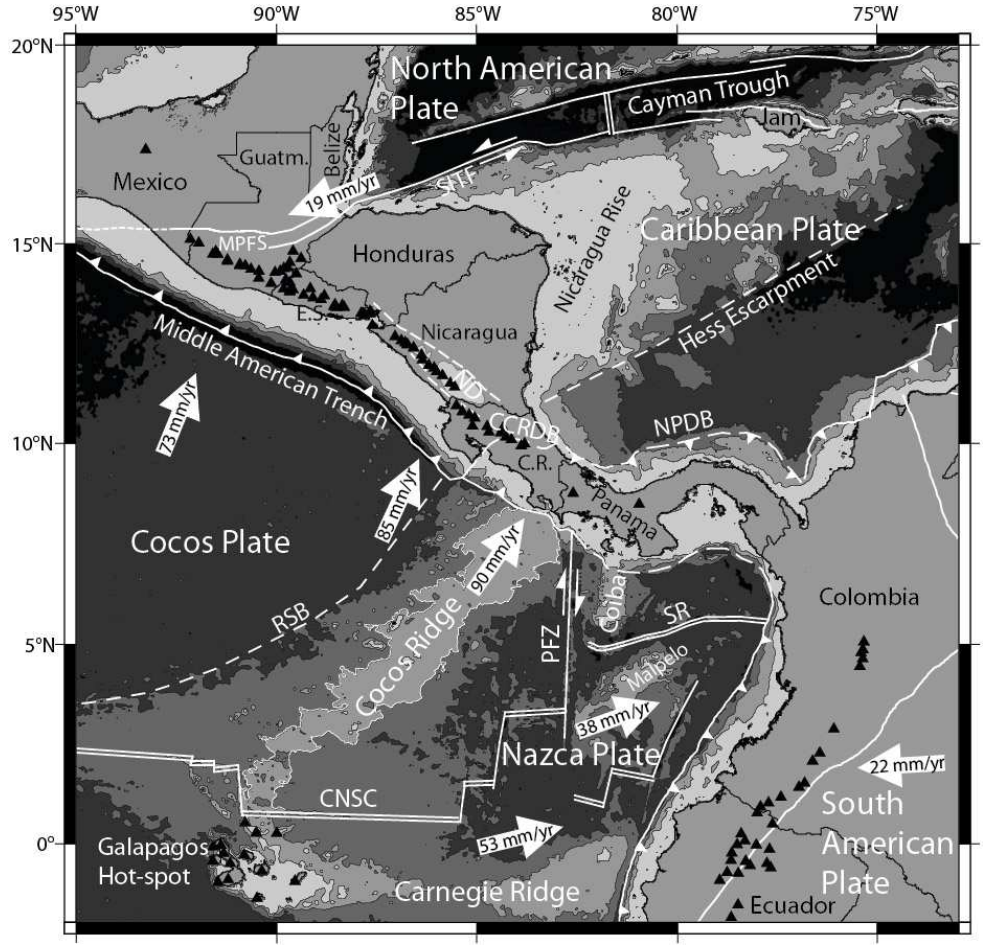

Figure 5.1. Tectonic setting of the Central American Isthmus. White lines show plate boundaries and major tectonic structures. Black triangles show main Quaternary volcanoes, modified from Siebert & Simkin (2002). White arrows show direction and rate of plate motions relative to the Caribbean Plate (fixed) according to: DeMets *et al.* (1994), DeMets (2001) and DeMets *et al.* (2010). Plate boundaries modified from Coffin *et al.* (1998) and Lonsdale (2005). Black lines depict the coastline and international borders. C.R.: Costa Rica; E.S.: El Salvador; Guatm.: Guatemala; Jam.: Jamaica; CCRDB: Central Costa Rica Deformed Belt; MPFS: Motagua-Polochic Fault System; ND: Nicaragua Depression; NPDB: North Panamá Deformed Belt; PFZ: Panamá Fracture Zone; RSB: Rough-Smooth Boundary modified from Hey (1977); SITF: Swan Islands Fault; SR: Sandra Rift (de Boer *et al.*, 1988). White contour represents the -2000 m bathymetric level outlining the Cocos Ridge, bathymetric data from Global Multi-Resolution Topography by Ryan *et al.* (2009).

5.3 Data

5.3.1 Seismological Data

Recent seismological studies (Arroyo *et al.*, 2009; DeShon *et al.*, 2003; DeShon *et al.*, 2006) have been used to constrain the slab geometry of the gravity model down to depths of ~40-50 km. In order to constrain the deeper parts of the model, earthquakes from four different catalogues were used or relocated. The earthquake catalogue from Husen *et al.* (2003a) consists of nearly 4000 events recorded by the two permanent networks in Costa Rica, Red Sismológica Nacional (RSN) and

Observatorio Vulcanologico y Sismológico de Costa Rica (Ovsicori) and is the result of their local earthquake tomography. The RSN catalogue from 1991, when digital recording started, to 2004 was also used. The network records seismic activity since the early 1980s, mainly with short-period, vertical-component stations installed throughout Costa Rica (Fig. 5.3).

Since the RSN network has a higher station density in Central Costa Rica, where most of the population of the country concentrates, two additional local catalogues were examined to in order to increase the amount of well constrained seismicity to the northwest and southeast (Fig. 5.3). The temporary Boruca network was operated by RSN in southeastern Costa Rica between May 1998 and November 2001 (Arroyo, 2001). This network consisted of two vertical-component stations and five three-component stations, all of them equipped with short-period seismometers. Readings from five short-period stations from Panama were added to the dataset, improving the coverage eastward (Fig. 5.3).

In NW Costa Rica, RSN operates the permanent network from Observatorio Sismológico y Vulcanológico Arenal y Miravalles (OSIVAM) since 1994. Originally intended to monitor the seismic activity around Arenal and Miravalles volcanoes, the network has expanded in the last decade with a two more permanent subnetworks around Tenorio and Rincón de la Vieja volcanoes and several temporal projects (Fig. 5.3). The network configuration has varied over time. Presently, the subnetworks consist of four to eight, three-component, short-period stations each and one broadband station at the Tenorio Volcano. Other temporary stations have been placed in the area of the Nicoya Peninsula and toward the border with Nicaragua. The catalogue used in this study extends from October 2006 until December 2010, when all four permanent sub-networks were recording simultaneously and includes readings from 44 stations.

5.3.2 Gravity Data

The EGM2008 combined geopotential model (Pavlis *et al.*, 2008) was used as the source of gravity data for the 3D density model and was obtained through the International Centre for Global Earth Models (ICGEM, under: http://icgem.gfz-

potsdam.de/ICGEM/ICGEM.html). With a maximum spatial resolution of approximately 10 km, this geopotential model combines data from the GRACE satellite mission as well as satellite altimetry data offshore and surface stations data onshore (where available), which are reduced to a 5'x5' grid. To this date, the latest combined geopotential model available is the EIGEN-6C (Förste *et al.*, 2011) which additionally includes data from the LAGEOS and GOCE satellite missions. However, for purposes of consistency with regional lithospheric density modeling carried out for Central America (Lücke, 2012) and in order to resolve the shorter wavelengths obtained from a higher degree, the local density model was based on EGM2008.

In order to assess which individual dataset was adequate for the density modeling, different anomalies were calculated and compared with surface station data. A detailed analysis of a data subset for Costa Rica was carried out by Köther *et al*. (2011). To provide a dataset consistent with previous solid Earth modeling (Lücke *et al.*, 2010; Lücke, 2012), the Bouguer anomaly for this work was calculated from the gravity disturbance. The gravity disturbance is calculated for a given point on the Earth's surface and for the satellite derived gravity disturbance data used for this study, the downward continuation takes place between the orbit and the surface of the Earth. Discussions on the use of gravity anomalies and disturbances in solid Earth modeling are given by Li and Götze (2001). Onshore, the effect of the Bouguer plate was subtracted from the value of the gravity disturbance using the orthometric height at the topographic level as station elevation resulting in Bouguer anomaly values. For data located offshore, values equivalent to the free-air anomaly were obtained for stations located on the ocean's surface. Figure 5.2 shows a compilation of the Bouguer anomaly onshore and the free-air anomaly offshore for the study area.

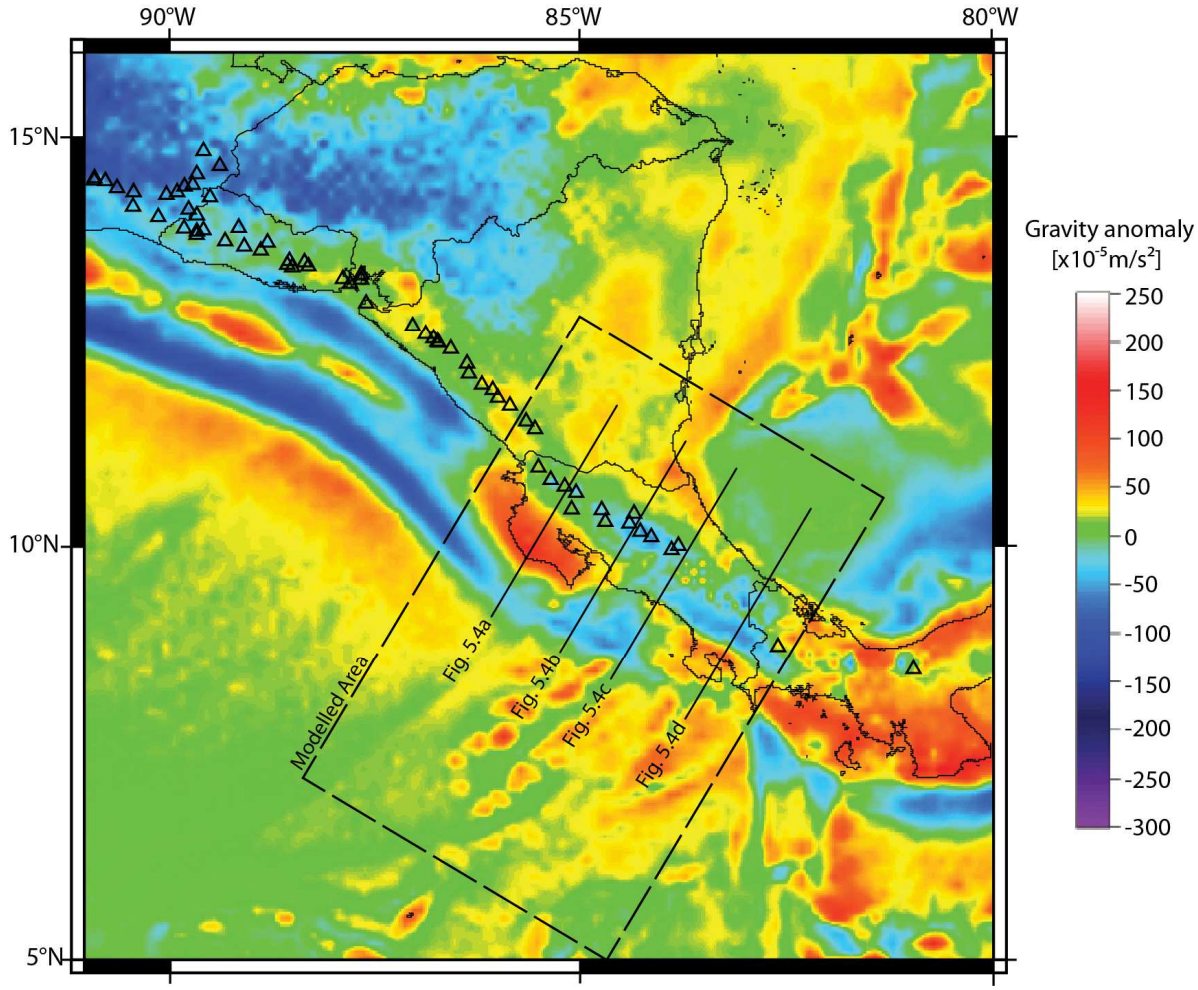

Figure 5.2. Gravity field data for the Central American isthmus and surrounding areas. Bouguer anomaly onshore and free-air anomaly offshore calculated for this study from gravity disturbance data from EGM2008. Location of the cross sections shown in figure 5.4 and the area of the local scale density model for Costa Rica are indicated. Triangles show the location of Quaternary volcanoes modified from Siebert and Simkin (2002). International borders and coastline are shown in black.

5.4 Methods

5.4.1 Earthquake Relocation

The tomography earthquake dataset from Husen *et al.* (2003a) has been used as published by those authors. An analysis of relocation uncertainties is included in their work. The 3D P-wave velocity model from Husen *et al.* (2003a) and the minimum 1D model for Costa Rica from Quintero and Kissling (2001) were used to relocate RSN, Boruca, and OSIVAM databases with the non-linear probabilistic approach (Moser *et al.*, 1992; Tarantola and Valette, 1982) implemented in the software package NonLinLoc (Lomax *et al.*, 2000).

The approach relies on the use of normalized and unnormalized probability density functions to express the available knowledge about the values of parameters. When the density functions, given the a priori information on the model parameters and on the observations, are independent and the theoretical relationship can be expressed as a conditional density function, a complete, probabilistic solution can be expressed as an a posteriori density function (PDF) (Tarantola and Valette, 1982). Final hypocenter locations are given by their maximum likelihood value, i.e. the minimum misfit point of the complete PDF. Further details are given by Tarantola and Valette (1982) and Moser *et al*. (1992).

The PDF solution includes location uncertainties due to the spatial relation between the network and the event measurement error in the observed arrival times and errors in the calculation of theoretical travel times. Because error estimates are included through covariance matrices and the solution is fully nonlinear, location uncertainties may assume irregular and multimodal shapes. In this case, the traditional error ellipsoids are not able to represent the location error (Husen and Smith, 2004). NonLinLoc also provides traditional Gaussian estimates, like the expectation hypocenter location and the 68% confidence ellipsoid (Lomax *et al.*, 2000).

5.4.2 Gravity Modeling

The density model was prepared by means of three-dimensional interactive forward modeling of gravity data using the software IGMAS+ (Götze *et al.*, 2010). With this software, parallel cross sections are constructed and can be modified interactively. Between these cross sections, the three dimensional structure is triangulated to form polyhedra of constant density which represent the structure of the subsurface. The calculation of the effect on the gravity field from each polyhedron is carried out by the algorithm of Götze (1976) and Götze and Lahmeyer (1988). The calculated gravity field is then compared with the measured gravity data to achieve the best fit. Available geophysical data were incorporated as

constraints to the model and visualized in three dimensions to aid the interactive modeling. For the regional reference model of Central America, 47 cross sections were constructed extending from the Yucatan Peninsula to eastern Panama. From the regional density model, a subset was defined and further detailed by taking into account the constraining seismological data prepared for this work and the previously available geophysical data. For this area, 24 cross sections were considered and modeled in detail with a focus on the subducting slab and the integration with the seismological results for Costa Rica.

5.5 Results

5.5.1 Seismology

Analysis of probabilistic earthquake relocation uncertainties in 3D velocity models (Husen *et al.*, 2003b; Husen and Smith, 2004) shows that, in general, hypocenter locations with less than six P-wave observations are poorly constrained, even with a good azimuthal distribution of stations (coverage gap < 180°). In addition, focal depths are not well constrained without a station located within a distance similar to the focal depth, regardless of the total number of observations. For this study, these criteria were used to select the datasets from the initial seismic catalogues.

The RSN, OSIVAM, and Boruca datasets were relocated and classified into four quality classes using NonLinLoc. For the two first datasets, the 3D P-wave velocity model from Husen *et al*. (2003a) was used. Since several Boruca-Panama stations were located out of that model (Fig. 5.3), the minimum 1D P-wave model for Costa Rica from Quintero and Kissling (2001) was used to relocate the events from that network. This 1D model served as initial model for the tomography by Husen *et al*. (2003a). In all three cases, only P-wave readings were considered.

The Oct-Tree importance sampling algorithm included in NonLinLoc was used. This algorithm gives an accurate, efficient and complete mapping of the earthquake location PDF in the 3D space. The Oct-Tree method uses recursive subdivision and sampling of cells in 3D space to generate a cascade of sampled cells, where the density of sampled cells follows the PDF values of the cell center leading to a higher density of cells in the areas of higher PDF.

Large differences between the maximum likelihood and the expectation hypocenter locations can result from an ill-conditioned location problem (Lomax *et al.*, 2000). Husen and Smith (2004) found that a difference greater than 0.5 km between both hypocenter estimations cause large uncertainties of several kilometers in epicenter and focal depth. Numerous scatter plots were investigated in order to confirm this observation for our datasets. Further following Husen and Smith (2004), the average of the three axes of the 68% confidence ellipsoid was taken into account to refine location quality. Figure 5.3 shows example scatter plots for each quality class used in this work.

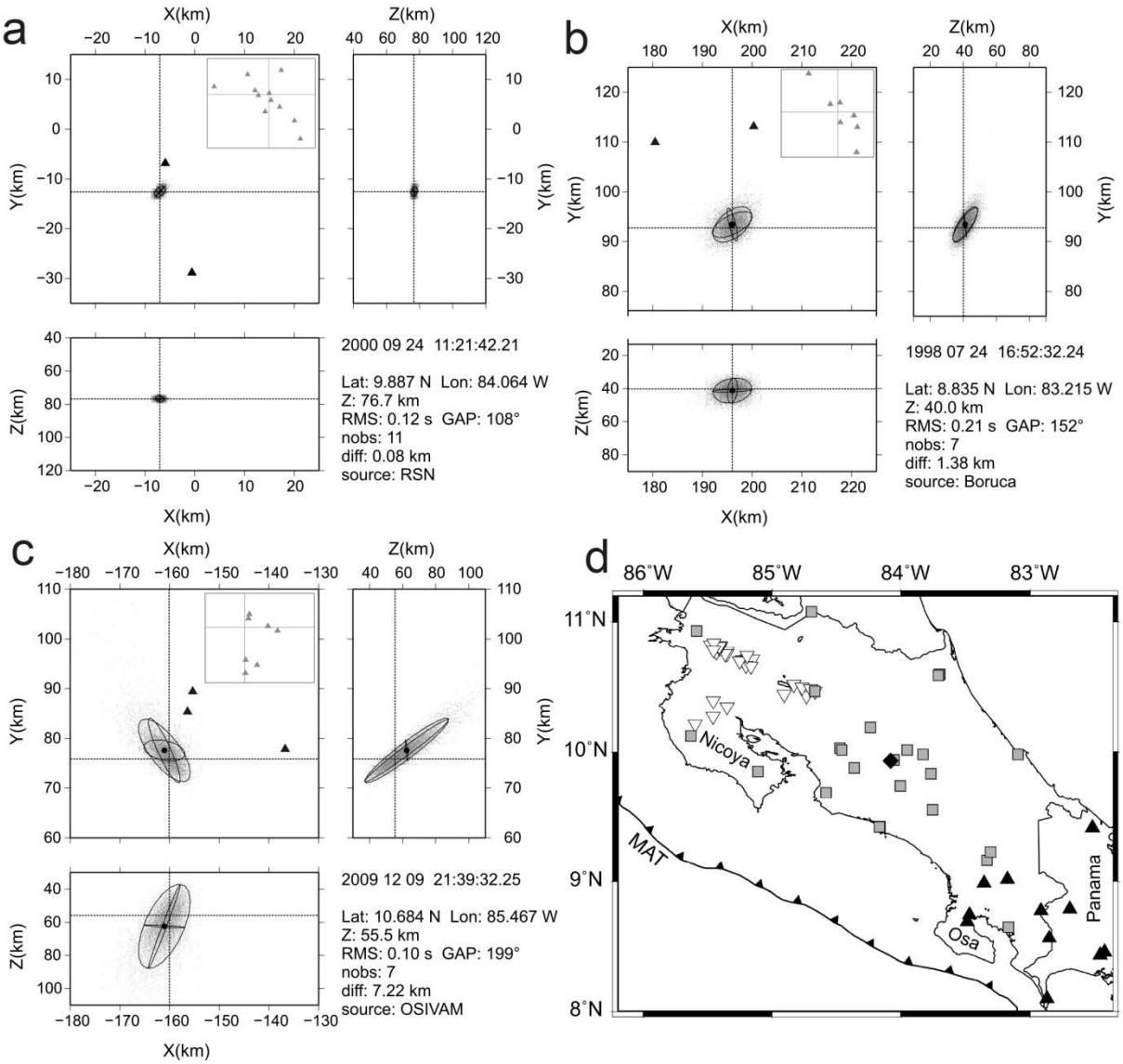

Figure 5.3. Density scatter plots of representative earthquakes for each quality class: A (a), B (b), and C (c) used in this study (see text) and seismic stations map (d). In the map, squares represent RSN stations, inverted triangles OSIVAM stations and black triangles Boruca stations (see text for network descriptions). The dented line marks the MAT axis. Scatter plots: plan view in x–y direction and cross sections in x–z and y–z directions are shown. The intersection of the dashed lines marks the maximum likelihood hypocenter locations. Black circles denote expectation hypocenter locations. Projection of the 68% confidence ellipsoid is shown by black lines. The insets include all the seismological stations (triangles) used to locate the earthquakes (intersection of bold lines). Nobs: number of observations, diff: difference between maximum likelihood and expectation hypocenter locations.

Earthquakes in class D have rms larger than 0.5 s and are not used. Events with location quality A, with well-defined PDFs, have differences between maximum-likelihood and expectation hypocenters of 0.5 km and lower, and maximum location uncertainties of 4 km. Differences above 0.5 km but under 3 km between both hypocenter estimations and average uncertainties lower than 4 km define quality B. Their epicenters and focal depths are still

relatively well defined. Earthquakes with a maximum rms of 0.5 s and differences in hypocenter estimations higher than 3 km are classified as C. They show large location uncertainties, of which the confidence ellipsoid is a poor approximation.

5.5.2 Density Model

The lithospheric density distribution was modeled in three dimensions to a depth of 200 km for a regional Central American model published by Lücke (2012). Using the regional model as reference, a subset was modeled in detail for Costa Rica considering the availability of geophysical constraints. Offshore Costa Rica, the Cocos Plate was modeled with a density of 2.80 Mg/m^3 for the crust, 3.3 Mg/m^3 for the upper mantle and 3.34 Mg/m^3 for the asthenospheric mantle. Density changes in the subducting slab were also modeled as an increase in density due to dehydration of the mantle and crust. The density of the crust of the subducting slab was constrained by petrological modeling by Bousquet *et al*. (2005) considering the lithostatic pressure on the plate interface and the temperature from thermal modeling by Peacock *et al*. (2005). A homogenous upper mantle with a density of 3.32 Mg/m^3 and a 3.34 Mg/m^3 asthenospheric mantle were modeled for the overriding plate, setting the lithosphere-asthenosphere boundary at a depth between 75 and 85 km. The crustal basement for the Caribbean Plate in Costa Rica was divided into a southeastern block with a density of 2.90 Mg/m^3 considering an overall basaltic composition of the basement related to the Caribbean Large Igneous Province (Hoernle *et al.*, 2004), and a northwestern block with a density of 3.00 Mg/m^3 for serpentinized ultramafic material related to the Mesquito Composite Oceanic Terrane (Baumgartner *et al.*, 2008). Densities in the upper crust of the Caribbean Plate are variable and were modeled depending on local structures such as predominant fore- and back-arc sedimentary basins (2.4 - 2.55 Mg/m^3), volcanic infill along the arc (2.6-2.7 Mg/m^3) and dioritoid intrusions in southeastern Costa Rica (2.75 Mg/m^3). The initial density of the crustal units of the Caribbean Plate was constrained by Vp values

and the correlation with local geology and regional tectonic models. A detailed discussion on the constraints of the densities used for the 3D model is given by Lücke (2012).

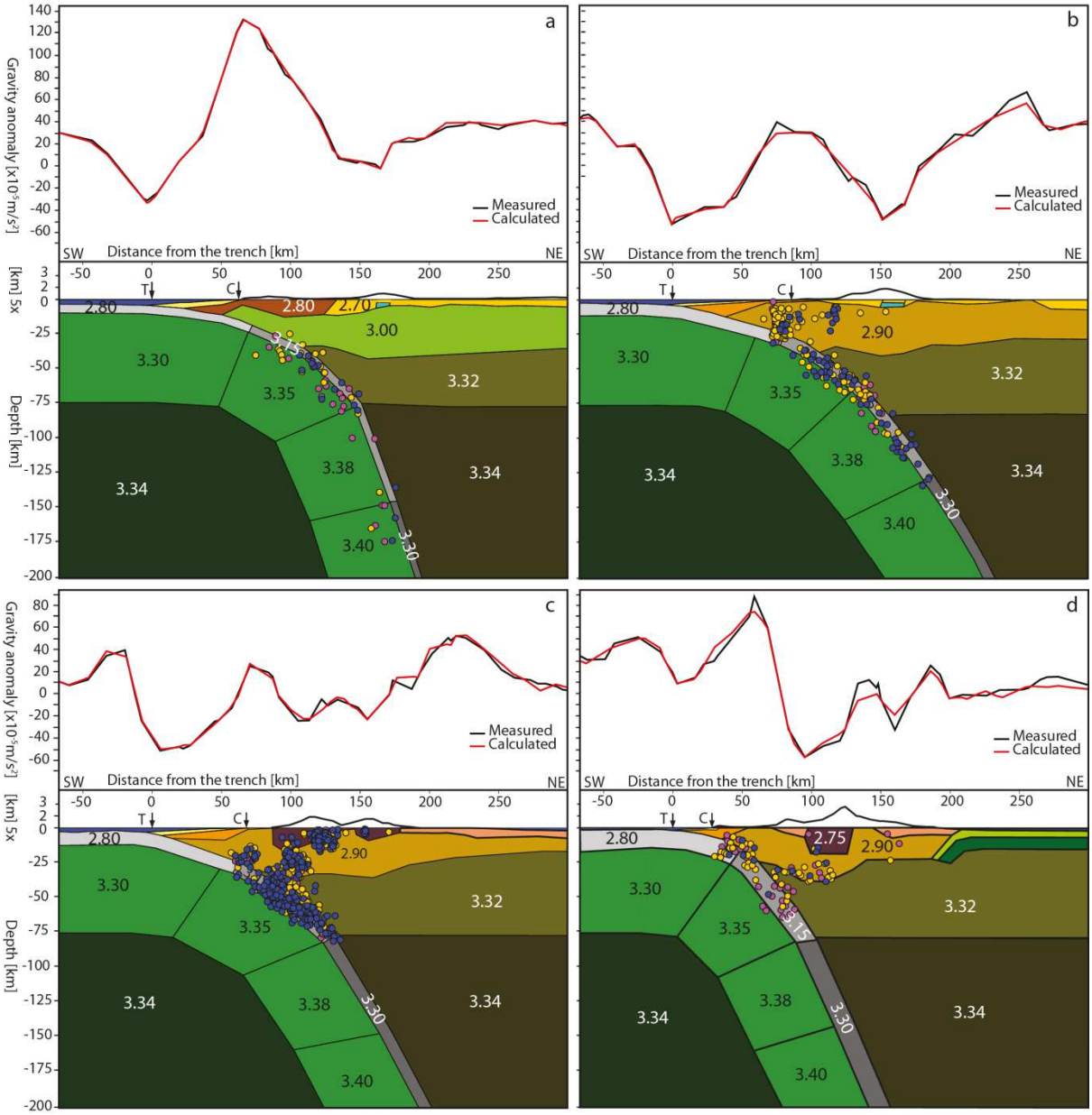

Figure 5.4. Vertical cross sections from the local scale 3D density model and relation to the integrated earthquake hypocenter locations for this work. The upper panels show the fit between the measured (black) and calculated (red) gravity anomaly. Circles show the earthquake hypocenters color coded for classes: A (blue), B (yellow) C (magenta). The modeled density distribution of the subducted oceanic crust is depicted in gray tones: 2.80 Mg/m^3 (light gray), 3.15 Mg/ m^3 (medium gray), 3.30 Mg/ m^3 (dark gray). Location of the cross-sections is shown in figure 5.2.

5.5.3 Regional Scale Slab Geometry as a Reference Model

Figure 5.5 shows the geometry of the Central American subduction zone, modeled on a regional scale to serve as a reference model for the Costa Rican subset. In order to constrain the regional geometry of the subduction zone, hypocenters from the catalogue of the Central American Seismic Center (CASC) hosted by the RSN were included. The CASC catalogue includes earthquakes with magnitudes above 3 and recorded by at least two national networks. The selected events have a minimum of 8 readings, a coverage gap of less than 250 degrees, a maximum rms of 0.6 s and Gaussian uncertainties lower than 10 km in depth. Additionally, earthquake hypocenters from the catalogue of the National Earthquake Information Center of the United States Geological Survey were included to constrain the regional slab structure for depths greater than 110 km which were not resolved by the CASC network in some areas.

The regional scale model provides the three-dimensional framework for the detailed interpretation of the Costa Rican subduction segment along the MAT, constrained by the local earthquake data presented for this work. The regional scale model considers the segmentation of the Central American crustal basement and the regional Moho structure for the Caribbean Plate published by Lücke (2012). The geometry obtained from the regional model shows a uniformly dipping slab for the segment between 91°W and 86°W. The subduction angle steepens for the southern Nicaragua segment and carries over to northwestern Costa Rica (Fig. 5.5). The larger heterogeneities in the geometry of the subduction zone are observed for the segment located eastward of the 86°W longitude and will be described in detail for the local scale model for the area.

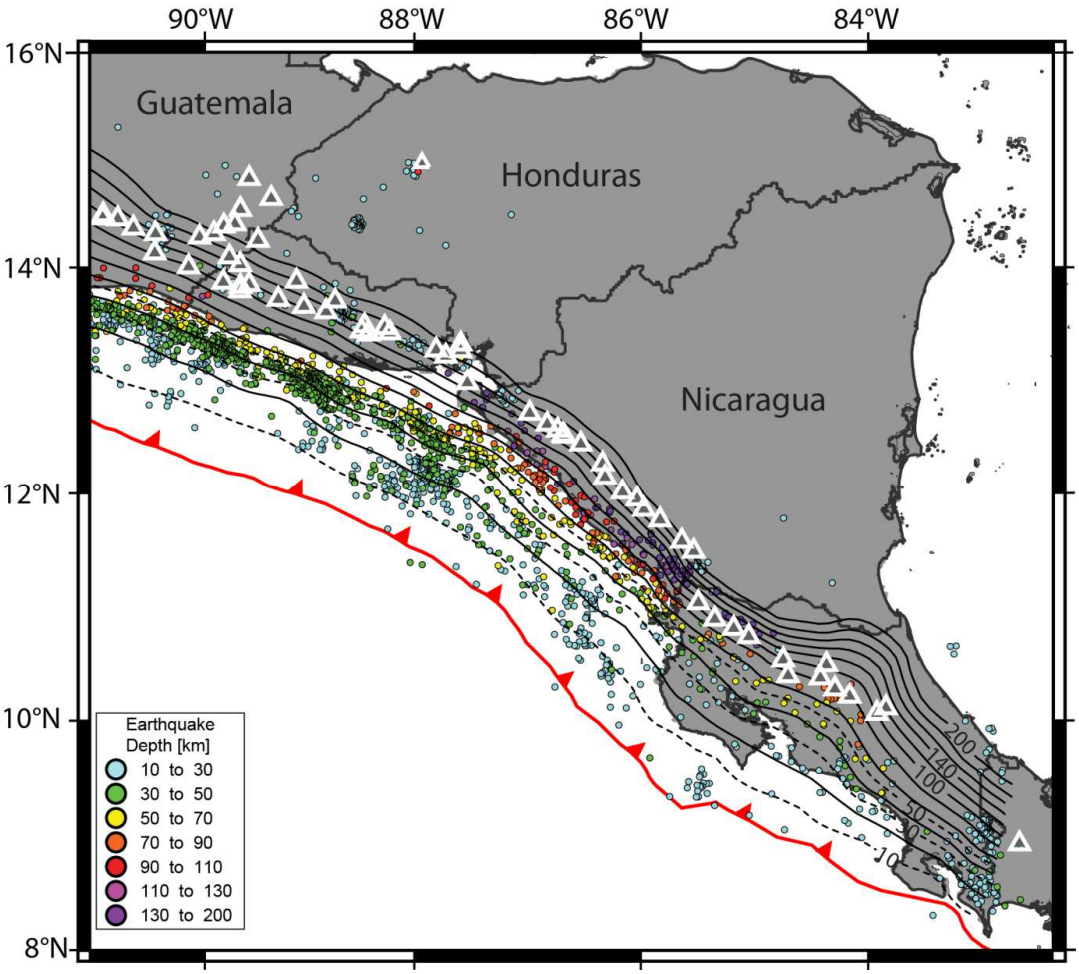

Figure 5.5. Slab depth contours for the Central American subduction zone from the regional scale 3D density model published by Lücke (2012) and integrated with the local scale interpretation for this study. Earthquake hypocenters from Central American Seismological Center. Earthquake depths as indicated in the inset. White triangles show the location of Quaternary volcanoes modified from Siebert and Simkin (2002). International borders and coastline are shown in black.

5.5.4 Local Integrated Interpretation of Slab Geometry for Costa Rica

In order to achieve a three-dimensional interpretation of the geometry of the subducting slab, the earthquake hypocenter results were integrated into the density model. By means of three-dimensional visualization and projection of results onto two-dimensional cross sections, the density model was modified interactively to achieve the best fit with the measured gravity data considering the structure outlined by the seismicity. The joint interpretation allowed to constrain the overall geometry of the density model while simultaneously accounting for a more precise determination of the plate interface.

The results are shown in in figures 5.6 and 5.7. Considerable changes in slab dip as well as in the density distribution of the subducted oceanic crust are observed. The Cocos Plate segmentation observed offshore Costa Rica (von Huene *et al.*, 2000) carries over to the structure of the subducted slab. The northwestern section of the Cocos Plate (originated from the EPR and CNS) was modeled with a thickness of 6 to 8 km and subducts at an angle of 14° to a depth of 30 km from which the slab dip steepens to an angle of 44° to a depth of 80 km and finally 71° to the terminal depth of the model at 200km (Fig. 5.4a). For Central Costa Rica, the slab dip transitions from an angle of 15° for the section between the trench and a depth of 30 km, 40° to a depth of 80 km and a relatively shallow angle for the final section with 58° to a depth of 200 km (Fig. 5.4b). This shallower section of the slab extends to the southwest toward the end of the Quaternary volcanic arc and corresponds to the subduction of the seamount province located between the Fisher Seamount and the Quepos Plateau on the oceanic plate.

At the southeastern end of the Quaternary volcanic arc, a change in the dip angle of the slab beneath 80 km depth is observed increasing from 40° to 60° (Fig. 5.4c). When observed as plotted depth contours (Fig. 5.6) this change in slab dip occurs 20 km to the northwest of the NNE-SSW axis formed by the Irazu and Turrialba volcanoes. This also coincides with the location of a feature in the gravity field which separates this volcanic complex from the three other stratovolcanoes that constitute the Central Cordillera of Costa Rica. This segmentation of the local Bouguer gravity low has been described by Lücke *et al.* (2010) for Central Costa Rica based on a local database compiled from surface gravity measurements and is present in the EGM2008 data. Southwest of this alignment, the earthquake hypocenters outline a steeply subducting slab with an angle of 50° to a depth of 70 km. This structure is consistent with gravity modeling carried out for this work. The density model considers a continuous slab structure with an angle of 64° for the final section

to a depth of 200 km (Fig. 5.4d). The geometry observed for the sections depicted in figures 5.4c and 5.4d is also consistent with local earthquake seismic tomography results by Dinc *et al*. (2010) and receiver functions results published by Dzierma *et al*. (2011).

Intraslab seismicity in the southeastern part of Costa Rica is interrupted by a 55 km long gap in the onshore area adjacent to the Coronado Bay (Fig. 5.6) and then resumes to the northeast of the Osa Peninsula (Arroyo, 2001).

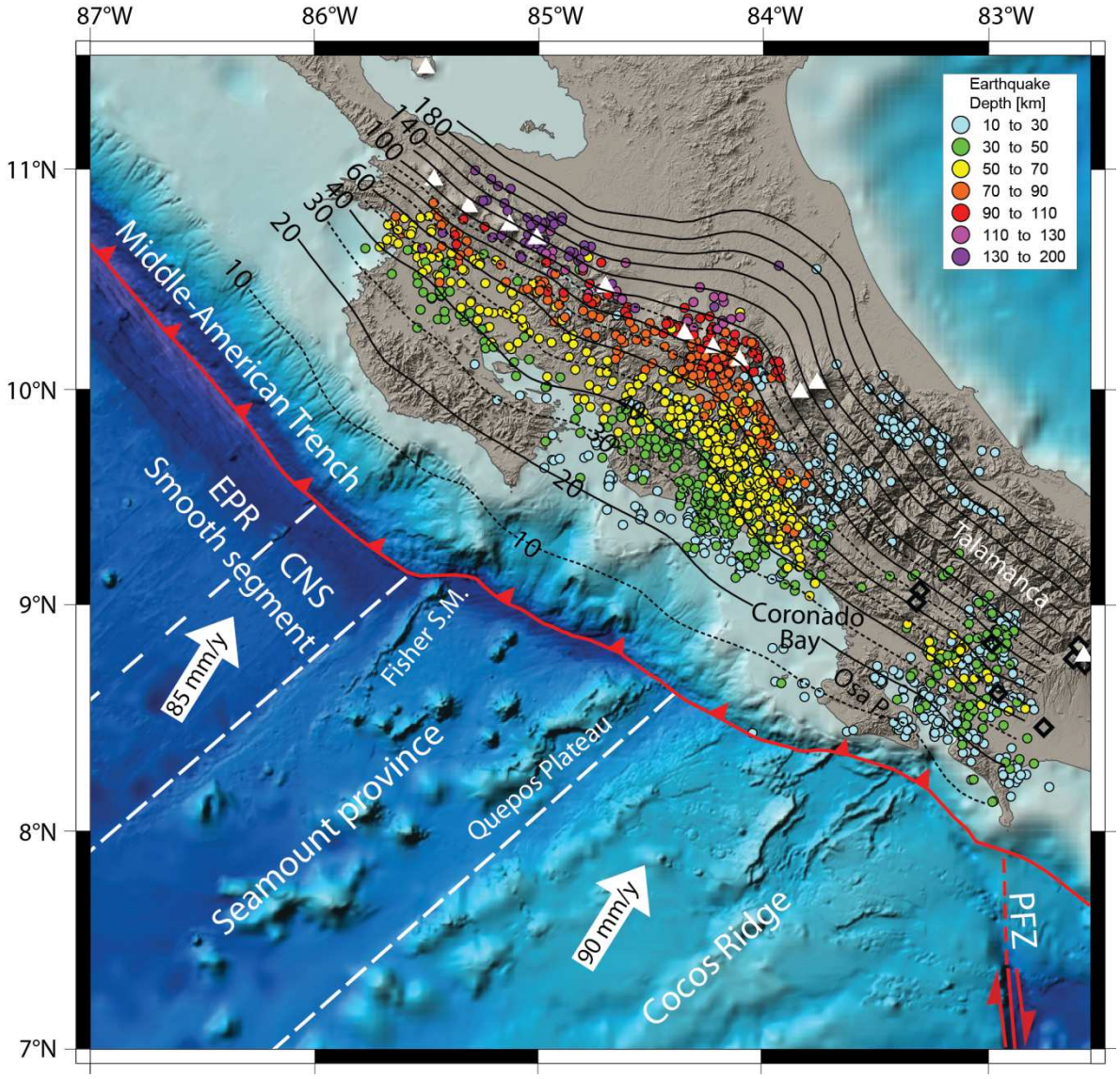

Figure 5.6. Slab depth contours for Costa Rica from the integrated interpretation of seismological and density modeling results. White arrows indicate direction and rate of plate motion from DeMets (2001) and DeMets *et al*. (1994). Earthquake depths as indicated in the inset. Tectonic features on the oceanic plate after *von* Huene *et al*. (2000) and Barckhausen *et al*. (2001). The dented line represents the axis of the Middle American Trench. EPR: East-Pacific Rise, CNS: Cocos-Nazca Spreading Center, PFZ: Panama Fracture Zone. Bathymetric data from Global Multi-Resolution Topography by Ryan *et al*. (2009). Open diamond symbols show the location of adakite samples from Hoernle *et al*. (2008) and Gazel *et al*. (2011).

In this southeastern most section of convergence of the Cocos Plate, the seismicity reaches 70 km in depth (Fig. 5.4d) and outlines a subducting slab consistent with the geometry observed westward of the seismic gap in the Coronado Bay region (Arroyo *et al.*, 2003). In spite of the presence of such gap, the gravity field does not show segmentation that could be related to major changes in subduction geometry. Overall, the results of the density modeling support the existence of a continuous slab structure.

The vertical extent of the Wadati-Benioff zone seismicity correlates with the section of the subducted oceanic crust with a density of 3.15 Mg/m^3. This part of the slab represents the zone in which dehydration reactions occur. The deepest part of the modeled subducted crust was assigned a density of 3.3 Mg/m^3 to account for an anhydrous slab. The downdip extension of the 3.15 Mg/m^3 zone is variable (Fig 5.7).

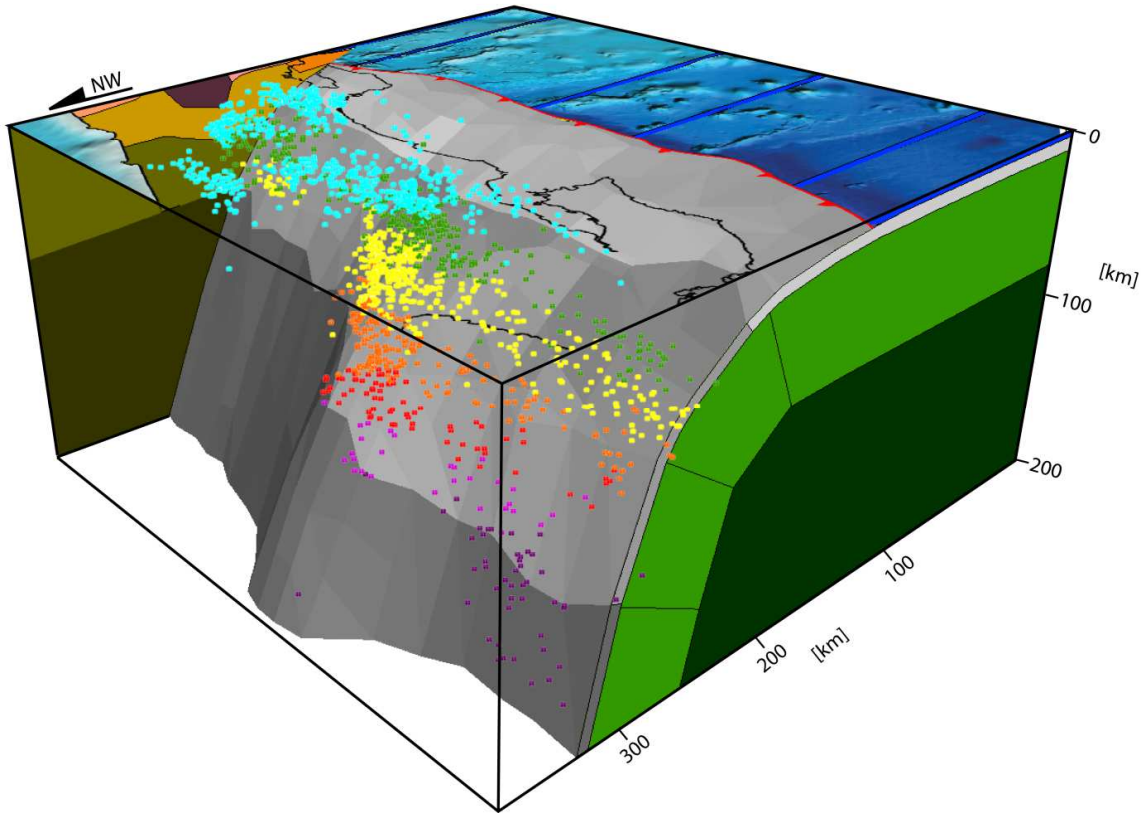

Figure 5.7. Three-dimensional perspective view of the top of the slab from the local density model integrated with seismic hypocenters. Earthquake depths as indicated in Figure 5.6. The modeled density distribution of the subducted oceanic crust is depicted in gray tones: 2.80 Mg/m^3 (light gray), 3.15 Mg/ m^3 (medium gray), 3.30 Mg/ m^3 (dark gray). Bathymetry data from Global Multi-Resolution Topography by Ryan *et al.* (2009).

For the southeastern part of Costa Rica it correlates with the lithosphere-asthenosphere boundary (LAB) modeled between 70 and 80 km, whereas it is located much deeper than the local LAB in the northwestern part of Costa Rica, between 130 and 160 km.

5.6 Discussion

The origin of the Wadati-Benioff seismicity has been a subject of discussion since its discovery because at depths superior than ~30 km the great pressures should prevent brittle or frictional processes. It is commonly believed that the intermediate-depth seismicity is enabled by slab dehydration (Hacker *et al.*, 2003; Kirby *et al.*, 1996). As the slab sinks, metamorphic reactions liberate fluids from hydrous phases. Dehydration increases pore pressure, thus reducing normal stress enough to bring the system into the brittle regime. Yet, the exact relationship between dehydration and earthquake nucleation is not yet well understood. Earthquakes could be generated by dehydration embrittlement creating new faults (Zhang *et al.*, 2004) or reactivating pre-existing weak zones (Peacock, 2001), depending on where hydration occurred (Ranero *et al.*, 2005).

Recently, Ranero *et al.* (2005) statistically compared the strike of bending-related faults in the oceanic plate with that of the nodal planes of intermediate-depth earthquakes (> 70 km) along different segments of the Middle America and Chile subduction zones. The similarity they found supports previous studies from other subduction zones of the world (Jiao *et al.*, 2000), attributing most of the intraslab seismicity to reactivation of faults rather than formation of new ones at the planes of maximum shear within the slab. *Ranero et al.* (2005) propose that seismicity starts between 60-80 km, when dehydration of the oceanic crust reactivates the upper segment of bend-faults, causing concentration of earthquakes on the upper part of the slab. Deeper than ~100 km, eclogitization is completed; here or slightly deeper, dehydration of the slab mantle occurs reactivating bend-faults and generating

seismicity within the upper slab mantle. The authors point out that this model may not be applicable to subduction of young lithosphere and broad aseismic ridges.

Tomographic studies (Arroyo *et al.*, 2009; DeShon *et al.*, 2006; Husen *et al.*, 2003a) indicate the existence of a low-velocity hydrous oceanic crust in the subducting plate in northwestern and central Costa Rica. The petrologic modeling from Husen *et al*. (2003a) show a good correlation between the predicted locations of hydrous minerals in the oceanic crust and the hypocenters of intermediate-depth earthquakes, further supporting the hypothesis of the latter being enabled by dehydration.

5.6.1 Continuous Slab Model for Costa Rica

In northwestern Costa Rica, the geometry of the subducting slab is consistent with the trench-normal subduction of the 24 to 25 m.y. oceanic crust generated at the EPR (Barckhausen *et al.*, 2001). This section presents a steeply subducting slab (Fig 5.4a) with a geometry consistent with that observed for the Nicaraguan section of the MAT (Syracuse *et al.*, 2008). Between the northwestern part of the volcanic arc and the central region of Costa Rica, a change in slab dip is observed. For the central part, results show slab dip angles between 40° and 50° consistent with previous local earthquake seismic tomography results by Arroyo *et al*. (2009) and Husen *et al*. (2003a). This section of the slab corresponds to the subduction of the seamount province of the Cocos Plate (von Huene *et al.*, 2000). The northwestern and central regions are separated by a transition zone in which the slab dip beneath 40 km decreases from 75° to 45° (Fig. 5.6). For this region, the trend of the slab contours changes from trench parallel for the northwestern region, to a 17° offset from trench parallel for the transition zone. This change in the strike of the depth contours is consistent with the section of the margin where oblique subduction occurs, located to the southeast of the Rough-Smooth-Boundary.

Southeast of the Cordillera Central, seismicity within a steep slab is observed to a depth of approximately 75 km, extending southwest to Uvita. The presence of a steeply subducting slab for this region is supported by seismic tomography results from Dinc *et al*. (2010) to a depth of 40 km and receiver functions results by Dzierma *et al*. (2011) where a steeply subducting slab is imaged to a depth of 100 km. Furthermore, by considering the structure beneath the northern part of Talamanca resolved by receiver functions, Dzierma *et al*. (2011) suggest that steep subduction below 50 km may extend eastward to the Panama Fracture Zone.

The results from the Boruca seismological network in southeastern Costa Rica show the structure of a subducting slab dipping at an angle of 50° for the region northeast of the Osa Peninsula to a depth of 70 km (Figs 5.4c and 5.6). These results, along with the receiver functions and seismic tomography data immediately to the northwest, were included as constraints into the density model. Regarding the slab geometry, the results from the three dimensional density modeling are in agreement with the seismological observations. Furthermore, the density model shows no large-scale lateral segmentation of the subducting oceanic lithosphere for the area in which a gap in the seismicity is observed (Coronado Bay, Fig. 5.6). This suggests that a continuous subducting slab is present for the margin from central Costa Rica to the Panama Fracture Zone.

Lateral changes in the density structure of the slab are limited to the section of the subducted oceanic crust with a density of 3.15 Mg/m^3 (Fig 5.4.). This three-dimensional polyhedron was modeled to represent the zone in which dehydration reactions occur contrasting with a of 3.3 Mg/m^3 zone for an anhydrous slab taking into account the maximum depth of the seismicity. From the joint seismological-density interpretation, an overall trend is observed in which the maximum depth for the dehydrating oceanic crust decreases toward the southeast from 160 km in the northwest, to 125 km for the central region and 75 km depth for

southeastern Costa Rica. This trend may be related to the extent of hydration of the upper mantle in the subducting oceanic plate in the form of serpentinization. Petrological models by Husen *et al*. (2003a) place the boundary in which the subducted crust transforms to anhydrous eclogite at 100 km for southeastern Costa Rica and 130 km for northwestern Costa Rica thus observing a similar trend. The depth of the 3.15 - 3.3 Mg/m^3 boundary in the subducted crust of the density model shows a correlation with the termination of the seismicity with depth (Fig. 5.4).

Within the conceptual model from Ranero *et al*. (2005), the degree of bend faulting occurring in the outer rise would directly influence the characteristics of the intraslab seismicity by determining both the extent of hydration through serpentinization of the upper mantle and the segmentation of the slab by means of fragile deformation. In this sense, the Costa-Rican subduction zone provides a wide spectrum of environments with different degrees of bending related faulting.

A smooth segment in which the oceanic plate presents pervasive, trench-parallel bending-related faulting subducts off Central America and northwestern Costa Rica. Here, pervasive faulting along the trench has been imaged by high-resolution seafloor mapping, near-vertical reflection lines and outer-rise seismicity (Grevemeyer *et al.*, 2007; Hinz *et al.*, 1996; Lefeldt and Grevemeyer, 2007; Ranero *et al.*, 2003; von Huene *et al.*, 2000). In the Central Pacific (seamount) segment though, the thicker oceanic crust promotes a smaller outer rise and less-developed faulting (von Huene *et al.*, 2000), while the Cocos Ridge section in the southeast, lacks bending related faulting. Moreover, Rüpke *et al*. (2002) show considerable differences in serpentinization of the upper mantle for the Cocos Plate for the smooth segment in comparison with the seamount province. In Nicaragua, the subducting oceanic plate generated at the EPR shares characteristics with the oceanic plate offshore northwestern Costa Rica in terms of origin, composition, age and thickness (Barckhausen *et*

al., 2001; von Huene *et al.*, 2000). Also, the tectonic fabric observed in bathymetric data for Nicaragua indicates the same magnitude of normal faulting of the outer rise observed offshore Costa Rica by Ranero *et al*. (2003). For this section of the Cocos plate, Rüpke *et al*. (2002) estimate a 10 km thick serpentinized mantle layer with a 5.5 wt% of water whereas for central Costa Rica, a 5 km thick 2 wt% H_2O layer is considered.

This considerable contrast in the serpentinization of the upper mantle via bend-faulting on the outer-rise indicates that the hydrated mantle may reach greater depths in northwestern Costa Rica, thus accounting for the greater depth of the 3.15 Mg/m^3 zone where intra-plate seismicity nucleates. Offshore southeastern Costa Rica, the bending-related faulting is absent and the structure of the oceanic plate is heavily influenced by the Cocos Ridge, which features a thickened crust with maximum Moho depths of 21 km (Sallarès *et al.*, 2003; Walther, 2003). The anomalous thickness of the Cocos Ridge and the absence of bending-related faulting near the trench may hinder the process of mantle serpentinization by interaction with seawater. We suggest that the shallow depth to which intraslab seismicity is observed northwest of the Osa Peninsula may be related to a lower percentage of chemically bound water in the slab due to a lack of mantle serpentinization through bending related faults.

The adakites found in southeastern Costa Rica and western Panama (de Boer *et al.*, 1991; Drummond *et al.*, 1995) have been linked to the melting of the edge of the slab by means of interaction with hot mantle through either a slab window (Abratis and Wörner, 2001; Johnston and Thorkelson, 1997) or a slab detachment (Gazel *et al.*, 2011) below the Costa Rican section of the Talamanca Range. These interpretations assume that the melting takes place at the leading edge of the subducting slab generating adakitic melts through the interaction of the subducted oceanic crust with the asthenospheric mantle underneath the western section of the Talamanca Range. The slab detachment model requires a segment of

the Cocos Plate slab to be absent and replaced by asthenospheric mantle. This detachment is inconsistent with the primary model of the density distribution in the lithosphere obtained from the interpretation of the gravity data for southeastern Costa Rica.

For this work, we propose a scenario in which the current Cocos Plate subducts with a continuous slab in southeastern Costa Rica and in which the melting may take place through interaction with mantle at the downdip projection of the Panama Fracture Zone, where the lithospheric segmentation caused by the Cocos-Nazca boundary may allow the subducted oceanic crust to come in contact with the mantle. The presence of the westernmost adakite outcroppings might be explained by the migration of the triple junction toward the southeast proposed by DeMets (2001). According to Gazel *et al*. (2011), this is consistent with a 35 mm/y migration in the adakites as evidenced by the age progression established by means of ^{40}AR/^{39}Ar dating. (Bindeman *et al.*, 2005) also mention the Panamanian adakites in relation to the Panama Fracture Zone. For adakites in general, Bindeman *et al*. (2005) discuss the possibility that their origin may not necessarily be the melting of the slab and discuss two alternative interpretations for adakite petrogenesis by means of melting processes in the overriding plate. One alternative mechanism may be the re-melting of basalts or mafic cumulates near the base of the crust while another scenario, considered less-likely by Bindeman *et al.* (2005), is the high-pressure crystallization–differentiation of wedge derived calc-alkaline hydrous basaltic magmas.

5.6.2 Alternative Model

As mentioned before, the seismological data presented in this work shows the termination of possible slab-related seismicity at a depth of approximately 70 km for the area located northeast of the Osa Peninsula. The hypocenters show the presence of a steeply subducting slab to that depth and have been used to constrain the geometry of the three-dimensional density model. However, in the primary density model, the continuity of the slab

to a greater depth has been modeled without seismological constraints. Considering the non-uniqueness of the gravity modeling, it may be possible to find an alternative solution to the existence of a steep slab in southeastern Costa Rica.

A prior seismological model of the slab geometry by Protti *et al*. (1994) based solely on routine located earthquake hypocenters registered intraslab seismicity eastward of the end of the Quaternary volcanic arc in Costa Rica. The apparent lack of registry of deep seismicity coupled with the presence of a gap in Quaternary volcanism and a OIB-type geochemical signature for the volcanic rocks (Hoernle *et al.*, 2008), has led to several interpretations for its source such as the presence of a slab window (Abratis and Wörner, 2001) or a slab detachment (Gazel *et al.*, 2011). Both of these alternative models do not consider the presence of the structure observed in receiver functions results from Dzierma *et al*. (2011) in which a steeply subducting slab is interpreted for the area east of the volcanic arc and beneath the northern edge of the Talamanca Range. Also, Dzierma *et al*. (2011) tested several alternative tectonic models for this area and compared them with their receiver functions results. From this comparison, they concluded that a slab break-off at a depth shallower than 70 km is not plausible. However, Dzierma *et al*. (2011) consider that scattering signals may be generated on the receiver functions and may produce similar results if the Cocos Plate subducts deeper than 70 km. Considering the ambiguity of the methods, the depth and extent of slab-related seismicity, the possible effects of scattering on the receiver function results and the presence of the OIB signature in volcanic rocks of the Quaternary arc, we generated an alternative model to the continuous slab, in which the asthenosphere (with a density of 3.34 Mg/m^3) replaces the subducting slab (Fig. 5.8).

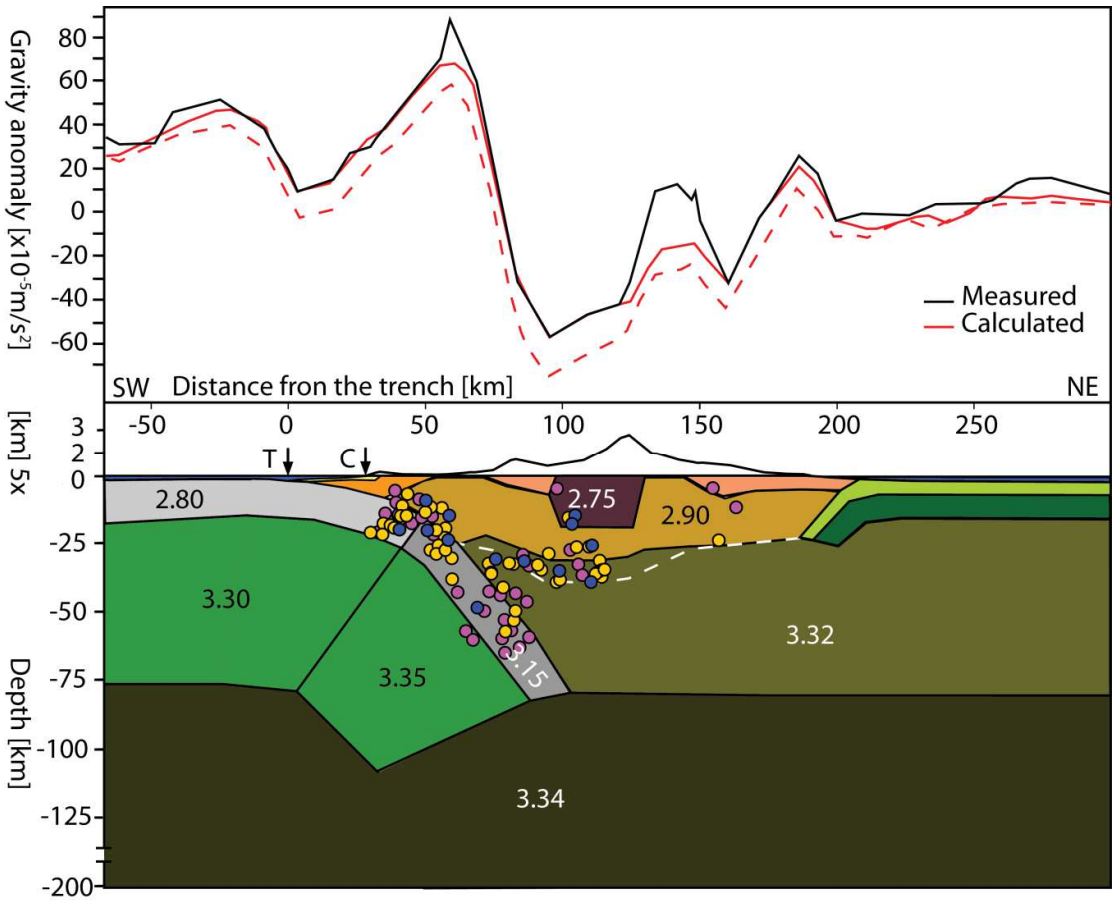

Figure 5.8. Cross section of the alternative density model considering a slab detachment at 80 km for the Cocos ridge. The upper box shows the fit between the measured (black) and calculated (red) gravity anomalies, the red stippled line shows the calculated gravity anomaly for the alternate slab detachment model with the Moho structure from Lücke (2012). The lower box shows the alternative model assuming a slab detachment at a depth of 70 to 80 km under the Talamanca region. White stippled line represents the location of the Moho from Lücke (2012) constrained by receiver function results from Dzierma *et al.* (2010). Blue dots show the location of earthquake hypocenters obtained for this study.

In order to achieve a proper fit between the measured and the calculated gravity for this alternative model, the 10 to 20 x10^{-5} m/s^2 misfit caused by the absence of the downgoing slab beyond approximately 80 km requires the replacement of lower crust material of the overriding plate (2.90 Mg/m^3) by lithospheric mantle material with a higher density (3.32 Mg/m^3), thus requiring a considerably shallower Moho (28 km). Isostatic compensation along the Talamanca range (which has the highest elevations of the southeastern Central American isthmus) contradicts the possibility of a shallow Moho. According to the model Airy-type isostasy modeling of the Moho depth carried out by Dzierma *et al.* (2010), in the presence of mass load from the Talamanca Range the Moho reaches depths greater than 40 km. Receiver function results from Dzierma *et al.* (2010) show a Moho at 35 km for areas of intermediate

topography and becomes deeper though less constrained below the areas with the highest topographic elevations. Regional three dimensional density modeling by Lücke (2012) shows Moho depths between 32 and 36 km for the Talamanca Range in Costa Rica and Panama.

5.7 Conclusions

The gravity modeling and local earthquake relocation results were successfully interpreted in a joint model showing the three-dimensional structure of the slab beneath Costa Rica. The depth of the intraslab seismicity varies from ~220 km for the northwestern part of Costa Rica, to 140 km for the central part and 70-75 km for the southeastern region. The depth reached by the intermediate density segment (3.15 Mg/m^3) of the subducted oceanic crust varies laterally along the Costa Rican section of the convergent margin. The progressively shallower depth at which the change from 3.15 to 3.30 Mg/m^3 occurs toward the southeastern segment of the Costa Rican subduction zone may be related to the initial state of hydration of the lithosphere.

The two plausible models for the Costa Rican southeastern Costa Rican subduction zone derived from the joint gravity-seismological interpretation are: (a) a steeply subducting slab which becomes a-seismic at a depth of approximately 75 km due to less mantle hydration through serpentinization at the Cocos Ridge; (b) a slab detachment occurring at a depth of 70 to 80 km and a shallow Moho underneath Talamanca. The previously constrained Moho depth and the inferred presence of a slab-structure at the northern edge of the Talamanca Range interpreted from receiver functions (Dzierma *et al.*, 2011) suggest that the presence of a continuous slab is more likely.

6 Conclusions and Outlook

6.1 Conclusions

- A new, homogenous surface gravity database has been compiled for Costa Rica. This gravity database is considered to be the state of the art in onshore coverage of surface stations for Costa Rica since it combines the previously available gravity database for Central America with data that has been newly released for academic research. The limitations in coverage of the current surface database for onshore Costa Rica were identified by the assessment of the detail achieved for local scale 3D modeling in Central Costa Rica. Offshore Costa Rica, the data collected by the research ships during the activities of the SFB574 in Central America has been included in the database. This marine data provides comprehensive coverage of the Middle American Trench and the Pacific continental shelf. The marine areas on the Caribbean side of Costa Rica were covered by open source data from NOAA which was thoroughly vetted. The newly compiled on- and offshore database was used as a reference for the comparison and assessment of the validity of the combined geopotential models for the modeling of the solid earth.

- The combined geopotential model EGM2008 has proven to be a viable and reliable source for gravity data as input for the forward modeling of the solid Earth. The satellite-only models are a consistent database that may be used for interpretation of the solid Earth on a global scale. However, for applications on a regional scale for areas like Central America, the input of the additional data in the form of satellite altimetry and surface station data is needed to provide a better spatial resolution. For the purpose of modeling the lithospheric density structure, a higher spatial resolution

than the maximum resolution achieved by satellite-only models is required since even the first order lithospheric discontinuities such as the Moho and the subducting slab were found to present significant heterogeneities that may result in gravity anomalies with wavelengths shorter than 55 km. From the modeling process it was found that even with the limitations in spatial resolution, the satellite component of the combined models is a valuable input for areas lacking onshore surface station coverage since the interpretation of trends in the longer wavelengths has been shown to provide information on areas where large gaps in coverage are present. The interpretation of these trends are also useful to identify areas in which aberrant values from gravity prediction were included at the maximum spatial resolution of the combined models and may not have been otherwise specified. Overall, the use of the geophysical anomaly (gravity disturbance) for the calculation of Bouguer anomalies onshore is more consistent with the use of data from surface stations when compared with the geodetic anomaly (classical gravity anomaly) since the downward continuation from the topographic surface to the geoid may be unreliable in areas of high topography.

- In this work, the first three-dimensional density model for the Central American Isthmus has been presented. This model incorporates the available geophysical constraints in the area and provides a three-dimensional interpretation of the tectonic models inferred from surface geology for the western part of the Caribbean Plate. The segmentation of the crustal basement along Central America is reflected in the gravity field and has been modeled successfully from the EGM2008 gravity data. The contrast in the modeled density for the boundaries between the continental component of the Chortis Terrane and the ultramafic oceanic component of the Mesquito / Siuna Terrane is consistent with the observed gravity. The boundary between the Mesquito /

Siuna Terrane and the Caribbean Large Igneous Province (CLIP) however, is not immediately identifiable in the Bouguer anomaly but has been constrained by surface geology and borehole data. This lack of contrast may be due to the similarity in density of the components of each unit.

- Regarding the modeled boundary surfaces, the main structures that are present throughout most of the modeled area and have the most effect on the modeled gravity are the Moho and the subducting slab. For the first time for Central America, the regional structure of the Moho has been interpreted via forward modeling and constrained by the integration of geophysical data. The changes in the depth of the Moho in the Cocos Plate follow the segmentation caused by the different origins of the oceanic crust and the observed morpho-tectonic domains on the oceanic plate. The shallowest Moho depth (~8 km) is present to the northwest of the Rough-Smooth-Boundary and corresponds to the Mid Ocean Ridge Basalts which are not significantly affected by hotspot interaction. The seamount segment features intermediate depths and constitutes a transition zone to the deepest segment of the Moho underneath the Cocos Ridge where it reaches consistent depths between 18 and 22 km. Onshore, the Moho structures is heavily influenced by the Quaternary volcanic front, with a maximum depth of 44 km beneath the Tacana volcano in Guatemala. Values of more than 40 km in depth are present at both ends of the arc and a trend toward a shallower Moho is observed for the Nicaraguan segment of the volcanic front which shows the effects of crustal extension along the Nicaragua depression. On the Caribbean side of the isthmus, the oceanic basins feature a thickened crust offshore Costa Rica and Panama (14 to 18 km) although the areas with the largest crustal thickness, related to the Caribbean Large Igneous Province, appear to be present outside of the modeled area.

- The geometry and density distribution of the subducting Cocos Plate has been modeled along the Middle American Trench, from Guatemala (16°N) to the Panama Fracture Zone. The plate interface has been constrained by available wide-angle seismic profiles, magnetotelluric information, local earthquake seismic tomography and receiver functions. The geometry of the subducting slab has been further constrained by earthquake hypocenters from global (USGS), regional (CASC) and local networks (RSN, OSIVAM, Boruca) with varying levels of accuracy. This seismological information was correlated in detail with the density distribution of the subducted oceanic crust for the Costa Rican section of the margin. From this correlation, a link between the initial state of hydration of the oceanic plate and the terminal depth of intraslab seismicity was investigated. Furthermore, an alternative model to the previous slab window / slab detachment interpretations for the convergent margin of southeastern Costa Rica has been proposed.

6.2 Outlook

The regional structure of the Central American convergent margin and the overriding Caribbean Plate that has been modeled for this dissertation provides an overview of the boundary layers of important tectonic structures. The tectonic processes that act upon this modeled surfaces will be studied further by means of calculation of the stress field (vertical and normal stress) and stress anomalies which result from the characteristics of the geometry of the boundaries, the density distribution of the surrounding lithosphere and the regional dynamic forces.

At the moment, the state of the static normal stress upon the Cocos-Caribbean plate interface (Fig. 6.1), has been calculated by considering the geometry for the Costa Rican subduction zone and the density distribution of the overriding plate described in chapter 5 of this dissertation. The stress calculation takes into account the topographic load assuming a 2.67 Mg/m^3 density for the masses above the geoid.

The absolute stress, calculated as a vector which is normal to the plate interface, is dominated by the increase in lithostatic pressure with depth. This provides a quantifiable parameter on the stress distribution on the subducting slab but makes the interpretation of the local effects of the changes in geometry and density structure difficult. The absolute value of the normal stress (or similarly, the calculation of the vertical stress at a given level) provides an important tool for determining the pressure parameters as boundary conditions for applications such as petrological modeling. Also, the state of stress at the plate interface may provide information for the further understanding of the conditions under which mineralogical changes, due to metamorphic dehydration reactions occur in the subduction zone (*sensu* Hacker *et al*., 2003 and Ranero *et al*., 2005) and the way they affect intermediate depth seismicity.

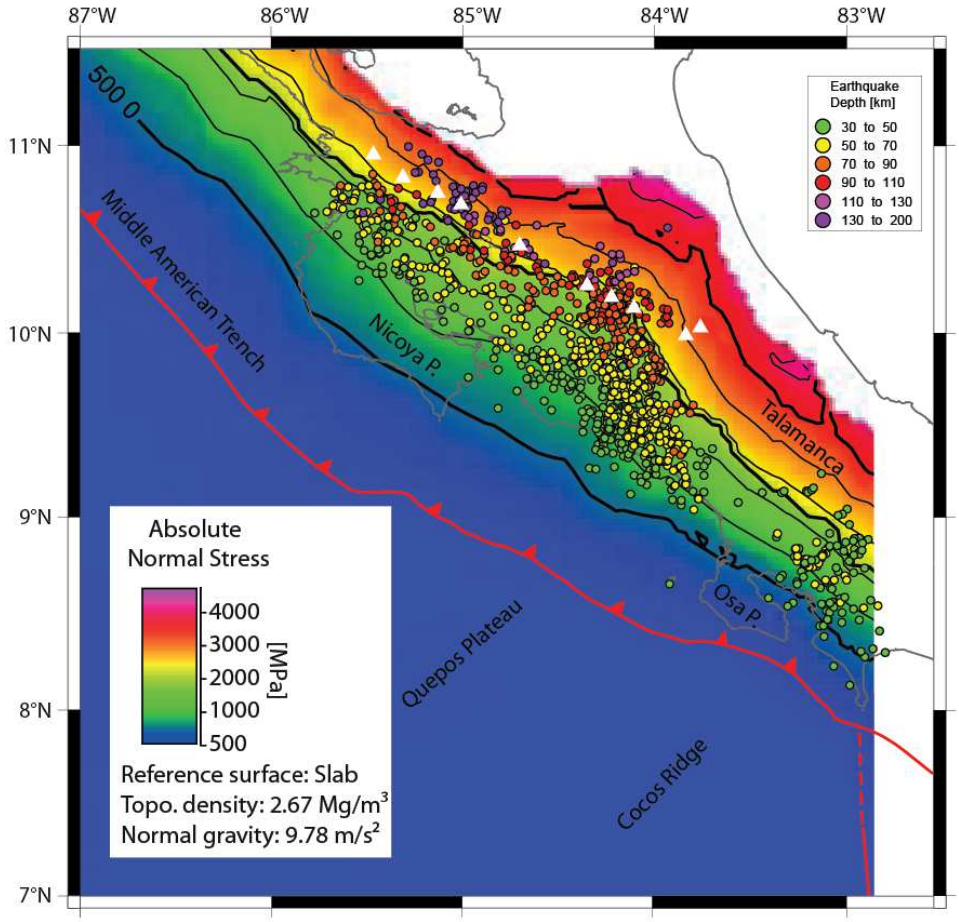

Figure 6.1. Magnitude of the absolute normal stress (σ_n) on the subducted Cocos slab an its relation to deep (>30 km) intraslab seismicity (colored circles) from the seismological database described in chapter 5. Slab reference surface from chapter 5 of this work. Contours every 500 MPa. Gray lines depict the coastline..

The calculation of stress anomalies by subtracting the influence of the lithostatic pressure, may provide information on the possible presence of asperities along the subduction zone. By considering the normal stress field generated by a reference body with a given density, it is possible to partially eliminate the effects of the depth gradient caused by the lithostatic pressure and focus on the effect of local heterogeneities.

Figure 6.2 shows the results of the anomalies of the normal stress, obtained by subtracting the normal stress field generated by a reference body with a constant density of 3.32 Mg/m^3. The resulting stress anomalies were integrated with the database of earthquake hypocenters presented in chapter 5.

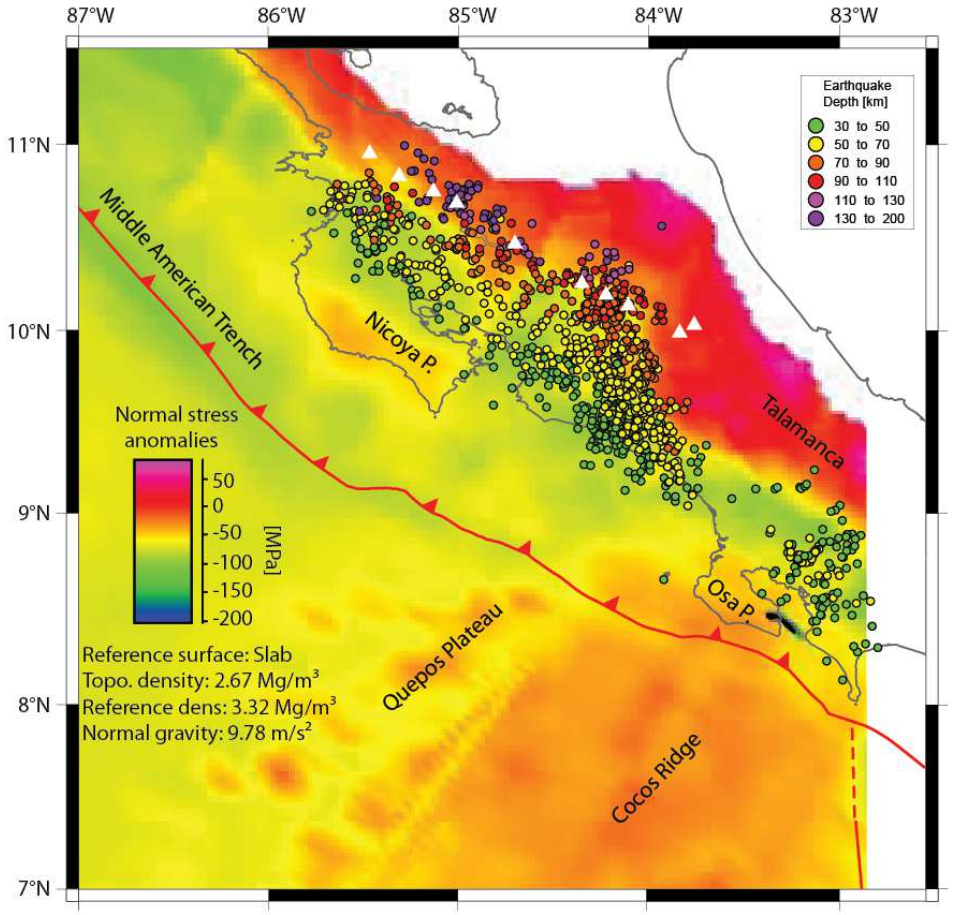

Figure 6.2. Normal stress anomaly on the Cocos Plate and the subducted slab, calculated by subtracting the mean normal stress with a reference density of 3.32 Mg/m^3 for the 3D model (2.67 Mg/m^3 density for the topography). Slab reference surface from chapter 5 of this work. Colored circles show the earthquake epicenters from the joint database described in chapter 5 for Costa Rica. Gray lines depict the Coastline.

The distribution of intraplate seismicity for the Costa Rican subduction zone shows a spatial correlation with the presence of the highest stress anomalies on the plate interface. The presence of these high normal stress anomalies in the order of 50 MPa relative to the reference body, correlate with the termination in depth of the intraplate seismicity.

Taking into account the density of the reference body (3.32 Mg/m^3), the change from positive values to negative values in the magnitude of the stress anomalies indicates the level at which the negative normal stress anomalies from the crustal material reach an equilibrium with the higher stress created by the asthenospheric material. This state is reached when the effect of the lower crustal densities is compensated by the higher densities of the lower mantle which consequently should occur at a depth located below the lithosphere-

asthenosphere boundary. However, the effect of the topographic load may be large enough to offset this equilibrium. This is the case for the area beneath the Talamanca region of Costa Rica where the stress anomalies relative to a reference body with a density of 3.32 Mg/m^3 become positive approximately at the depth contour of 60 km for the slab, between 10 and 15 km shallower than the lithosphere-asthenosphere boundary. This is observed in areas where the Moho is constrained by receiver functions and/or seismic tomography which provide appropriate constraints on the crustal thickness.

Although a correlation between the terminal depth of the seismicity and the level of compensation of the normal stress anomalies relative to an upper mantle density can be observed, the interpretation of the mechanism by which the stress may play a role in controlling this depth is still not clear. The joint interpretation of the static stress with seismological information, dynamic models, and correlation with the analysis of flexural rigidity, may provide valuable information for the assessment of seismological hazards. Furthermore, the calculation of the effect of the topographic load and the density distribution in the upper crust may provide information on isostasy in the region.

Another important boundary surface to consider in terms of static stress is the Moho. The calculation of the static stress upon this surface yields information on the combined effect of the geometry of the boundary and the composition of the masses above it. Figure 6.3 shows the results obtained for the absolute vertical stress on the surface, modeled for the Moho and described in chapter 4. In this case the vertical load imparted on the Moho by the topography is considered by assigning a density of 2.67 Mg/m^3 to the material between the geoid and the height of the gravity station. The values obtained are thus dependant on the depth to the Moho, the topography, and the mass distribution modeled for the Earth's crust.

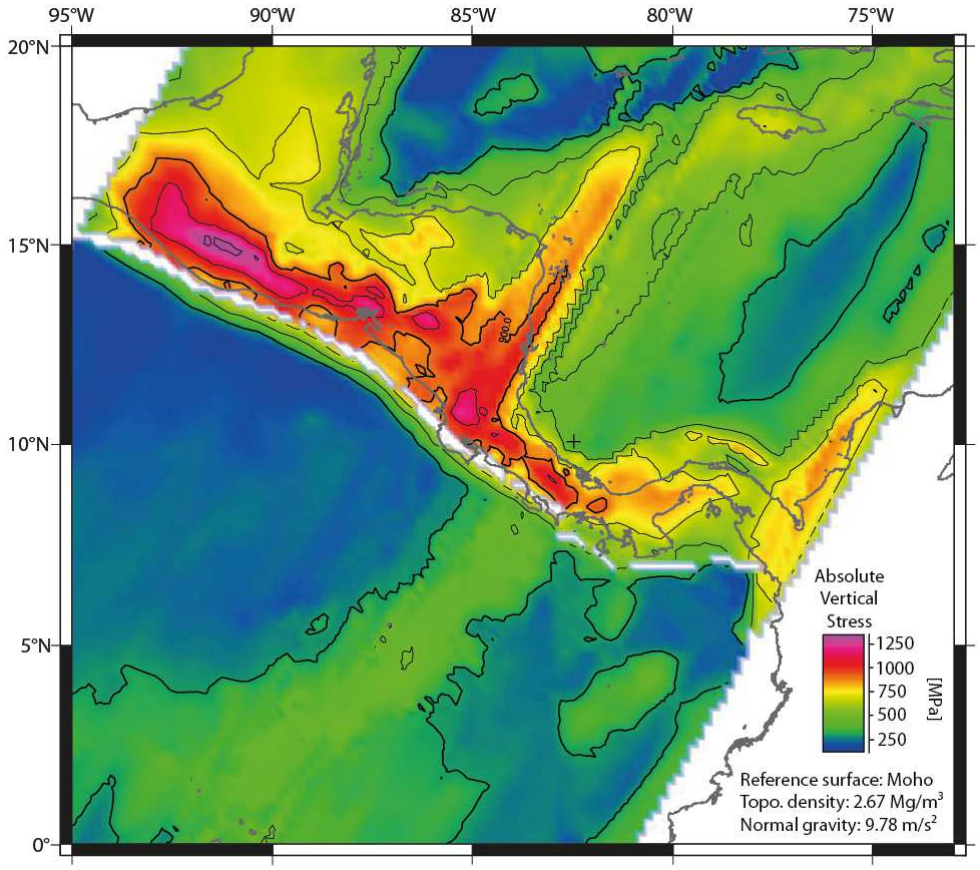

Figure 6.3. Magnitude of the absolute vertical stress (σ_v) calculated at the Moho for the Cocos, Nazca, and Caribbean plates in the modeled region (2.67 Mg/m^3 density for the topography). Moho structure and model densities from chapters 4 and 5 of this work. Gray lines depict the Coastline.

The regional density model coupled with the tool for the calculation of static stress, enable the possibility of obtaining quantifiable lithostatic pressure parameters either at a given modeled boundary layer (e.g. Moho) or at a constant depth. This parameters allow to constrain conditions under which metamorphic and magmatic processes occur

Regarding the implementation of new sources of data for the interpretation of the lithospheric density distribution in the region, the existing model will be improved by incorporating gravity data from the GOCE mission which will provide a better resolution for the satellite-only component (longer wavelengths). Although the latest geopotential model to date, the EIGEN-6C (Förste *et al.*, 2011) already incorporates gravity data derived from GOCE, it already operates at the present technical limitations for a satellite mission. For this reason, the spatial resolution of the combined geopotential models at the shortest wavelengths

is still dependent on the availability of surface data. For this reason, the maximum spatial resolution has not improved relative to EGM2008 (Pavlis *et al.*, 2008).

Taking into account the intrinsic limitations of ground access for the purpose of acquiring surface gravity data in the Central American region, and the present limitations in terms of spatial resolution posed by measuring the gravity field from orbit, an intermediate level of measurement is required. Currently, advanced plans are in place to carry out an airborne gravity campaign in Costa Rica. Such data acquisition campaign may provide the required compromise between spatial resolution and coverage of gravity data, as well as solve the uncertainties posed by the quality and provenance of the available surface data.

Furthermore, the implementation of gravity gradients either from satellites (GOCE) or airborne measurements in the modeling of the solid Earth must be studied. The regional density model will also provide a framework for the analysis of the effects of large scale structures (e.g. Slab, Moho) on the measured gravity field and contribute to the understanding of the sources of the signals and the significance of the coefficients and degree of the spherical harmonics in the calculation of the combined geopotential models.

7 References

Abratis, M. and Wörner, G. (2001). Ridge collision, slab-window formation, and the flux of Pacific asthenosphere into the Caribbean realm, *Geology*, **29**(2): 127-130, doi: 10.1130/0091-7613(2001)029<0127:RCSWFA>2.0.CO;2

Alasonati-Tašárová, Z. (2007). Towards understanding the lithospheric structure of the southern Chilean subduction zone (36°S–42°S) and its role in the gravity field, *Geophys. J. Int.*, **170**(3): 995-1014.

Allmendinger, R.W., Jordan, T.E., Kay, S.M. and Isacks, B.L. (1997). The evolution of the Altiplano-Puna Plateau of the Central Andes, *Earth planet. Sci.*, **25**: 139-174.

Alvarado, G.E. (2000). *Los volcanes de Costa Rica: geología, historia y riqueza natural*, 2 ed., 269 pp., EUNED, San José.

Alvarado, G.E., Dengo, C., Martens, U., Bundschuh, J., Aguilar, T. and Bonis, S.B. (2007). Stratigraphy and geologic history, in *Central America: Geology, Resources and Hazards*, vol. 1, edited by Alvarado G.E. and Bundschuh J. pp 345-393, Taylor & Francis, London.

ANCORP Working Group (2003). Seismic imaging of a convergent continental margin and plateau in the Central Andes: Andean continental research project 1996: ANCORP 96, *J. geophys. Res.*, **108**: 2328.

Andersen, O.B. and Knudsen, P. (1998). Clobal marine gravity field from the ERS-1 and Geosat geodetic mission altimetry, *J. geophys. Res.*, **103**: 8129-8137.

Aochi, H., Madariaga, R. and Fukuyama, E. (2003). Constraint of fault parameters inferred from nonplanar fault modeling, *Geochem. Geophys. Geosyst.*, **4**(16): 1020.

Arroyo, I.G. (2001). Sismicidad y Neotectónica en la región de influencia del Proyecto Boruca: hacia una mejor definición sismogénica del sureste de Costa Rica, Licenciate thesis, University of Costa Rica, San José, Costa Rica.

Arroyo, I.G, Alvarado, G.E. and Flueh, E.R. (2003). Local seismicity at the Cocos Ridge - Osa Peninsula subduction Zone, Costa Rica, paper presented at AGU Fall Meeting, San Francisco, USA, 08 - 12 Dec.

Arroyo, I.G. (2008). Local earthquake tomography at the Central Pacific Margin of Costa Rica, Ph.D. thesis, Christian-Albrechts, Kiel.

Arroyo, I.G., Husen, S., Flueh, E.R., Gossler, J., Kissling, E. and Alvarado, G.E. (2009). Three-dimensional P-wave velocity structure on the shallow part of the Central Costa Rican Pacific margin from local earthquake tomography using off- and onshore networks, *Geophys. J. Int.*, doi: 10.1111/j.1365-246X.2009.04342.x.

Babeyko, A.Y., Sobolev, S.V., Vietor, T., Oncken, O. and Trumbull, R.B. (2006). Numerical study of weakening processes in the central Andean back-arc, in *The Andes – Active Subduction Orogeny*, edited by Oncken, O., Chong, G., Franz, G., Giese, P., Götze, H.-J., Ramos, V.A., Strecker, M. and Wigger, P., pp. 495-512, Springer-Verlag, Berlin, Germany.

Barckhausen, U., Roeser, H.A. and von Huene, R. (1998). Magnetic signature of upper plate structures and subducting seamounts at the convergent margin of Costa Rica, *J. geophys. Res.*, **103**: 7079-7093.

Barckhausen, U., Ranero, C.R., von Huene, R., Cande, S.C. and Roeser, H.A. (2001). Revised tectonic boundaries in the Cocos Plate off Costa Rica: Implications for the segmentation of the convergent margin and for plate tectonic models, *J. geophys. Res.*, **106**(B9): 19207-19229.

Barthelmes, F. (2009). Definition of functionals of the geopotential and their calculation from spherical harmonic models. *GFZ Scientific Technical Report*, **STR09/02.**

Baumgartner, P., Kennet, F., Bandini, A., Girault, F. and Cruz, D. (2008). Upper Triassic to Cretaceous radiolaria from Nicaragua and northern Costa Rica - The Mesquito composite oceanic terrane, *Ofioliti*, **33**(1): 1-19.

Bindeman, I.N., Eiler, J.M., Yogodzinski, G.M., Tatsumi, Y., Stern, C.R., Grove, T.L., Portnyagin, M., Hoernle, K. and Danyushevsky, L.V. (2005). Oxygen isotope evidence for slab melting in modern and acient subduction zones, *Earth planet. Sci. Lett.*, **235**: 480-496, doi: 10.1016/j.epsl.2005.04.014.

Birch, F. (1960). The Velocity of Compressional Waves in Rocks to 10 Kilobars, Part 1, *J. geophys. Res*, **65**(4): 1083-1102, doi: 10.1029/JZ065i004p01083.

Bohm, M., Lüth, S., Echtler, H., Asch, G., Bataille, K., Bruhn, C., Rietbrock, A. and Wigger, P. (2002). The southern Andes between 36◦S and 40◦S latitude: seismicity and average seismic velocities, *Tectonophysics*, **356**: 275-289.

Bolge, L.L., Carr, M.J., Milidakis, K.I., Lindsay, F.N. and Feigenson, M.D. (2009). Correlating geochemistry, tectonics, and volcanic volume along the Central American volcanic front, *Geochem. Geophys. Geosyst.*, **10**(Q12S18).

Bousquet, R., Goffé, B., deCapitani, C., Chopin, C., Le Pichon, X. and Henry, P. (2005). Comment on "Subduction factory: 1. Theoretical mineralogy, densities, seismic wave speeds, and H2O contents" by Bradley R. Hacker, Geoffrey A. Abers, and Simon M. Peacock, *J. geophys. Res*, **110**(B02206), doi: 10.1029/2004JB003450.

Boutelier, D.A. and Oncken, O. (2010). The role of the plate margin curvature in the plateau build-up: consequences for the Central Andes, *J. geophys. Res.*, **115**(B04402), doi: 10.1029/2009JB006296.

Brasse, H., Kapinos, G., Mütschard, L., Alvarado, G.E., Worzewski, T. and Jegen, M. (2009). Deep electrical resistivity structure of northwestern Costa Rica, *Geophys. Res. Lett.*, **36**(L02310), doi: 10.1029/2008GL036397.

Brocher, T.M. (2005). Empirical Relations between Elastic Wavespeeds and Density in the Earth's Crust, *Bull. seism. Soc. Am.*, **95**(6): 2081-2092, doi: 10.1785/0120050077.

Buchs, D.M., Arculus, R.J., Baumgartner, P.O., Baumgartner-Mora, C. and Ulianov, A. (2010). Late Cretaceous arc development on the SW margin of the Caribbean Plate: Insights from the Golfito, Costa Rica, and Azuero, Panama, complexes, *Geochem. Geophys. Geosyst.*, **11**(7), doi: 10.1029/2009GC002901.

Buske, S., Lüth, S., Meyer, H., Patzig, R., Reichert, C., Shapiro, S., Wigger, P. and Yoon, M. (2002). Broad depth range seismic imaging of the subducted Nazca slab, north Chile, *Tectonophysics*, **350**: 273-282.

Carr, M.J. (1984). Symetrical and segmented variation of physical and geochemical characteristics of the Central American volcanic front, *J. Volc. geoth. Res.*, **20**: 231-252.

Carr, M.J., Saginor, I., Alvarado, G.E., Bolge, L.L., Lindsay, F.N., Milidakis, K., Turrin, B.D., Feigenson, M.D. and Swisher, C.C. (2007). Element fluxes from the volcanic front of Nicaragua and Costa Rica, *Geochem. Geophys. Geosyst.*, **8**(6): 1-22, doi: 10.1029/2006GC001396.

Christensen, N.I. and Mooney, W.D. (1995). Seismic velocity structure and composition of the continental crust: A global view, *J. geophys. Res.*, **100**(B6): 9761-9788, doi: 10.1029/95jb00259.

Cloos, M. (1992). Thrust-type subduction-zone earthquakes and seamount asperities: a physical model for seismic rupture, *Geology*, **20**: 601-604.

Coffin, M.F., Gahaga, L.M. and Lawyer, L.A. (1998). Present-day Plate Boundary Digital Data Compilation, *University of Texas Institute for Geophysics Technical Report*(174): 5.

Colombo, D., Cimini, G.B. and DeFranco, R. (1997). Three-dimensional velocity structure of the upper mantle beneath Costa Rica from teleseismic tomography study, *Geophys. J. Int.*, **131**: 189-208.

deBoer, J.Z., Defant, M.J., Stewart, R.H., Restrepo, J.F., Clark, L.F. and Ramirez, A.H. (1988). Quaternary calc-alkaline volcanism in western Panama: Regional variation and implication for the plate tectonic framework, *J. South Am. Earth Sci.*, **1**(3): 275-293.

deBoer, J.Z., Defant, M.J., Stewart, R.H. and Bellon, H. (1991). Evidence for actve subduction below western Panama, *Geology*, **24**: 649-652.

DeMets, C., Gordon, R.G., Argus, D.F. and Stein, S. (1994). Effect of Recent Revisions to the Geomagnetic Reversal Time Scale on Estimates of Current Plate Motions, *Geophys. Res. Lett.*, **21**(20): 2191–2194, doi: 10.1029/94gl02118.

DeMets, C. (2001). A new estimate for present-day Cocos-Caribbean plate motion: Implications for slip along the Central American volcanic arc, *Geophys Res Lett*, **28**(21): 4043-4046, doi: 10.1029/2001GL013518.

DeMets, C., Gordon, R.G. and Argus, D.F. (2010). Geologically current plate motions, *Geophys. J. Int.*, **181**: 1-80, doi: 10.1111/j.1365-246X.2009.04491.x.

Dengo, G. (1969). Problems of tectonic relations between Central America and the Caribbean, *Gulf Coast Association of Geological Societies Transactions*, **19**: 311-320.

Dengo, G. (1985). Mid America: Tectonic setting for the Pacific margin from southern Mexico to northwestern Columbia, in *The Ocean Basins and Margins*, edited by Nairn, A., Stehli, F. and Uyeda, S., pp. 123-180, Plenum Press, New York.

Denyer, P. and Alvarado, G.E. (2007). Mapa geológico de Costa Rica, Editorial Francesa, San José, Costa Rica.

DeShon, H.R., Schwartz, S.Y., Bilek, S.L., Dorman, L.M., Gonzalez, V., Protti, J.M., Flueh, E.R. and Dixon, T.H. (2003). Seismogenic zone structure of the southern Middle America Trench, Costa Rica, *J. geophys. Res.*, **108**(14).

DeShon, H.R., Schwartz, S.Y., Newman, A.V., González, V., Protti, M., Dorman, L.R.M., Dixon, T.H., Sampson, D.E. and Flueh, E.R. (2006). Seismogenic zone structure beneath the Nicoya Peninsula, Costa Rica, from three-dimensional local earthquake P- and S-wave tomography, *Geophys. J. Int.*, **164**(1): 109-124, doi: 10.1111/j.1365-246X.2005.02809.x.

Dinc, A.N., Koulakov, I., Thorwart, M., Rabbel, W., Flueh, E., Arroyo, I.G., Taylor, W. and Alvarado, G.E. (2010). Local earthquake tomography of Central Costa Rica: Transition from seamount to ridge subduction, *Geophys. J. Int.*, **183**(1): 286-302, doi: 10.1111/j.1365-246X.2010.04717.x.

Döring, J. (1995). Tiefenabschäztung von Massenverteilungen im Untergrund mit Hilfe des Fourier Amplitudenspektrums, Diploma Thesis thesis, Freie Universität Berlin.

Drummond, M.S., Bordelon, M., deBoer, J.Z., Defant, M.J., Bellon, H. and Feigenson, M.D. (1995). Igneous petrogenesis and tectonic setting of plutonic and volcanic rocks of the Cordillera de Talamanca, Costa Rica-Panama, Central American arc, *Am. J. Sci.*, **295**: 875-919.

Dzierma, Y., Thorwart, M.M., Rabbel, W., Flueh, E.R., Alvarado, G.E. and Mora, M.M. (2010). Imaging crustal structure in south central Costa Rica with receiver functions, *Geochem. Geophys. Geosyst.*, **11**(8), doi: 10.1029/2009GC002936.

Dzierma, Y., Rabbel, W., Thorwart, M.M., Flueh, E.R., Mora, M.M. and Alvarado, G.E. (2011). The steeply subducting edge of the Cocos Ridge : evidence from receiver functions beneath the northern Talamanca Range, south-central Costa Rica, *Geochem. Geophys. Geosyst.*, **12**(4), doi: doi:10.1029/2010GC003477.

Ewing, J., Antoine, J. and Ewing, M. (1960). Geophysical measurements in the western Caribbean Sea and in the Gulf of Mexico, *Journal of Geophysical Research*, **65**(12): 4087-4126.

Fedi, M., Ferranti, L., Florio, G., Giori, I. and Italiano, F. (2005). Understanding the structural setting in the Southern Apennines (Italy): insight from Gravity Gradient Tensor, *Tectonophysics*, **397**: 21-36.

Förste, C., Flechtner, F., Schmidt, R., Stubenvoll, R., Rothacher, M., Kusche, J., Neumayer, K.-H., Biancale, R., Lemoine, J.-M., Barthelmes, F., Bruinsma, J., König, R. and Meyer, U. (2008). EIGEN-GL05C – a new global combined high-resolution GRACE-based gravity field model of the GFZ-GRGS cooperation, paper presented at European Geosciences Union General Assembly, *Geophys. Res. Abstr.*, **10**.

Förste, C., Bruinsma, S., Shako, R., Marty, J.-C., Flechtner, F., Abrikosov, O., Dahle, C., Lemoine, J.-M., Neumayer, K.H., Biancale, R., Barthelmes, F., König, R., and Balmino, G. (2011). EIGEN-6 - A new combined global gravity field model including GOCE data from the collaboration of GFZ-Potsdam and GRGS-Toulouse, paper presented at European Geosciences Union General Assembly, *Geophys. Res. Abstr.*, **13**.

Freymueller, J.T., Kellogg, J.N. and Vega, V. (1993). Plate Motions in the North Andean Region, *J. geophys. Res*, **98**, doi: 10.1029/93jb00520.

Fuller, C.W., Willett, S.D. and Brandon, M.T. (2006). Formation of forearc basins and their influence on subduction zone earthquakes, *Geology*, **34**: 65-68.

Gardner, G.H.F., Gardner, L.W. and Gregory, A.R. (1974). Formation, velocity and density - the diagnostic basics for stratigraphic traps, *Geophysics*, **39**: 770-780.

Gazel, E., Hoernle, K., Carr, M.J., Herzberg, C., Saginor, I., van den Bogaard, P., Hauff, F., Feigenson, M. and Swisher III, C. (2011). Plume-subduction interaction in southern Central

America: mantle upwelling and slab melting, *Lithos*, **121**: 117-134, doi: 10.1016/j.lithos.2010.10.008.

Giese, P., Asch, G., Brasse, H., Götze, H.-J., Haberland, C. and Wigger, P. (Eds.) (1999). *Procesos geodinámicos en los andes centrales, representados mediante observaciones geofsícas*, 15-17 pp., Relatorio, Salta, Argentina.

Gödde, H. (1999). Die Krustenstrukturen am konvergenten Plattenrand Costa Ricas, *Geoforschungszentrum Potsdam, Scientific Technical Report*, **99**(17).

Godfrey, N.J., Beaudoin, B.C., Klempererthe, S.L. and MendocinoWorkingGroupUSA (1997). Ophiolitic basement to the Great Valley forearc basin, California, from seismic and gravity data: implications for crustal growth at the North American continental margin, *Geol. Soc. Am. Bull.*, **109**: 1536-1562.

Götze, H.J. (1976). Ein numerisches Verfahren zur Berechnung der gravimetrischen und magnetischen Feldgrößen für dreidimensionale Modellkörper, Ph.D. thesis, TU Clausthal, Clausthal, Germany.

Götze, H.J. (1984). Über den Einsatz interaktiver Computergraphik im Rahmen 3-dimensionaler Interpretationstechniken in Gravimetrie und Magnetik, Habil. thesis, Techn. Univ. Clausthal, Germany.

Götze, H.J. and Lahmeyer, B. (1988). Application of three-dimensional interactive modeling in gravity and magnetics, *Geophysics*, **53**(8): 1096-1108.

Götze, H.-J., Lahmeyer, B., Schmidt, S. and Strunk, S. (Eds.) (1994). *The lithospheric structure of the central Andes (20°S–26°S) as inferred from interpretation of regional gravity*, 7-21 pp., Springer Verlag, Berlin.

Götze, H.-J. and Krause, S. (2002). The Central Andean gravity high, a relic of an old subduction complex?, *J. South Am. Earth Sci.*, **14**: 799-811.

Götze, H.-J., Schmidt, S., Fichler, C. and Plonka, C. (2010). IGMAS+ a new 3D Gravity, FTG and Magnetic Modeling Software, paper presented at *European Geosciences Union General Assembly*, Geophys. Res. Abstr., Vienna, Austria.

Grevemeyer, I., Ranero, C.R., Flueh, E.R., Kläschen, D. and Bialas, J. (2007). Passive and active seismological study of bending-related faulting and mantle serpentinization at the Middle America Trench, *Earth planet. Sci. Lett.*, **258**: 528-542.

Gutscher, M.A., Spakman, W., Bijwaard, H. and Engdahl, E.R. (2000). Geodynamics of flat subduction: seismicity and tomographic constraints from the Andean margin, *Tectonics*, **19**: 814-833.

Hacker, B.R., Peacock, S.M., Abers, G.A. and Holloway, S.D. (2003). Subduction factory 2: Are intermediate depth earthquakes in subducting slabs linked to metamorphic dehydration reactions?, *J. geophys. Res.*, **108**(B1): 2030, doi: 10.1029/2001JB001129.

Hackney, R.I. and Featherstone, W.E. (2003). Geodetic versus geophysical perspectives of the `gravity anomaly', *Geophys. J. Int.*, **154**: 35-43.

Hackney, R., et al. (2006). The segmented overriding plate and coupling at the south-central Chile margin (36°S–42°S), in *The Andes – Active Subduction Orogeny*, edited by Oncken, O., Chong, G., Franz, G., Giese, P., Götze, H.-J., Ramos, V.A., Strecker, M. and Wigger, P., pp. 355-374, Springer Verlag, Berlin, Germany.

Heuret, A. and Lallemand, S. (2005). Plate motions, slab dynamics and back-arc deformation, *Phys. Earth planet. Intr.*, **149**: 31-51.

Hey, R. (1977). Tectonic evolution of the Cocos-Nazca spreading center, *Geological Society of America Bulletin*, **88**: 1404-1420.

Hinz, K.R., von Huene, R., Ranero, C.R. and PACOMARWorkingGroup (1996). Tectonic structure of the convergent margin offshore Costa Rica from multichannel seismic reflection data, *Tectonics*, **15**: 54-66.

Hoernle, K., Hauff, F. and van den Bogaard, P. (2004). A 70 m.y. history (139-69 Ma) for the Caribbean large igneous province, *Geology*, **32**(8): 697-700.

Hoernle, K., et al. (2008). Arc-parallel flow in the mantle wedge beneath Costa Rica and Nicaragua, *Nature*, **451**(1094-1097), doi: 10.1038/nature06550.

Holstein, H., Sherratt, E.M. and Reid, A.B. (2007). Gravimagnetic field tensor gradiometry formulas for uniform polyhedra, paper presented at SEG Tech. Prog. Exp.

Husen, S. (1999). Local earthquake tomography of a convergent margin, North Chile, Ph.D. thesis, Christian-Albrechts-University, Kiel, Germany.

Husen, S., Quintero, R., Kissling, E. and Hacker, B. (2003a). Subduction zone structure and magmatic processes beneath Costa Rica constrained by local earthquake tomography and petrological modelling, *Geophys. J. Int.*(155): 11-32.

Husen, S., Kissling, E., Deischmann, N., Wiemer, S., Giardini, D. and Baer, M. (2003b). Probabilistic earthquake location in complex three-dimensional velocity models: Application to Switzerland, *J. geophys. Res.*, **108**(2077), doi: 10.1029/2002JB001778.

Husen, S. and Smith, R.B. (2004). Probabilistic eathquake relocation in three-dimensional velocity models for the Yellowstone National Park region, Wyoming, *Bull. seism. Soc. Am.*, **94**(3): 880-896.

Jiao, W., Silver, P.G., Fei, Y. and Prewitt, C.T. (2000). Do intermediate- and deep-focus earthquakes occur on preexisting weak zones? An examination of the Tonga subduction zone, *J. geophys. Res.*, **105**(28): 125-138.

Johnston, S.T. and Thorkelson, D.J. (1997). Cocos-Nazca slab window beneath Central America, *Earth planet. Sci. Lett.*, **146**: 465-474.

Jordan, T.E., Reynolds III, J.H. and Erikson, J.P. (Eds.) (1997). *Variability in age of initial shortening and uplift in the Central Andes*, 41-61 pp., Plenum Press, New York, USA.

Kellogg, J.N. and Vega, V. (1995). Tectonic development of Panama, Costa Rica, and the Colombian Andes: constraints from global positioning system geodetic studies and gravity, *Geol. Soc. Am. Spec. Paper*, **V**(295): 75- 90.

Kim, J., Matumoto, T. and Latham, G.V. (1982). A crustal section of northern Central America as inferred from wide-angle reflections from shallow earthquakes, *Bull. seism. Soc. Am.*, **72**(3): 940-952.

Kirby, S., E.R, E. and Denlinger, R. (1996). Intermediate-depth intraslab earthquakes and arc volcanism as physical expressions of crustal and uppermost mantle metamorphism in subducting slabs, in *Subduction: Top to Bottom*, edited by Bebout, G.E., Scholl, D.W., Kirby, S.H. and Platt, J.P., pp. 195-214, American Geophysical Union, Washington DC, USA.

Kirchner, A., Götze, H.-J. and Schmitz, M. (1996). 3d-density modelling with seismic constraints in the central Andes, *Phys. Chem. Earth*, **21**: 289-293.

Klotz, J., Khazaradze, G., Angermann, D., Reigber, G., Perdomo, R. and Cifuentes, O. (2001). Earthquake cycle dominates contemporary crustal deformation in Central and Southern Andes, *Earth planet. Sci. Lett.*, **193**(3-4): 437-446, doi: 10.1016/S0012-821X(01)00532-5.

Klotz, J., Abolghasem, A., Khazaradze, G., Heinze, B., Vietor, T., Hackney, R., Bataille, K., Maturana, R., Viramonte, J. and Perdomo, R. (2006). Long-Term signals in the present-day deformation field of the central andes and constraints on the viscosity of the earth's upper mantle, in *The Andes – Active Subduction Orogeny*, edited by Oncken, O., Chong, G., Franz, G., Giese, P., Götze, H.-J., Ramos, V.A., Strecker, M. and Wigger, P., pp. 65-89, Springer Verlag, Berlin, Germany.

Köther, N., Götze, H.-J., Gutknecht, B.D., Jahr, T., Jentzsch, G., Lücke, O.H., Mahatsente, R., Sharma, R. and Zeumann, S. (2011). The seismically active Andean and Central American margins: Can satellite gravity map lithospheric structures?, *J. Geodyn.*, **In press**, doi: 10.1016/j.jog.2011.11.004.

Lefeldt, M. and Grevemeyer, I. (2007). Centroid depth and mechanism of trench-outer rise earthquakes, *Geophys. J. Int.*, **172**: 240-251, doi: 10.1111/j.1365-246X.2007.03616x.

Lessel, K. (1997). Die Krustenstruktur der zentralen Anden in Nordchile (21◦S–24◦S), abgeleitet aus 3D-Modellierungen refraktionsseismischer Daten, Ph.D. thesis, Freie Universität Berlin, Berlin, Germany.

Li, X. and Götze, H.-J. (2001). Ellipsoid, geoid, gravity, geodesy, and geophysics, *Geophysics*, **66**: 1660-1668.

Linkimer, L., Beck, S.L., Schwartz, S.Y., Zandt, G. and Levin, V. (2010). Nature of crustal terranes and the Moho in northern Costa Rica from receiver function analysis, *Geochem. Geophys. Geosyst.*, **11**(1): 1-24, doi: Q01S19, doi:10.1029/2009GC002795.

Lizarralde, D., Holbrook, W.S., VanAvendonk, H., Alvarado, G.E., Mora, M., Harder, S. and Bullock, A. (2007). Crustal structure along strike beneath the Costa Rican arc, paper presented at

Margins Workshop to Integrate Subduction Factory and Seismogenic Zone Studies in Central America, Heredia, Costa Rica.

Lomax, A., Virieux, J., Volant, P. and Berge-Thierry, C. (2000). Probabilistic earthquake location in 3D layered models, in *Advances in seismic event location*, edited by Thurber, C.H. and Rabinowitz, N., pp. 101-134, Kluwer Academic Publishers, Dordrecht.

Lonsdale, P. and Klitgord, K.D. (1978). Structure and tectonic history of the eastern Panama basin, *Geol. Soc. Am. Bull.*, **89**: 981-999.

Lonsdale, P. (2005). Creation of the Cocos and Nazca plates by fission of the Farallon plate, *Tectonophysics*, **404**: 237-264, doi: 10.1016/j.tecto.2005.05.011.

Lücke, O.H. (2008). Modelo tridimensional de densidades de la corteza superior en el sector Central de Costa Rica, basado en interpretación del campo gravimétrico, Licenciate thesis, University of Costa Rica, San José.

Lücke, O.H., Götze, H.-J. and Alvarado, G.E. (2010). A constrained 3D density model of the upper crust from gravity data interpretation for central Costa Rica, *International Journal of Geophysics*, doi: 10.1155/2010/860902.

Lücke, O.H. (2012). Moho structure of Central America based on three-dimensional lithospheric density modelling of satellite derived gravity data, *Intl. J. Earth Sci.*, **In press**, doi: 10.1007/s00531-012-0787-y.

Lüth, S., et al. (2003). A crustal model along 39°S from a seismic refraction profile – ISSA 2000, *Rev. geol. Chile*, **30**: 83-101.

MacKenzie, L., Abers, G.A., Fischer, K.M., Syracuse, E.M., Protti, J.M., Gonzalez, V. and Strauch, W. (2008). Crustal structure along the Central American volcanic front, *Geochem. Geophys. Geosyst.*, **9**(8), doi: 10.1029/2008GC001991.

Madariaga, R. and Cochard, A. (1996). Dynamic friction and the origin of the complexity of earthquake sources, *Proc. Natl. Acad. Sci. U.S.A*, **93**: 3819-3824.

Marsan, D. (2006). Can coseismic stress variability suppress seismicity shadows? Insights from a rate-and-state friction model, *J. geophys. Res.*, **111**(B06305), doi: 10.1029/2005JB004060.

Marshall, J.S., Fisher, D.M. and Gardner, T.W. (2000). Central Costa RIca deformed belt: Kinematics of diffuse faulting across the western Panama block, *Tectonics*, **19**(3): 468-492.

Marshall, J.S. (2007) The Geomorphology and Physiographic Provinces of Central America, in *Central America: Geology, Resources and Hazards*, vol. 1, edited by Alvarado G.E. and Bundschuh J. pp 75-121, Taylor & Francis, London.

Matumoto, T., Ohtake, M., Latham, G. and Umaña, J. (1977). Crustal Structure in Southern Central America, *Bull. seism. Soc. Am.*(67): 121-134.

Mayer-Guerr, T. (2007). ITG-Grace03s: the latest GRACE gravity field solution computed in Bonn, paper presented at *GSTM+SPP Conference*, Potsdam, Germany.

Meschede, M., Barckhausen, U. and Worm, H.U. (1998). Extinct spreading on the cocos ridge, *Terra Nova*, **10**: 211-216.

Montero, W., Paniagua, S., Kussmaul, S. and Rivier, F. (1992). Geodinámica interna de Costa Rica, *Rev. geol. Am. Centr.*(14): 1-12.

Moser, T.J., van Eck, T. and Nolet, G. (1992). Hypocenter determination in strongly heterogeneous Earth models using the shortest path method, *J. geophys. Res.*, **97**(B5): 6563-6572, doi: 10.1029/91JB03176.

Müller, R.D., Sdrolias, M., Gaina, C. and Roest, W.R. (2008). Age, spreading rates and spreading symmetry of the world's ocean crust, *Geochem. Geophys. Geosyst.*(9), doi: 10.1029/2007GC001743.

Norabuena, E.O., Dixon, T.H., Stein, S. and Harrison, C.G.A. (1999). Decelerating nazca–south America and nazca–pacific plate motions, *Geophys. Res. Lett.*, **26**: 3405-3408.

Oncken, O., Chong, G., Franz, G., Giese, P., Götze, H.-J., Ramos, V.A., Strecker, M. and Wigger, P. (2006). *The Andes – Active Subduction Orogeny*, Springer Verlag, Berlin, Germany.

Pail, R., Goiginger, H., Schuh, W.-D., Höck, E., Brockmann, J.M., Fecher, T., Gruber, T., Mayer-Gürr, T., Kusche, J., Jäggi, A. and Rieser, D. (2010). Combined satellite gravity field model GOCO01S derived from GOCE and GRACE, *Geophys. Res. Lett.*, **37**(L20314), doi: 10.1029/2010GL044906.

Pašteka, R. and Richter, R. (2005). Improvement of the Euler deconvolution algorithm by means of the introduction of regularized derivatives, *Geophys Geod*, **35**(1): 19-32.

Pašteka, R. (2006). RegDer software, user's manual, Comenius University Bratislava, Slovakia.

Pavlis, N.K., Factor, J. and Holmes, S. (2007). Terrain-related gravimetric quantities computed for the next EGM, paper presented at 1st International Symposium of the International Gravity Field Service (IGFS), Istambul, Turkey.

Pavlis, N.K., Holmes, S.A., Kenyon, S.C. and Factor, J.K. (2008). An Earth Gravitational Model to Degree 2160: EGM2008, paper presented at *European Geosciences Union General Assembly*, Vienna, Austria, April 13-18th.

Peacock, S.M. (2001). Are the lower planes of double seismic zones caused by serpentine dehydration in subducting oceanic mantle?, *Geology*, **29**: 299-302.

Peacock, S.M., vanKeken, P.E., Holloway, S.D., Hacker, B.R., Abers, G.A. and Fergason, R.L. (2005). Thermal structure of the Costa Rica – Nicaragua subduction zone, *Phys. Earth planet. Intr.*, **149**(1-2): 187-200, doi: 10.1016/j.pepi.2004.08.030.

Pedersen, L.B. and Rasmussen, T.M. (1990). The gradient tensor of potential field anomalies: Some implications on data collection and data processing of maps, *Geophysics*, **55**: 1558-1566.

Pindell, J. and Keenan, L. (2009). Tectonic evolution of the Gulf of Mexico, Caribbean and South America in the mantle reference frame: An update, in *The origin and evolution of the Caribbean Plate*, edited by James, K.H., Lorente, M.A. and Pindell, J., pp. 1-55.

Pizarro, D. (1993). Los pozos profundos perforados en Costa Rica: aspectos litológicos y bioestratigráficos, *Rev. geol. Am. Centr.*(15): 81-85.

Ponce, D.A. and Case, J.E. (1987). Geophysical interpretation of Costa Rica, in *U.S. Geol. Surv. Misc. Inv. Series Map*, edited by Survey, U.S.G., Hidrocarburos, D.d.G.M.e. and Rica, U.d.C., p. 75, U.S. Department of the Interior, Virginia.

Prezzi, C.B., Götze, H.-J. and Schmidt, S. (2009). 3D density model of the Central Andes, *Phys. Earth planet. Intr.*, **177**: 217-234.

Protti, M., Gundel, F. and McNally, K. (1994). The geometry of the Wadati-Benioff Zone under southern Central America and its tectonic significance—Results from a high-resolution local seismographic network, *Phys. Earth planet. Intr.*, **84**: 271-287, doi: 10.1016/0031-9201(94)90046-9.

Protti, M., Schwartz, S.Y. and Zandt, G. (1996). Simultaneous inversion for earthquake location and velocity structure beneath central Costa Rica, *Bull. seism. Soc. Am.*, **86**(1A): 19-31.

Quintero, R. and Kissling, E. (2001). An improved P-wave velocity reference model for Costa Rica, *Geofisica Int.*, **40**: 3-19.

Ramos, V. and Aleman, A. (2000). Tectonic evolution of the Andes, paper presented at 31st International Geological Congress, Rio de Janeiro, Brazil.

Ranero, C.R. and von Huene, R. (2000). Subduction erosion along the Middle America convergent margin, *Nature*, **404**: 748-752.

Ranero, C., Morgan, P., McIntosh, K. and Reichert, C. (2003). Bending-related faulting and mantle serpentinization at the Middle America Trench, *Nature*, **425**: 367-373, doi: 10.1038/nature01961.

Ranero, C.R., Villaseñor, A., PhippsMorgan, J. and Weinrebe, W. (2005). Relationship between bend-faulting at trenches and intermediate-depth seismicity, *Geochem. Geophys. Geosyst.*, **6**(12), doi: 10.1029/2005GC000997.

Reichert, C. and Schreckenberger, B. (2002). Cruise report SO-161 leg 2 & 3, SPOC (Subduction Processes Off Chile) *Rep.*: 142 pp, Hannover.

Reigber, C., Schmidt, R., Flechtner, F., König, R., Meyer, U., Neumayer, K.H., Schwintzer, P. and Zhu, S.Y. (2005). An earth gravity field model complete to degree and order 150 from Grace: Eigen-grace02s, *J. Geodyn.*, **39**: 1-10.

Reutter, K. and Götze, H.-J. (Eds.) (1994). *Comments on the geological and geophysical maps*, 329-333 pp., Springer Verlag, Heidelberg, Germany.

Rogers, R.D., Mann, P. and Emmet, P.A. (2007). Tectonic terranes of the Chortis block based on integration of regional aeromagnetic and geologic data, *GEological Society of America Special Paper*, **248**: 65-88, doi: 10.1130/2007.2428(04).

Rüpke, L., Phipps Morgan, J., Hort, M. and Connolly, J.A.D. (2002). Are the regional variations in Central American arc lavas due to differing basaltic versus peridotitic slab sources of fluids?, *Geology*, **30**(11): 1035-1038, doi: 10.1130/0091-7613(2002)030.

Ryan, B.F., Carbotte, S.M., Coplan, J.O., O'Hara, S., Melkonian, A., Arko, R., Weissel, R. A., Ferrini, V., Goodwillie, A., Nitsche, F., Bonczkowski, J. and Zemsky, R. (2009). Global Multi-Resolution Topography Synthesis, *Geochem. Geophys. Geosyst.*, **10**: doi:10.1029/2008GC002332.

Sallarès, V., Dañobeitia, J.J. and Flueh, E.R. (2001). Lithospheric structure of the Costa Rican Isthmus: Effects of subduction zone magmatism on an oceanic plateau, *J. geophys. Res*, **106**(B1): 621-643.

Sallarès, V., Charvis, P., Flueh, E.R. and Bialas, J. (2003). Seismic structure of Cocos and Malpelo Volcanic Ridges and implications for hot spot-ridge interactions, *J. geophys. Res*, **108**(B12, 2564), doi: 10.1029/2002JB002431, 2003.

Scheuber, E., Bogdanic, T., Jensen, A. and Reutter, K. (1994). Tectonic development of the north Chilean Andes relation to plate convergence magmatism since the Jurassic, in *Tectonics of the Southern Central Andes*, edited by Reutter, K., Scheuber, E. and Wigger, P., pp. 7-22, Springer Verlag, Berlin, Germany.

Schmidt, S. and Götze, H.J. (1998). Interactive visualization and modification of 3D-models using GIS-functions, *Phys. Chem. Earth*, **23**(3): 289-295.

Schmidt, S. and Götze, H.J. (1999). Integration of data constraints and potential field modelling -- an example from southern lower saxony, Germany, *Phys. Chem. Earth*, **24**(3): 191-196.

Schmidt, S. and Götze, H.-J. (2006). Bouguer and isostatic maps of the Central Andes, in *The Andes – Active Subduction Orogeny*, edited by Oncken, O., Chong, G., Franz, G., Giese, P., Götze, H.-J., Ramos, V.A., Strecker, M. and Wigger, P., pp. 559-565, Springer Verlag, Berlin, Germany.

Schmidt, S., Götze, H.-J., Fichler, C. and Alvers, M. (2010). IGMAS+ – a new 3D Gravity, FTG and Magnetic Modeling Software, in *GEO-INFORMATIK 2010, Die Welt im Netz*, edited by Zipf, A., Behncke, K., Hillen, F. and Schefermeyer, J., pp. 57-63, Akademische Verlagsgesellschaft.

Schmitz, M., Lessel, K., Giese, P., Wigger, P., Araneda, M., Bribach, J., Graeber, F., Grunewald, S., Haberland, C., Lüth, S., Röwer, P., Ryberg, T. and Schulze, A. (1999). The crustal structure beneath the central andean fore-arc and magmatic arc as derived from seismic studies – the PISCO 94 experiment in northern Chile (21◦–23◦S), *J. South Am. Earth Sci.*, **12**: 237-260.

Sick, C. (2006). Structural investigations of Chile: Kirchhoff Prestack Depth Migration versus Fresnel Volume Migration, Ph.D thesis, Freie Universität Berlin, Berlin, Germany.

Siebert, L. and Simkin, T. (2002). Volcanoes of the World: An Illustrated Catalogue of Holocene Volcanoes and their Eruptions, *Smithsonian Institution, Global Volcanism Program Digital Information Series*,, **GVP-3**(http://wwww.volcano.si.edu/world/)).

Sobiesiak, M., Meyer, U., Schmidt, S., Götze, H.-J. and Krawczyk, C.M. (2007). Asperity generating upper crustal sources revealed by b-value and isostatic residual anomaly grids in the area of Antofagasta, Chile, *J. geophys. Res.*, **112**(B12308).

Sobolev, S.V., Babeyko, A.Y., Koulakov, I. and Oncken, O. (2006). Mechanism of the Andean Orogeny: insight from numerical modeling, in *The Andes – Active Subduction Orogeny*, edited by Oncken, O., Chong, G., Franz, G., Giese, P., Götze, H.-J., Ramos, V.A., Strecker, M.R. and Wigger, P., pp. 513-535, Springer Verlag, Berlin, Germany.

Somoza, R. (1998). Updated Nazca (Farallon)-South America relative motions during the last 40 My: implications for mountain building in the central Andean region, *J. South Am. Earth Sci.*, **11**(3): 211-215.

Song, T.R.A. and Simons, M. (2003). Large trench-parallel gravity variations predict seismogenic behavior in subduction zones, *Science*, **301**: 630-633.

SRTM3 Version 2, Courtesy NASA/JPL-Caltech, January 2009, http://www2.jpl.nasa.gov/srtm/.

Stavenhagen, A.U., Flueh, E.R., Ranero, C., McIntosh, K.D., Shipley, T., Leandro, G., Schulze, A. and Dañobeitia, J.J. (1997). Seismic wide-angle investigations in Costa Rica: A crustal velocity model from the Pacific to the Caribbean coast, *Zbl. Geol. Paläeont.*, **6**(1-3): 393-408.

Syracuse, E.M., Abers, G.A., Fischer, K., MacKenzie, L., Rychert, C., Protti, M., González, V. and Strauch, W. (2008). Seismic tomography and earthquake locations in the Nicaraguan and Costa Rican upper mantle, *Geochem. Geophys. Geosyst.*, **9**(7), doi: 10.1029/2008GC001963.

Tarantola, A. and Valette, B. (1982). Inverse problems = quest for information, *J. Geophys.*, **50**: 159-170, doi: 10.1038/nrm1011.

Tassara, A., Götze, H.-J., Schmidt, S. and Hackney, R. (2006). Three-dimensional density model of the nazca plate and the andean continental margin, *J. geophys. Res.*, **111**(B09404), doi:10.1029/2005JB003976.

Tassara, A. (2010). Control of forearc density structure on megathrust shear strength along the Chilean subduction zone, *Tectonophysics*, **495**(1-2): 34-47.

Thorpe, R.S., Locke, C.A., Brown, G.C., Francis, P.W. and Randal, M. (1981). Magma chamber below Poás volcano, Costa Rica, *J. geol. Soc. London*, **138**: 367-373.

Tournon, J., Seyler, M. and Astorga, A. (1995). Les péridotites du rio San Juan (Nicaragua et C.R.): jalons posible dune suture ultrabasique E-W en Amérique Centrale méridionale C.R. , *Académie des Sciencies*, **320**(11).

Tournon, J. and Alvarado, G.E. (1997). Mapa geológico de Costa Rica, Editorial Tecnológica de Costa Rica, Cartago, Costa Rica.

Venable, M.E. (1994). A geologic, tectonic, and metallogenic evaluation of the Siuna terrane, PhD thesis, University of Arizona, Tucson.

von Huene, R., Ranero, C.R., Weinrebe, W. and Hinz, K. (2000). Quaternary convergent margin tectonics of Costa Rica, segmentation of the Cocos Plate, and Central American volcanism, *Tectonics*, **19**(2): 314-334.

Walther, C.H.E., Flueh, E.R., Ranero, C.R., von Huene, R. and Strauch, W. (2000). Crustal structure across the Pacific margin of Nicaragua, evidence for ophiolitic basement and a shallow mantle sliver, *Geophys. J. Int.*, **141**: 759-777.

Walther, C.H.E. (2003). The crustal structure of the Cocos Ridge off Costa Rica, *J. geophys. Res.*, **108**(B3): 2136, doi: doi:10.1029/2001JB000888.

Wells, R.E., Blakely, R.J., Sugiyama, Y., Scholl, D.W. and Dinterman, P.A. (2003). Basin-centered asperities in great subduction zone earthquakes: a link between slip, subsidence, and subduction erosion?, *J. geophys. Res.*, **108**(30).

Wollard, G.P. (1969). Regional variations in gravity, in *The Earth's crust and upper mantle*, edited by Hart, P.J., pp. 320-340, Am. Geophys. Union.

Worzewski, T., Jegen, M., Kopp, H., Brasse, H. and Taylor, W. (2011). Magnetotelluric image of the fluid cycle in the Costa Rican subduction zone, *Nature Geosci.*, **4**, doi: 10.1038/NGEO1041.

Ye, S., Bialas, J., Flueh, E.R., Stavenhagen, A., von Huene, R., Leandro, G. and Hinz, K. (1996). Crustal structure of the Middle American Trench off Costa Rica from wide-angle seismic data, *Tectonics*, **15**(5): 1006-1021, doi: 10.1029/96TC00827.

Zhang, J., Green II, H.W., Bozhilov, K. and Jim, Z. (2004). Faulting induced by precipitation of water at grain boundaries in hot subducting oceanic crust, *Nature*, **428**: 633-636.

Acknowledgements

O. Lücke thankfully acknowledges the support of the German Academic Exchange Service (DAAD) for financing the studies leading to this dissertation. Also the University of Costa Rica (UCR), the Special Priority Program 1257 “Mass Transport and Mass Distribution in the Earth System” of the German Research Foundation (DFG) and the Collaborative Research Center 574: Volatiles and Fluids in Subduction Zones, for providing additional support at various stages.

Special thanks to the members of the Geophysics and Geoinformation Research Group of the Institute of Geosciences at the University of Kiel, lead by Prof. Dr. Hans-Jürgen Götze who has provided guidance for all of my research activities in the field of Geophysics. Thanks to Dr. Rezene Mahatsente, Benjamin Gutknecht and Nils Köther as well as researchers of the NOGAPSGRAV and IMOSAGA subprojects of the SPP1257 for their collaboration in the analysis and interpretation of satellite derived data. Thanks to Dr. Sabine Schmidt for her assistance with the IGMAS+ software and Prof. Dr. Rabbel for his research group's contribution of constraining data and for his contributions as examiner of this work.

Thanks to all my family and friends in Costa Rica, Switzerland and Germany, for their invaluable support throughout this experience and for tolerating the countless hours of talk about cycling.

Eidesstattliche Erklärung

Hiermit versichere ich, dass ich vorliegende Arbeit selbständig verfaßt und keine anderen als die angegebenen Hilfsmittel benutzt habe. Die Stellen der Arbeit, die anderen Werken wörtlich oder inhaltlich entnommen sind, wurden durch entsprechende Angaben der Quellen kenntlich gemacht. Diese Arbeit hat in gleicher oder ähnlicher Form noch keiner Prüfungsbehörde vorgelegen. Hiermit versichere ich, dass die Arbeit unter Einhaltung der Regeln guter wissenschaftlicher Praxis der Deutschen Forschungsgemeinschaft entstanden ist.

I certify that this thesis is my own composition, all sources have been acknowledged and my contribution to the thesis is clearly identified. The thesis has not previously been accepted for a degree at this or another institution. I certify that the work has been undertaken in compliance with the German Research Foundation’s (Deutsche Forschungsgemeinschaft, DFG) rules of good academic practice.

Curriculum Vitae

Oscar Herbert Lücke Castro

Date of Birth:	October 1st, 1982
Place of Birth:	San José, Costa Rica
Nationality:	Costa Rican
Languages:	Spanish (native language), English, German

Education

- 2003-2006: Bachelor of Science degree in geology at the University of Costa Rica, Ciudad Universitaria Rodrigo Facio, San José.
- 2007-2008: Licentiate degree in Geology at the University of Costa Rica.